

# **Live cell methods to visualize translocated *Salmonella* effectors and monitor Ca<sup>2+</sup> transients during infection**

**By**

**Alexandra Marie Young**

**B.S. Illinois State University, Normal Illinois, 2008**

**M.S. Illinois State University, Normal Illinois, 2010**

**A thesis submitted to the faculty of the graduate school of the University of Colorado  
in partial fulfillment of the requirement for the degree of Doctor of Philosophy,  
Department of Chemistry and Biochemistry, 2017.**

This thesis for the Doctor of Philosophy degree entitled:  
Live cell methods to visualize translocated *Salmonella* effectors  
and monitor Ca<sup>2+</sup> transients during infection

written by Alexandra Marie Young  
has been approved for the  
Department of Chemistry and Biochemistry

---

Amy E. Palmer

---

Joel Kralj

---

Date

The final copy of this thesis has been examined by the signatories,  
and we find that both the content and the form meet acceptable presentation standards of  
scholarly work in the above mentioned discipline.

## ABSTRACT

**Alexandra Marie Young (Ph.D. Chemistry and Biochemistry)**

**Live cell methods to visualize translocated *Salmonella* effectors and monitor Ca<sup>2+</sup> transients during infection**

**Thesis directed by Professor Amy E. Palmer**

*Salmonella* species invade and survive within eukaryotic host cells by using a Type Three Secretion System (T3SS) to translocate bacterial effector proteins into the host cell and commandeer host-cell signaling processes, including Ca<sup>2+</sup> regulation. T3SS effector activity is tightly regulated, in part by their different spatial distribution within the host cell, to coordinate each stage of the infection process. To date, more than 40 T3SS effector proteins have been identified, but their biochemical functions and role in the infection process are often poorly understood. Complexity of effector regulation coupled with growing evidence for cell-to-cell heterogeneity of infection underscores the importance of being able to localize and monitor effectors directly in living infected host cells. However, progress in understanding the dynamics of when and where effectors localize within host cells has been challenging due to limited tools to study these proteins in the native cellular environment throughout the course of infection. Here we discuss two novel imaging methods, one was created to study the host cell localization of specific effector proteins and the other to monitor host cell Ca<sup>2+</sup> transients that occur upon *Salmonella* internalization.

# CONTENTS

## Chapter

<b>1. Introduction</b> .....	1
1.1 <i>Salmonella</i> Infection: Background and Significance.....	1
1.2 T3SS-1 Translocated Effector Proteins.....	5
1.3 T3SS-2 Translocated Effector Proteins.....	11
1.4 Effector Proteins Translocated Through Both T3SS-1 and T3SS-2.....	19
1.5 Current Methods Used to Study Effector Proteins.....	22
1.6 Development of a New Modular Split-GFP Labeling Platform.....	34
<b>2. Fluorescence complementation platform for visualizing <i>Salmonella</i> effector proteins by live cell microscopy</b> .....	35
2.1 Introduction.....	35
2.2 Results.....	39
2.3 Discussion.....	67
2.4 Methods.....	70
2.5 Supplementary Effector Proteins.....	77
<b>3. Future Directions</b> .....	85
<b>Appendix: Development of Fluorescence Microscopy Assays to Examine Host Cell Ca<sup>2+</sup> Transients During <i>Salmonella</i> Invasion of HeLa Cells</b> .....	90
A.1 Introduction.....	90
A.2 Results and Discussion.....	92
A.3 Methods.....	108
<b>References</b> .....	112

## TABLES

### Table

1.1. T3SS-1 translocated effector proteins.....	8
1.2. T3SS-2 translocated effector proteins.....	12
1.3. T3SS-1/2 translocated effector proteins.....	21
2.1. Comparison of bacterial expression assay and split-GFP complementation in infected host cells.....	47
S.1. Comparison of bacterial expression assay and split-GFP complementation in infected host cells for supplementary effector proteins.....	78
S.2. Comparison of bacterial expression assay and split-GFP complementation in infected host cells for SopD2 expressed in different plasmid layouts.....	83

## FIGURES

### Figure

1.1. Overview of <i>Salmonella</i> infection of epithelial cells and macrophage.....	4
1.2. Overview of T3SS-1 effector protein roles in epithelial cell invasion by <i>Salmonella</i> .....	10
1.3. Overview of T3SS-2 effector protein roles during epithelial cell or macrophage infection .....	15
1.4. Outline of methods used to study effector protein roles in infection.....	31
1.5. The split-GFP system.....	33
2.1. Platforms for labeling <i>Salmonella</i> effector proteins with split-GFP.....	41
2.2. Cloning layout of the pACYC plasmid based GFP11 effector protein labeling platform.....	42
2.3. Bacterial expression assay to validate effector protein expression and split-GFP complementation efficiencies.....	44
2.4. GFP <sub>comp</sub> intensity profiles for effector proteins tested with the bacterial expression assay .....	50
2.5. In vitro growth curves of <i>Salmonella</i> strains used in this study.....	51
2.6. Visualizing translocated effector proteins inside live host cells.....	52
2.7. Time course images for GFP <sub>comp</sub> -labeled effector proteins in infected HeLa cells .....	54
2.8. SseG gathers at the host cell periphery in the absence of SseF.....	57
2.9. SseG filaments are thin and punctate in the absence of SseF.....	58
2.10. Defining subcellular localization of SlrP during live cell infections.....	60
2.11. Fluorescence images demonstrating split-GFP fluorescence complementation in cells nucleofected with GFP1-10-IRES-NLS-mTagBFP.....	64
2.12. Fluorescence images demonstrating split-GFP fluorescence complementation in BMDMs nucleofected with GFP1-10-IRES-NLS- mTagBFP.....	65
2.13. Images of infected primary BMDMs illustrating dispersed as opposed to compact bacteria.....	66

<b>S.1.</b> GFP <sub>comp</sub> intensity profiles for supplementary effector proteins tested with the bacterial expression assay .....	79
<b>S.2.</b> Cloning layouts for different versions of GFP11 effector protein labeling platforms .....	82
<b>S.3.</b> The presence of the EcoRI restriction site between the promoter and the initiation codon effects the expression of SopD2.....	84
<b>A.1.</b> Imaging rate impacts the amount of observed Ca <sup>2+</sup> transients with Fura-2.....	93
<b>A.2.</b> <i>Salmonella</i> infection efficiency is temperature dependent.....	95
<b>A.3.</b> Measuring membrane ruffling localized host cell Ca <sup>2+</sup> responses to <i>Salmonella</i> internalization with the genetically encodable FRET sensor lynD3cpv.....	96
<b>A.4.</b> Ca <sup>2+</sup> transients near the plasma membrane of infected host cells are dependent on extracellular Ca <sup>2+</sup> .....	98
<b>A.5.</b> <i>Salmonella</i> infection does not create large host cell membrane pores.....	101
<b>A.6.</b> <i>Salmonella</i> induced host cell Ca <sup>2+</sup> transients have multiple phenotypes...	103
<b>A.7.</b> Extracellular Ca <sup>2+</sup> is not essential for <i>Salmonella</i> internalization in HeLa cells.....	105
<b>A.8.</b> Extracellular Ca <sup>2+</sup> is not essential for <i>Salmonella</i> infection or replication in HeLa cells .....	106

## CHAPTER 1

### 1.1 *SALMONELLA* INFECTION: BACKGROUND AND SIGNIFICANCE

*Salmonella* is a Gram-negative, facultative anaerobic, rod-shaped bacteria that belongs to the family Enterobacteriaceae<sup>1</sup>. Almost all strains of *Salmonella* are pathogenic and thus have the ability to invade, replicate and survive in a variety of plant and animal hosts, including humans<sup>2</sup>. In fact *Salmonella* is one of the most frequently isolated foodborne pathogens and remains a major public health concern, accounting for approximately 94 million foodborne illnesses and 200,000 deaths per year worldwide<sup>3</sup>. With the emergence of antibiotic-resistant strains of *Salmonella*, infections pose an increasing public health concern and contribute to an economic burden, for both industrialized and underdeveloped countries, through the costs associated with surveillance, prevention and treatment of disease<sup>3-5</sup>. It is therefore pertinent to better understand the mechanisms behind these infections in order to identify new ways of mitigating disease.

The genus *Salmonella* consists of two main species, *Salmonella enterica* and *Salmonella bongori*, that were classified based on 16S rRNA sequence variation. *Salmonella enterica* is further categorized into six subspecies based on genomic relatedness and biochemical features<sup>6,7</sup>. In addition to these classifications based on phylogeny, *Salmonella* subspecies are further divided into serotypes (or serovars) based on the presence of specific antigens on the surface of the bacteria. Within the genus *Salmonella*, over 2600 serotypes have been identified and these differ in antigen presentation, host preference, and disease manifestation<sup>8</sup>. Over half of the identified serotypes belong to *Salmonella enterica* subspecies *enterica*, which accounts for the majority of *Salmonella* infections in humans<sup>3</sup>. Two of the most abundant and well-characterized *Salmonella enterica* serovars are Typhi and Typhimurium,

commonly referred to as *S. Typhi* and *S. Typhimurium*, respectively<sup>7</sup>. *S. Typhi* is restricted to human hosts and is responsible for causing the life-threatening systemic disease typhoid fever. *S. Typhimurium* infection, on the other hand, causes gastroenteritis in humans and other hosts, and less commonly bacteremia. *S. Typhimurium* is not restricted to human hosts and produces a typhoid-like systemic disease in mice<sup>9</sup>, making it an attractive model for better understanding the mechanisms of both gastroenteritis and systemic disease. In this work, we exclusively use *S. Typhimurium* to study infection, and we will refer to this serovar simply as “*Salmonella*” from this point forward.

When *Salmonella* enter the digestive tract of a host organism via consumption of contaminated food or water, the bacteria have the ability to penetrate nonphagocytic epithelial cells as well as microfold (M) cells that line the intestinal wall (**Figure 1.1A**)<sup>10</sup>. This invasion occurs preferentially at Peyer’s patches in the small intestine and enables *Salmonella* uptake and colonization of host cells which triggers an immune inflammatory response thought to be the major cause of gastroenteritis symptoms due to acute infection<sup>11,12</sup>. In the case of systemic *Salmonella* infections and bacteremia, *Salmonella* breach the epithelial layer of the intestine and become engulfed by macrophages that reside in the blood stream. *Salmonella* can persist within macrophage cells and travel through the bloodstream to new sites of infection and colonization, such as the spleen, liver or gall bladder to sustain prolonged infection of the host organism<sup>13,14</sup>.

The ability of *Salmonella* to persist within host cells is crucial for pathogenesis, as strains lacking this ability are non-virulent and are rapidly cleared by the host<sup>15</sup>. To invade and colonize different types of host cells in order to maintain an intracellular existence, *Salmonella* is dependent on two specialized type III secretion systems (T3SSs). T3SSs are complex multi-protein translocons that penetrate the host cell plasma membrane and function to transport bacterial proteins, called effector proteins, across both bacterial membranes as well as the epithelial cell membrane directly to the cytoplasm of the host cell<sup>16,17</sup>. The two T3SSs are encoded at distinct locations on the chromosome, *Salmonella* pathogenicity island-1 (SPI-1) and

*Salmonella* pathogenicity island-2 (SPI-2). Analysis of the genome suggests that these regions were both acquired by horizontal gene transfer<sup>18</sup>. The use of two distinct T3SSs by *Salmonella* is thought to be linked to the differential use of these secretion systems under different conditions<sup>19</sup>. For the invasion of non-phagocytic epithelial cells *Salmonella* use the SPI-1 encoded secretion system T3SS-1 and a specific set of effector proteins that are expressed upon T3SS-1 activation. These T3SS-1 effectors induce profound reorganization of the host actin cytoskeleton that results in ruffling of the host cell membrane and forces *Salmonella* uptake by macropinocytosis (**Figure 1.1B**)<sup>9,20,21</sup>. For macrophage infections, *Salmonella* are phagocytosed by the host cells and T3SS-1 is not required for invasion, although its presence has been linked to higher *Salmonella* survival rates and persistence<sup>16,22</sup> (**Figure 1.1B**). Once internalized into either epithelial or macrophage host cells, *Salmonella* reside in a membrane bound vacuole called the *Salmonella* containing vacuole, or SCV. As the SCV matures down the host endocytic pathway the evolving intravacuolar environment triggers expression of the SPI-2 encoded secretion system T3SS-2 and a new set of effector proteins which are translocated across the vacuolar membrane into the cytosol, functioning to allow for maturation of the vacuole and the continuation of *Salmonella* infection<sup>9,16,20,21,23</sup>.

Both the establishment and maintenance of the SCV are essential for *Salmonella* to successfully replicate and persist intracellularly<sup>24</sup>. It is perhaps because of this that many effector proteins have been suggested to play a role in the formation and maturation of the SCV. Other critical roles for effector proteins that are necessary for the persistence of *Salmonella* infection include modulation of host immune responses and host cell viability. However, most of the mechanisms used by effector proteins to promote successful *Salmonella* infection are not completely understood. By determining the specific roles of these essential effector proteins in generating and sustaining an intracellular niche for *Salmonella*, we can better understand the mechanism behind *Salmonella* virulence.

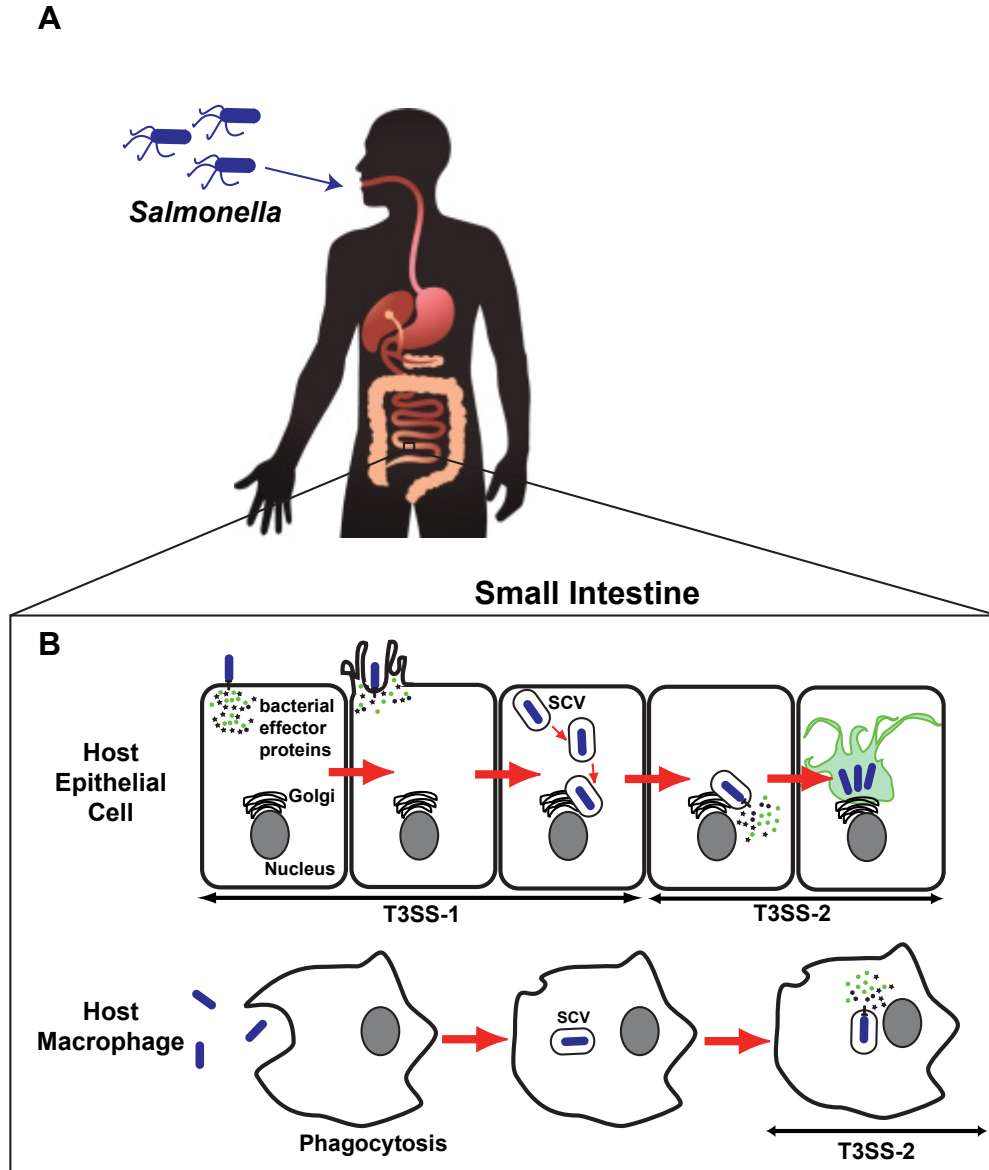


**Figure 1.1. Overview of *Salmonella* infection of epithelial cells and macrophage**

(A) *Salmonella* infection is initiated by ingestion of the bacteria, which then travel down the digestive system to the small intestine and are able to infect host cells, including the epithelial cells that line the small intestine and macrophages that reside beneath the epithelial layer. (B) *Salmonella* use two Type III secretion systems (T3SS) to invade and colonize host cells. For the invasion of epithelial cells, *Salmonella* use T3SS-1 to translocate effector proteins that induce membrane ruffling and bacterial uptake into the host cell. For the invasion of macrophages, *Salmonella* are phagocytosed. Following internalization into either epithelial cells or macrophages, *Salmonella* reside within a membrane bound compartment called the *Salmonella* containing vacuole or SCV, which is trafficked to a perinuclear region within the host cell. Upon maturation of the SCV, T3SS-2 translocates a second set of effector proteins that enable the continuation of *Salmonella* infection.

Figure adapted from Sarah McQate, Amy Palmer, and GettyImages

## 1.2 T3SS-1 TRANSLOCATED EFFECTOR PROTEINS

Following consumption, *Salmonella* enters the gut lumen mucosa of a host where the low oxygen concentration, high osmolarity, and near neutral pH of the small intestine induce the expression of SPI-1, including the T3SS-1 translocon and the associated set of effector proteins which can be translocated across the host cell membrane upon contact<sup>25-27</sup>. *Salmonella* must use T3SS-1 translocated effector proteins to mediate invasion of non-phagocytic epithelial cells (**Table 1.1, Figure 1.2**). A few early effector proteins, SipB, SipC and SipD, are known as translocases and function to assist in the successful translocation of other effector proteins<sup>28</sup>. These effector proteins are translocated themselves and have additional roles in the early infection process. SipC, along with SipA, SopE and SopE2 is required for reorganizing the host cell actin cytoskeleton to promote ruffling of the membrane surrounding the extracellular bacterium in order to initiate bacterial uptake<sup>29</sup>. SipA and SipC directly promote actin polymerization, and SopE and SopE2 function by activating Rho GTPases that can drive actin assembly<sup>30-34</sup>. Following the initiation of membrane ruffling, the formation of the vacuole around the bacterium begins, generating bacterial internalization and the formation of the early SCV. SCV formation is mediated by the effector protein SopB, an inositol phosphatase that contributes to cytoskeleton reorganization and manipulation of lipid dynamics on the cellular membrane<sup>28,35,36</sup>. Once bacteria are successfully internalized, the host cell cytoskeleton is returned to its resting state through the activity of SptP, which functions as a GTPase-activating protein (GAP) for activated Rho GTPases. By stimulating the conversion of GTP into GDP and deactivating Rho GTPases, SptP down regulates actin polymerization and membrane ruffling<sup>37</sup>.

As the early SCV matures down the endocytic pathway it is trafficked toward the nucleus. This process is mediated by effector proteins that recruit and manipulate host cell markers associated with the endo-lysosomal pathway<sup>9,38</sup>. For example, SopE and SopB recruit many host cell factors, including Rab5, sorting nexin-1, and early endosomal antigen 1 to the SCV<sup>38</sup>. Within about an hour, these early endosomal markers are replaced with the late

endosomal markers: v-ATPases, LAMP1, and Rab7, as the vacuole matures to the intermediate SCV. SipA is thought to be responsible for recruiting F-actin to the site of the SCV and controlling tethering of the SCV to actin to secure its location in a perinuclear position<sup>39</sup>. In addition to its role down regulating membrane ruffling, SptP recruits and dephosphorylates the AAA+ ATPase vasolin-containing protein (VCP, which is also known as p97 or Cdc48) at the SCV<sup>40,41</sup>. This SptP mediated process is thought to allow VCP to increase membrane fusion events, thus promoting the membrane integrity of the SCV<sup>41</sup>.

In addition to forming and maintaining the intracellular niche, effector proteins are able to regulate host cell immune signaling processes and host cell viability in order to benefit the intracellular fate of *Salmonella*. At least two effector proteins, AvrA and SopB, have been shown to have anti-apoptotic roles. AvrA is a deubiquitinase that targets  $\beta$ -catenin, I $\kappa$ B $\alpha$  and NF- $\kappa$ B, whose actions lead to a decrease in the expression of the pro-inflammatory cytokine IL-6<sup>42</sup>. The activity of AvrA suppresses the JNK MAPK apoptotic pathway<sup>43</sup> and SopB activates Akt, a kinase that can exert pro-survival effects<sup>44</sup>. On the other hand, some T3SS-1 translocated effector proteins have activities that are pro-inflammatory or can promote cell death. For example, SopA is a HECT-like E3 ubiquitin ligase that localizes to mitochondria and whose activity is involved in *Salmonella*-induced polymorphonuclear leukocytes (PMN) migration<sup>45-47</sup>. SopA facilitates stimulation of the host innate immune response and is required for efficient inflammation in animal models of *Salmonella* infection<sup>48</sup>. Recently, SopA was shown to directly target two host E3 ubiquitin ligases, TRIM56 and TRIM65, which signal through mitochondrial anti-viral signal adapter proteins (MAVs) to stimulate interferon- $\beta$  signaling and the production of pro-inflammatory cytokines<sup>49</sup>. The effector protein SipB is involved in the induction of a caspase-1 dependent form of macrophage cell death that is known as pyroptosis<sup>50,51</sup>. This ability of *Salmonella* to influence the fate of the host cell contributes to successful infection. Pro-survival and anti-inflammatory functions are important for the intracellular survival of *Salmonella*,

whereas pro-death activities enable dissemination of the bacteria to new sites of infection in other tissues within a single host, as well as bacterial clearance for the infection a new host.

The effector proteins translocated by T3SS-1 are present early in the infection process; some of these effector proteins exclusively contribute to the initial stages of infection and are present only transiently in the cell<sup>52</sup>, whereas others persist and function throughout the infection process<sup>39</sup>. The T3SS-1 effector proteins are essential for infection of epithelial cells, yet they are not required for the invasion of macrophages<sup>16,22</sup>. It has been shown, however, that the phagocytosis of *Salmonella* by macrophages induces the expression of SPI1 and the associated T3SS-1 translocated effector proteins, the presence of which results in higher *Salmonella* survival rates and persistence within macrophage cells<sup>53</sup>. This observation suggests that T3SS-1 effector proteins contribute to the macrophage infection model as well, likely by providing mechanisms for proper SCV formation and maintenance.

**Table 1.1. T3SS-1 translocated effector proteins**(modified from refs <sup>9,20,21,28</sup>)

<b>Effector Protein</b>	<b>Host Cell Localization</b>	<b>Molecular Activity</b>	<b>Function</b>	<b>Host Cell Targets</b>
AvrA	unknown	Acetyltransferase, deubiquitinase	Anti-apoptotic, anti-inflammatory	$\beta$ -catenin, ERK2, I $\kappa$ B $\alpha$ , NF- $\kappa$ B, MKK4, MKK7, p53
SipA (SspA)	Cytosol	unknown	Stabilizes actin polymerization and assembly, disruption of tight junctions, PMN migration, SCV positioning	Caspase-3, F-actin, T-plastin
SipB	unknown	unknown	Component of the T3SS translocase, induces pyroptosis by activation of IL-1 $\beta$	Caspase-1
SipC (SspC)	Cytosol	Actin bundling	Component of the T3SS translocase, promotes actin nucleation for membrane ruffling, aids in SCV maturation	F-actin, syntaxin6, Cytokeratin 8, cytokeratin 18, Exo70
SipD	unknown	unknown	Component of the T3SS translocase, assists with translocation of other effector proteins	unknown
SopA	Mitochondria	E3 ubiquitin ligase	Invasion, PMN migration, inflammation	Caspase-3, HsRMA1, UbcH7, TRIM56, TRIM65

**Table 1.1 continued. T3SS-1 translocated effector proteins**(modified from refs<sup>9,20,21,28</sup>)

<b>Effector Protein</b>	<b>Host Cell Localization</b>	<b>Molecular Activity</b>	<b>Function</b>	<b>Host Cell Targets</b>
SopB (SigD)	Plasma membrane, SCV	Phosphoinositide phosphatase, Guanine nucleotide-dissociation inhibitor (GDI): inhibits activation of GTPases	Invasion of epithelial cells, promotes vacuole formation, maturation and localization, modulates PIP lipids associated with the SCV, recruits Rab5 and Vps34 to the SCV	Inositol phosphates, Cdc24, Cdc42
SopE	Cytosol	Guanine-nucleotide exchange factor (GEF): causes activation of GTPases	Causes membrane ruffling during invasion of epithelial cells through actin remodeling, recruits early endosome fusion with the vacuole, associated with inflammation	Cdc42, Rab5, Rac1
SopE2	Cytosol	Guanine-nucleotide exchange factor (GEF): causes activation of GTPases.	Causes membrane ruffling during invasion of epithelial cells through actin remodeling, recruits early endosome fusion with the vacuole, associated with inflammation	Cdc42, Rac1
SptP	Cytosol	GTPase-activating protein (GAP): causes inactivation of GTPases, tyrosine phosphatase	Reversion of actin reorganization to restore the host cell plasma membrane after invasion of epithelial cells, mediates membrane integrity of the vacuole, inhibits ERK activation	Cdc42, Rac1, VCP, vimentin

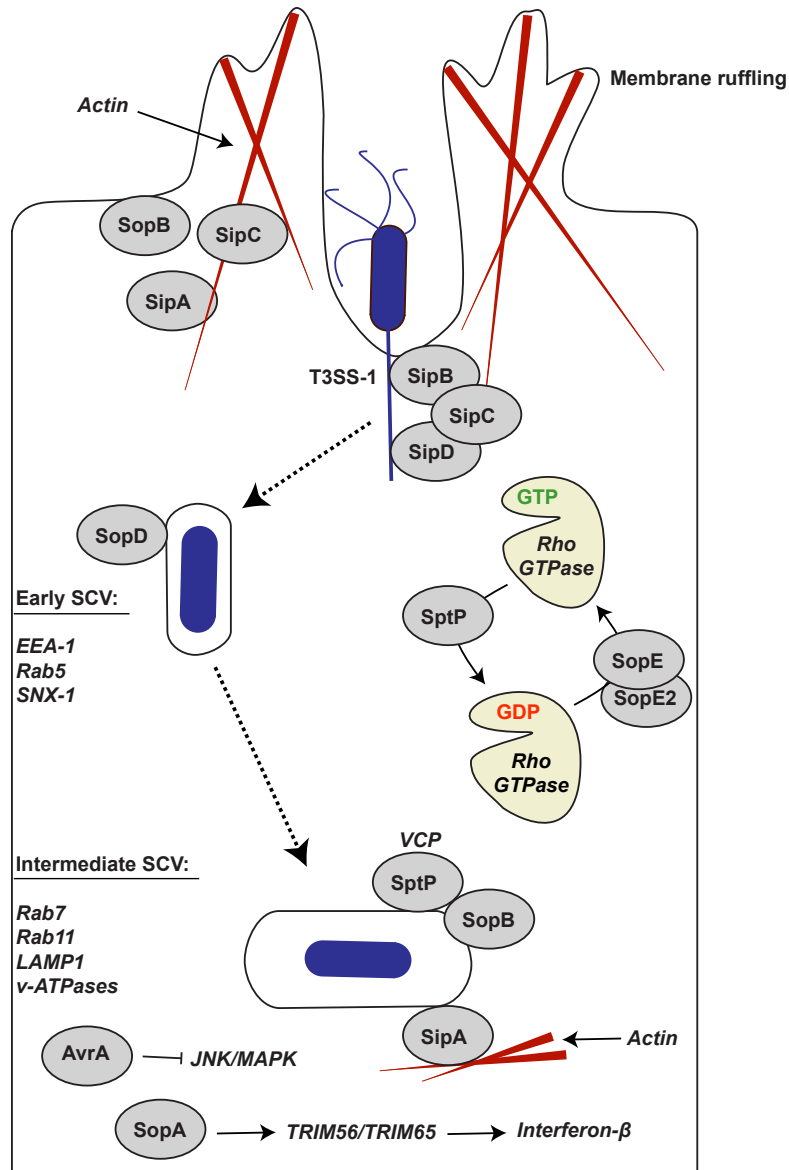


**Figure 1.2. Overview of T3SS-1 effector protein roles in epithelial cell invasion by *Salmonella***

T3SS-1 translocated effector proteins function cooperatively to induce bacterial uptake into the host cell via reorganization of the actin cytoskeleton, which results in macropinocytosis. These effector proteins are essential for the establishment of the SCV as well as early and intermediate stages of SCV maturation. T3SS-1 translocated effectors are depicted as grey ovals and host cell factors associated with both early and intermediate stages are listed on the left in *italics*. Host cell factors that are targeted by specific effector proteins are depicted in *italics* near to their respective effector protein. Abbreviations: EEA-1: early endosomal antigen 1, SNX-1: sorting nexin-1, VCP: AAA+ ATPase VCP (p97), LAMP1: lysosomal-associated membrane protein-1.

Figure adapted from Sarah McQuate

### 1.3 T3SS-2 TRANSLOCATED EFFECTOR PROTEINS

Inside of the host cell further along in the infection process, SPI2 is activated and the intravacuolar bacteria express a second secretion system and set of effector proteins, T3SS-2. T3SS-2 translocated effector proteins play a significant role in further controlling SCV development and maintenance as well as modulating host signaling events and immune responses (**Table 1.2, Figure 1.3**). The induction of T3SS-2 is stimulated by changes in the SCV environment as it matures down the endo-lysosomal pathway. One of the significant changes that contributes to SPI2 activation and expression of T3SS-2 is a steep decrease in  $Mg^{2+}$  within the SCV, although the identity of the host cell transporter responsible for removing the  $Mg^{2+}$  remains unknown<sup>16,54,55</sup>. In addition, the recruitment of v-ATPases to the SCV causes the intravacuolar pH to drop significantly ( $pH < 4.5$ )<sup>9,53,56</sup>. This pH drop induces the assembly of the T3SS-2 translocon which, upon sensing the neutral environment of the cytosol, begins to translocate T3SS-2 effector proteins<sup>16,57</sup>. This translocation process is aided by the activity of the effector protein SpiC, which is also important for preventing SCV fusion with the lysosome<sup>58-</sup>

60

**Table 1.2. T3SS-2 translocated effector proteins**(modified from refs<sup>9,20,21,28</sup>)

<b>Effector Protein</b>	<b>Host Cell Localization</b>	<b>Molecular Activity</b>	<b>Function</b>	<b>Host Cell Targets</b>
CigR	unknown	unknown	unknown	unknown
GogB	Cytosol	unknown	Anti-inflammatory, inhibition of NFκB dependent gene signaling	FBXO22, Skp1
GtgA	unknown	unknown	unknown	unknown
PipB	SCV and filaments	unknown	Stimulates inducible NO synthase, represses β-defensins in avian epithelial cells	Host cell membranes, lipid rafts
SifA	SCV and filaments	Guanine-nucleotide exchange factor (GEF): causes activation of GTPases	Required for SCV filament formation and vacuolar membrane integrity, contributes to vacuolar maintenance	Rab7, Rab9, RhoA, SKIP
SifB	SCV and filaments	Guanine-nucleotide exchange factor (GEF): causes activation of GTPases	unknown	unknown
SopD2	SCV and filaments	unknown	Mediates tubule formation by inhibiting LAMP1 negative tubules (LNTs)	Late endosomal membranes
SpiC (SsaB)	unknown	unknown	Regulates translocation of T3SS-2 effector proteins, prevents the fusion of lysosomes to the SCV	Hook3, TassC

**Table 1.2 continued. T3SS-2 translocated effector proteins**(modified from refs<sup>9,20,21,28</sup>)

<b>Effector Protein</b>	<b>Host Cell Localization</b>	<b>Molecular Activity</b>	<b>Function</b>	<b>Host Cell Targets</b>
SpvB	Cytosol	Actin ribosyltransferase	Inhibits vacuole associated actin polymerization and tubule formation, delays cytotoxicity in macrophage, stimulates P-body disassembly in infected cells	G-actin
SrfJ	unknown	unknown	unknown	unknown
SseF	SCV and filaments	unknown	Promotes filament formation and SCV positioning by forming microtubule bundles, redirecting late endosomal and exocytic traffic, and recruiting dynein to the SCV	Junction plakoglobin, TIP60, ACBD3
SseG	SCV and filaments	unknown	Promotes filament formation and SCV positioning by forming microtubule bundles, redirecting late endosomal and exocytic traffic, and recruiting dynein to the SCV	Caprin-1, desmoplakin, ACBD3
Ssel	SCV-associated F-actin meshwork	unknown	Modulates the migration of infected macrophage	TRIP6, IQGAP1, Filamin A
SseJ	SCV and filaments	acyltransferase, deacylase, phospholipase A1	Esterification of cholesterol in infected cells, regulates the integrity of SCV and filaments	Phospholipids, cholesterol, RhoA, RhoC
SseK1	Cytosol	unknown	unknown	unknown

**Table 1.2 continued. T3SS-2 translocated effector proteins**(modified from refs<sup>9,20,21,28</sup>)

<b>Effector Protein</b>	<b>Host Cell Localization</b>	<b>Molecular Activity</b>	<b>Function</b>	<b>Host Cell Targets</b>
SseK2	unknown	unknown	unknown	unknown
SseK3	unknown	unknown	unknown	unknown
SseL	unknown	Deubiquitinase	Delays cytotoxicity in macrophage, down-regulates NFκB dependent cytokine production, alters lipid metabolism in infected cells, autophagy	IκB, OSBP
SspH2	SCV-associated F-actin meshwork	E3 ubiquitin ligase	Modulates host cell innate immunity by enhancing Nod1-mediated IL-8 secretion	14-3-3γ, AIP, BAG2, Bub3, Filamin A, Profilin-1, Sgt1, UbcH5-Ub, AIP
SteC	SCV-associated F-actin meshwork	Serine/threonine kinase	Required for the formation of the SCV associated F-actin meshwork, actin polymerization	MEK
SteD	unknown	unknown	unknown	unknown



The coordinated activity of T3SS-2 effector proteins is critical for the survival and replication of intravacuolar *Salmonella*. Many T3SS-2 translocated effector proteins have roles in modulating host cell immune responses or manipulating host processes in order to maintain the replicative niche, the SCV. Several of these effector proteins have been found to localize to the SCV and associated membrane filaments, which emanate from the SCV towards the periphery of the host cell. The precise role of these filaments during *Salmonella* infection is still under investigation, though they are hypothesized to participate in activities such as membrane gathering, nutrient recruitment, SCV stabilization, and *Salmonella* spread to neighboring cells<sup>61-63</sup>. *Salmonella* strains that lack effector proteins known to localize to SCV filaments, due to genetic manipulation, are less virulent in mouse infection models<sup>61</sup>. It has therefore been suggested that these SCV filaments play an important role in supporting successful *Salmonella* infection. Some T3SS-2 effector proteins that localize to SCV filaments have well characterized roles in SCV maintenance and their functions can be divided into two general categories: SCV membrane integrity or host cytoskeleton manipulation.

Numerous T3SS-2 effector proteins have been found to promote recruitment of host cell factors to the SCV, leading to manipulation of SCV membrane integrity. SseF and SseG are similar effector proteins that have been shown to recruit lysosomal-associated membrane proteins-1, 2, and 3 (LAMP1, 2, and 3) to the SCV and filaments, indicating that they enable diversion of endocytic traffic to the SCV<sup>64,65</sup>. SseF and SseG were also shown to recruit a glycoprotein from the vesicular stomatitis virus (VSVG) to the SCV, suggesting that they are able recruit exocytic traffic to the SCV as well<sup>66</sup>. Another T3SS-2 effector protein SifA regulates membrane integrity of the SCV and filaments<sup>67</sup> by recruiting the host cell protein SKIP which activates kinesin-1 at the SCV<sup>68</sup>. The activity of SifA is essential for promoting an intact SCV. Consistent with this role, a deletion mutant of SifA allows *Salmonella* to escape from the SCV and hyperreplicate within the cytosol<sup>69,70</sup>. Another effector protein, SseJ, functions along with SifA to regulate the membrane composition of the SCV and filaments by recruiting the GTPase

RhoA to the SCV<sup>71,72</sup>. The presence of the active GTP-bound form of RhoA increases the ability of SseJ to modulate the levels of cholesterol associated with the SCV through acyltransferase activity<sup>73,74</sup>. The presence of cholesterol in the SCV membrane has been suggested to be significant for the recruitment of glycoproteins, which may be important in allowing for nutrient uptake and consequently successful *Salmonella* replication<sup>75</sup>. *Salmonella* is also able to down regulate SCV and filament growth through the activity of the effector protein SopD2, which is thought to be an agonist of vacuole integrity by disrupting vesicle transport to the SCV and subsequently restricting filament outgrowth<sup>76,77</sup>. SpvB may also be involved in the negative regulation of filament formation<sup>78</sup>. Finally, the effector protein SifB was also shown to localize to the SCV and filaments and functions as a GEF, however, its specific role in infection is currently unknown<sup>79</sup>. Similarly, a variety of host cell factors, including Rab11, SCAMP3, and Arl8b have been shown to localize to the late SCV, although the mechanism behind their recruitment is still unknown<sup>80-82</sup>. Collectively these effector proteins and recruited host cell factors are essential for maintaining the growing and maturing SCV in order for the replicating *Salmonella* population to continue an intracellular life.

In addition to their role in modifying SCV membrane composition, T3SS-2 translocated effector proteins are responsible for causing a reorganization of host cytoskeleton components around the SCV as well as maintaining the SCV in its perinuclear location. SseF and SseG localize to the SCV and filaments, however they have also been shown to colocalize with microtubules in infected HeLa cells and are responsible for inducing bundling of microtubules at the SCV at late time points of infection<sup>83</sup>. These microtubule bundles were shown to serve as a scaffold for filament extension<sup>83</sup>. SseF and SseG recruit the molecular motor dynein to the vacuole<sup>64</sup>, and have been shown to physically and functionally interact with each other to restrict the SCV to a perinuclear position near the *trans*-Golgi<sup>84</sup>. The SseF/SseG control of SCV localization to the Golgi is thought to occur by the manipulation of molecular motors such as dynein, or through a physical interaction with the Golgi associated protein ACBD3 that tethers

the SCV to the Golgi<sup>85</sup>, or by some combination of both methods<sup>28,65,86</sup>. T3SS-2 translocated effector proteins also manipulate actin surrounding the SCV. Though it is the T3SS-1 effector protein SipA that is responsible for targeting F-actin to the SCV, the T3SS-2 effector protein SteC is also involved in actin manipulation during infection. SteC enables the reorganization of vacuole associated F-actin to form “actin nests” around the SCV by phosphorylating the MAP kinase MEK<sup>87,88</sup>. It is hypothesized that one role for SteC activity involves regulating *Salmonella* outgrowth by constraining the actin nests around the SCV<sup>87</sup>. SpvB is also involved in actin reorganization over the course of infection and is hypothesized to antagonize SteC activity by negatively regulating the formation of actin nests<sup>89</sup>. Another T3SS-2 effector that localizes to actin nests is SseI, which functions to regulate the migration of infected macrophage cells by interacting with the host cell factors TRIP6 (thyroid hormone receptor interactor 6), IQGAP1 and Filamin A<sup>90,91</sup>. SspH2 also localizes to the SCV associated F-actin meshwork during infection and is able to bind actin<sup>89</sup>. SspH2 functions as an E3 ubiquitin ligase that is hypothesized to be responsible for tagging host cell proteins for proteasomal degradation<sup>92</sup>.

In addition to modulating the host cell in order to maintain the maturing SCV, T3SS-2 translocated effector proteins are also able to regulate host cell signaling events and control innate immune responses. SspH2 has been shown to interfere with antigen presentation and modulate host cell innate immunity by enhancing Nod1-mediated IL-8 secretion<sup>93</sup>. The effector proteins GogB and SseL have anti-inflammatory roles in infection by down regulating NF- $\kappa$ B dependent cytokine production<sup>94,95</sup>. Finally another effector protein, PipB, localizes to the SCV and filaments and has a role in activating host cell nitric oxide synthases and was shown to repress  $\beta$ -defensins in an avian model of infection<sup>96,97</sup>. The exploitation of these host cell-signaling systems is an important feature of *Salmonellas* adaption to intracellular life.

#### 1.4 EFFECTOR PROTEINS TRANSLOCATED THROUGH BOTH T3SS-1 AND T3SS-2

Of the approximately 40 known *Salmonella* effector proteins, ten have been shown to be translocated by both T3SSs (**Table 1.3**). Of these, four are known to play a role in vacuole maturation or have been found to localize to the SCV, three have roles in immune signaling or apoptosis and the rest have roles that are yet to be determined<sup>28</sup>. Among the effector proteins that function in SCV maintenance, SopD is hypothesized to work along with SopB in manipulating lipid dynamics and allowing for successful vacuole formation<sup>29,98</sup>. GtgE is an effector protein that was discovered to only be expressed in *S. Typhimurium* (not *S. Typhi* or *S. Paratyphi*) and was shown to prevent the recruitment of Rab29 to the *S. Typhimurium* SCV<sup>99</sup>. GtgE is a protease that functions by cleaving Rab29, a Rab GTPase that is recruited to the *S. Typhi*-containing vacuole and is necessary for the export of typhoid toxin, which is exclusively encoded by the human-specific serotypes *S. Typhi* and *S. Paratyphi*. Although there is no known biological role for Rab29, its recruitment to the *S. Typhi* SCV is associated with decreased replication<sup>99</sup>. Therefore, GtgE is important for allowing successful replication in *S. Typhimurium* infections. PipB2 was largely established as a T3SS-2 effector protein that promotes SCV filament formation and recruits kinesin-1 to the SCV<sup>96,100,101</sup>. However, it has recently been suggested that PipB2 may also be translocated by T3SS-1<sup>102</sup>, though its role early in infection has not yet been established. Finally, the effector protein SteA is known to localize to the SCV and filaments but its specific role in *Salmonella* infection has not yet been established, though it has been hypothesized to manipulate SCV membrane dynamics<sup>103,104</sup> and redirect exocytic traffic<sup>105</sup>.

SpvC, SspH1, and SlrP are among the effector proteins that participate in manipulating host immune responses. SpvC is a phosphothreonine lyase whose activity down regulates the MAPK signaling pathway by irreversibly inactivating ERK2<sup>106</sup>. Inactivation of MAPK by SpvC is proposed to modulate the host immune response by reducing inflammatory cytokines during the early stages of infection<sup>28</sup>. SspH1, on the other hand, is an E3 ubiquitin ligase that localizes to

the nucleus where it plays a role in inhibiting pro-inflammatory NF- $\kappa$ B dependent gene signaling. This activity is hypothesized to be mediated by an interaction between SspH1 and the host cell protein kinase PKN1<sup>107,108</sup>. SlrP is also an E3 ubiquitin ligase, and has been shown to interact with mammalian thioredoxin-1 (Trx)<sup>109</sup>. Transient transfection of SlrP into cultured epithelial cells showed that the localization of SlrP is mainly cytosolic<sup>110</sup>. However it is hypothesized that a part of the SlrP protein is transported into the endoplasmic reticulum (ER) based on interaction studies using yeast two-hybrid and immunoprecipitation that implicates a binding interaction between SlrP and the ER chaperone ERdj3<sup>110</sup>. SlrP has been shown to have a role in stimulating host cell death, and the current working model suggests that SlrP promotes apoptosis in host cells by interfering with the functions of its targets Trx and ERdj3<sup>109,110</sup>. As this set of effector proteins has the potential to be translocated at both early and late stages of infection, they may play important roles throughout the infection process. This includes participating in SCV maturation and maintenance as well as in modulating host cell responses throughout the stages of infection. It is possible that the roles of effector proteins translocated by both T3SS could evolve over the course of infection, however, many current established methods for studying the cellular roles of these effector proteins lack the sensitivity needed to address their specific mechanisms and whether they change over time.

**Table 1.3. T3SS-1/2 translocated effector proteins**(modified from refs establishment (modified from refs<sup>9,20,21,28</sup>)

<b>Effector Protein</b>	<b>Host Cell Localization</b>	<b>Molecular Activity</b>	<b>Function</b>	<b>Host Cell Targets</b>
GtgE (Not expressed in Typhi or Paratyphi)	unknown	protease	Prevents recruitment of Rab29 to the vacuole	Rab29
PipB2	SCV and filaments	unknown	Promotes tubulation and vacuole dynamics	Kinesin-1
SlrP	Cytosol, ER	E3 ubiquitin ligase	Apoptosis, host cell death	Thioredoxin, ERdj3
SopD	unknown	unknown	Vacuole formation	unknown
SpvC	unknown	Phosphothreonine lyase	Host immune signaling, dephosphorylation of MAP kinases	MAPKs (ERK2)
SpvD	unknown	unknown	unknown	unknown
SspH1	Nucleus	E3 ubiquitin ligase	Inhibition of NF- $\kappa$ B dependent gene signaling	PKN1
SteA	SCV and filaments	unknown	unknown	<i>trans</i> -Golgi network, PI(4)P
SteB	unknown	unknown	unknown	Unknown
SteE	unknown	unknown	unknown	Unknown

## 1.5 CURRENT METHODS USED TO STUDY THE ROLE OF EFFECTOR PROTEINS DURING INFECTION

### *Sequence and structure based methods*

There are many methods used to identify effector proteins and to probe how they mediate infection. The majority of studies aim to establish the biochemical function of individual effector proteins, their role at the cellular level, and how each effector protein influences acute and chronic infection in animal models. A common approach for gaining preliminary insight into the function of a newly identified protein is to compare its sequence to the sequence of proteins with known functions. Sequence alignments are often done using algorithms, such as BLAST, in order to identify regions of homology in the hopes that identifying a previously characterized domain in the new protein might signify function. A few *Salmonella* effector proteins share sequence homology across pathogenic species and this has aided in the identification of some *Salmonella* effector proteins. For example, AvrA is a T3SS-1 translocated effector that shares sequence similarity with YopJ of the animal pathogen *Yersinia pseudo-tuberculosis* and AvrRxv of the plant pathogen *Xanthomonas campestris* pv. *vesicatoria*<sup>111</sup>. Also, SptP shares sequence similarity with both bacterial and eukaryotic tyrosine phosphatases and was shown to possess potent tyrosine phosphatase activity<sup>112</sup>. However, many effector proteins share little to no amino acid sequence similarity compared to other effector proteins or to eukaryotic host cell proteins<sup>113</sup>, therefore alignment methods based on sequence are often not successful in determining potential functions for newly identified effector proteins. Though effector proteins do not share similar sequences with host cell factors, they often do mimic the structure of host cell factors whose function is emulated<sup>71,114</sup>. However, structural studies can often be challenging and time consuming as proteins must be stable and amenable to purification. For these reasons only a few *Salmonella* effector proteins have been structurally characterized. Though sequence and structure based studies are an extremely useful component in characterizing effector proteins and elucidating how they may function, these methods do not reveal information on

how, when, or why an effector protein performs influence on the infection process. Therefore, other methods aside from sequence and structure profiling to probe effector protein function during infection are highly valuable.

### ***Detection of translocation***

To detect whether a putative effector protein is indeed translocated into a host cell, the calmodulin-dependent adenylate cyclase (Cya) domain (derived from the cyclolysin toxin from *Bordetella pertussis*) is routinely used as a reporter<sup>115</sup>. This reporter assay works by fusing the N-terminal portion of an effector protein to Cya. If bacteria translocate the resulting effector-Cya hybrid protein into the cytosol of host cells, it will bind to calmodulin and produce a detectable accumulation of cyclic AMP (cAMP) from ATP. Because bacteria do not possess calmodulin, Cya is not active prior to translocation and it is not naturally translocated by the T3SSs. The Cya system is widely exploited to report on the translocation of effector proteins, however this system relies on measurements of transient and reversible modifications to host cell levels of cyclic AMP which necessitates previous knowledge on the time frame within which protein translocation will occur. Additionally, this method is limited in that it can only detect whether or not an effector protein is translocated into the host and is unable to address details of translocation kinetics, location, or expression over time.

To address this limitation for use with new putative effector proteins, another method based on the use of the bacteriophage P1 Cre-Lox system was generated to report on effector protein translocation<sup>116</sup>. This Cre system was used to demonstrate the T3SS-1 dependent translocation of *Salmonella* effector protein SopE<sup>116</sup>. The first 104 amino acids of SopE were fused to the full length Cre recombinase and translocation was assessed by Cre mediated excision of intervening sequences on a firefly luciferase or green fluorescent protein (GFP) reporter expressed within the host cell.

Another approach for detecting effector protein translocation uses a  $\beta$ -lactamase/CCF2 based reporter system<sup>117</sup>. This approach involves fusion of  $\beta$ -lactamase to an effector protein of interest and the introduction of a freely diffusing dye (CCF2) that undergoes a color-change upon hydrolytic cleavage by  $\beta$ -lactamase into the host cell. Pretreatment of mammalian cells with CCF2 prior to infection enables the system to report on the delivery of effector proteins into the host cytosol upon infection due to the different color of the cleavage product.

### ***Methods to assess a role in virulence***

Once the translocation of an effector protein has been established, it is important to assess whether it has an impact on the infection process. One commonly used technique to assess whether an effector protein plays a role in virulence, is to infect cells or model organisms with strains of *Salmonella* lacking the effector protein. Such studies seek to define and determine changes to infection phenotypes compared to the wild type strain in order to gain insight into an effector protein's function during infection. These differences may include the level of *Salmonella* invasiveness, the ability for bacteria to replicate, persist and disseminate within an organism or cell, or more specific features of infection at the cellular level such as perturbation of cellular organelles, location of the SCV or bacteria within the host cell and host inflammatory responses. One of the hallmarks of successful *Salmonella* infection in a mouse model is a persistent infection that breaches the small intestine and spreads to other organs. A primary method used to examine the role of an effector protein in virulence during a mouse model of infection is called a competitive index (CI) assay. In a CI assay, strains of *Salmonella* expressing the effector protein of interest are pitted against strains lacking the effector protein, and both strains are used simultaneously to infect a live mouse<sup>118</sup>. Infected mice are sacrificed at 2-4 days post infection and organs are examined for the presence of *Salmonella* by colony forming units (CFUs). For CFU assessment, the organ lysate is plated on agar with appropriate antibiotics for each strain and incubated for bacterial growth. The number of colonies recovered

is proportional to the bacterial load at a particular time point and is indicative of each strain's invasion or replication ability<sup>119</sup>. The CFU results are used to indicate which strain fared better within the mouse and reveal whether or not the effector protein had an impact on infection efficiency<sup>118</sup>. The CI/CFU assay is an instrumental starting point for investigating the role of an effector protein during infection. By incorporating a time parameter, the CFU approach can also be used to differentiate between a role in promoting invasion or replication, as both of these mechanisms of an effector protein allow for the increase of bacterial load within cells. Cells or tissues assessed at 1 to 2 hours post infection reveal invasion efficiency<sup>101,120</sup>, whereas 6 to 22 hours post infection are used to indicate replication efficiency<sup>70,84,96</sup>.

Although the CFU assay is useful in establishing whether an effector protein has a role in promoting *Salmonella* virulence, it fails to show invasion or replication on the single cell level and can therefore mask cell-to-cell heterogeneity. To overcome this, there are other methods available to examine invasiveness or replicative ability on the single cell level. For example, a differential “inside/outside” immunostaining method<sup>121,122</sup> can be used to determine invasion efficiencies. For the inside/outside assay, cells are fixed with paraformaldehyde at discrete time points post infection (often 15 minutes to 1 hour). The extracellular bacteria are stained using fluorescently labeled antibodies prior to host cell permeabilization. Following membrane permeabilization, host cell markers and internalized bacteria may be labeled with differently colored probes. Thus, upon visualization of infected cells using fluorescence microscopy, extracellular bacteria may be enumerated as they are clearly differentiated from intracellular bacteria and the internalization efficiency of mutant strains can be scored<sup>34,123,124</sup>.

### ***Methods to monitor intracellular bacterial replication verses persistence:***

Intracellular bacteria can proliferate, persist or be subjected to killing over the course of infection and these processes are difficult to distinguish. The fate of bacteria is often assessed through CI/CFU assays that determine net bacterial load, which is the product of both replication

and death undergone by the population. However, this measurement of net bacterial load does not reveal heterogeneity within bacterial populations. This distinction has been shown to be particularly important in persistent infections in which slow or nongrowing bacteria are thought to have a major impact<sup>125</sup>.

To address the heterogeneity of intracellular bacterial populations Helaine *et al.*<sup>125</sup> developed a reporter system based on fluorescence dilution that enables direct quantification of the replication dynamics of *Salmonella* at both the population and single-cell level. This dual fluorescence reporter functions by measuring a preformed pool of arabinose induced DsRed protein in replicating bacteria also expressing EGFP constitutively or by isopropyl  $\beta$ -D-thiogalactoside (IPTG) induction. Upon each bacterial division event in the absence of arabinose, DsRed fluorescence signal intensity is halved. Therefore, as the bacterial population replicates DsRed fluorescence undergoes a signal dilution that can be monitored and which corresponds to the number of replications for up to ten generations. This approach identified that many bacteria internalized by macrophage cells do not replicate, but appear to enter a dormant-like state which could represent an important reservoir of persistent bacteria in the macrophage model of infection<sup>125</sup>.

Another single-cell method of tracking intracellular bacterial replication was developed by McQuate *et al.*<sup>126</sup> using long-term (17h) live-cell imaging of infected cells and subsequent image analysis methods. This image analysis pipeline approach was applied to track bacterial replication within the SCV in epithelial cells as well as to quantify vacuolar replication versus survival in macrophages. Consistent with Helaine *et al.*, this long-term imaging method revealed a persistent non-replicating population of *Salmonella* in macrophage. Additionally, the growth of replicating bacterial populations in both epithelial cells and macrophage cells were shown to be diverse and fell into three major categories of: (1) delayed initiation of growth, (2) steady growth that plateaued over time, or (3) consistent, steady growth. The role of the individual effector proteins SteA and SseG in impacting these growth parameters was shown to differ between

epithelial cells and macrophages, suggesting that effector proteins may play different roles in infection that depend on the type of host cell and/or the infection model (acute versus systemic infection)<sup>126</sup>.

### ***Methods to visualize effector proteins in fixed host cells***

Approaches involving fixing and staining infected host cells or tissue slices at discrete time points post infection can be used to address the localization of effector proteins within the context of infection. Because these assays allow for the visualization of *Salmonella* within the host cell in relation to effector proteins or host cell markers, they have the potential to provide information about effector protein functions during infection. For example, the effector protein SopB was shown to promote membrane fusion following invasion through the hydrolysis of PI(4,5)P<sub>2</sub> and a localization at the host cell membrane local to ruffling events<sup>35,36</sup>. At later stages in infection SopB relocates from the plasma membrane to the SCV, which helps explain another role for SopB in promoting SCV maturation and tubule formation through the recruitment of Rab5 and PI3P accumulation on the SCV<sup>28</sup>. Defining the localization of effector proteins within the host cell at different stages of infection is important for elucidating how the pathogen manipulates host cell processes in different subcellular regions.

Visualization techniques based on immunofluorescence use fluorescently conjugated antibodies coupled with the expression of epitope tagged effector proteins. Such approaches typically involve expression of an epitope tagged version of the effector protein of interest as there are very few antibodies against individual effector proteins available. Studies based on immunofluorescence have shown that SCV associated filaments are diverse and vary in the presence of host cell markers and effector proteins that colocalize to individual filament extensions<sup>61</sup>. Immunofluorescence has also been essential for defining the involvement of specific effector proteins in established *Salmonella* infection phenotypes such as the roles of SopB in the recruitment of sorting nexin-1 to the SCV<sup>127</sup>, SifA, SseJ, SseG, and SseF in tubule

formation<sup>67,78,83</sup>, the role of SptP in allowing *Salmonella* to spread between organs within the mouse<sup>128</sup>, the role of SPI-1 (but not SPI-2) in promoting escape from the SCV<sup>129</sup>, and the roles of SifA, SseJ, and SopD2 in SCV membrane integrity<sup>69,71</sup>.

Another approach for visualizing effector proteins, both within the bacteria prior to translocation as well as within the host cell after translocation, is the FIAsh/tetracysteine labeling system<sup>26,130</sup>. This system uses the fluorescein-based biarsenical dye (FIAsh), which binds a 15 amino acid tetracysteine motif that can be appended to an effector protein for detection. The unbound FIAsh dye is weakly fluorescent and undergoes a large increase in fluorescence signal upon coordination to the tetracysteine motif<sup>131</sup>. The FIAsh labeling system was used to show that the *Shigella flexneri* T3SS effector proteins IpaB and IpaC localize to actin foci at invasion sites in fixed cells<sup>130</sup>.

These approaches for visualizing effector proteins in fixed cells are powerful tools for revealing spatial relationships between *Salmonella*, effector proteins and the host environment. However, isolated snap shots can misrepresent or fail to capture complex dynamic phenotypes including the dispersion and coalescence of the SCV over the course of infection<sup>126</sup>. Furthermore, cell fixation has been shown to significantly alter infection phenotypes, such as the integrity of the membrane that composes SCV filaments<sup>132</sup>. Thus there is a growing need to develop new tools that capture and highlight effector protein localization in live infected cells in order to unravel specific effector protein roles in a spatial and temporal context of infection while preserving cell-to-cell heterogeneity.

### ***Live cell techniques to visualize effector proteins***

Live cell imaging approaches allow for the observation of cellular events unfolding in real time, and are therefore desirable for elucidating dynamic processes. However, monitoring bacterial effector proteins during the infection of live cells is technically challenging due to the mechanism of effector protein translocation through the T3SS into the host cell. Effector

proteins are escorted and unfolded by chaperones in the bacterial cytosol in order to be threaded through the needle-like T3SS translocon for transport into the host cell, where the effectors are then refolded following delivery into the host cytosol<sup>133,134</sup>. This process of threading through the translocon is incompatible with fluorescent protein (FP) tagging due to the high thermodynamic stability of FPs<sup>135</sup>. Therefore, tagging and visualizing T3SS translocated bacterial effector proteins during live cell infections must use alternate approaches. Several established techniques rely on small affinity tags that label an effector protein within bacteria coupled with complementary components that are either introduced to the bacteria or to a host cell to generate a fluorescent label when the two components join together.

Though previously mentioned for use in visualizing effector proteins in fixed cells, FIAsH has also been used for live cell imaging. The FIAsH labeling system was used to visualize real time effector protein translocation into host cells upon infection by monitoring the depletion of effectors from the bacterial cytosol<sup>26,130</sup>. This technique was used to demonstrate that two *Salmonella* effector proteins, SopE2 and SptP, exhibit different secretion kinetics<sup>26</sup>. Additionally, because this system involves a physically tethered fluorescent label, it can be used to monitor effector proteins before and throughout the translocation process. However, poor signal to noise limits the use of this system in visualizing diffuse effector protein populations in live host cells.

Another system that is capable of monitoring the fate of translocated effector proteins within living host cells during infection uses a light-oxygen-voltage-sensing (LOV) domain. When conjugated to an effector protein of interest the LOV-domain functions as a reporter that binds to cellular flavin mononucleotides to produce a fluorescent tag. This LOV-domain technology has been used to monitor real time effector protein expression and translocation, as well as to track effector localization upon introduction into the host cell<sup>136,137</sup>. The-LOV domain reporter system remains ideal for capturing these early events in infection and was used to track the *Shigella flexneri* effector protein IpaB, which was shown to localize preferentially at bacterial poles before rapid translocation and final localization at the bacterial entry site within membrane ruffles<sup>137</sup>.

However, with a relatively low quantum yield (0.2-0.4)<sup>138</sup>, the LOV-domain reporter may not be ideal for visualizing all effector proteins because some *Salmonella* effectors have been shown to express and translocate at low levels<sup>139</sup>. The only other approach currently available for visualizing translocated effector protein localization within the host cell is based on fluorescence complementation using the split-GFP system<sup>103</sup>. The current methods discussed in the sections above for assessing effector protein roles during infection are listed in Figure 1.4.

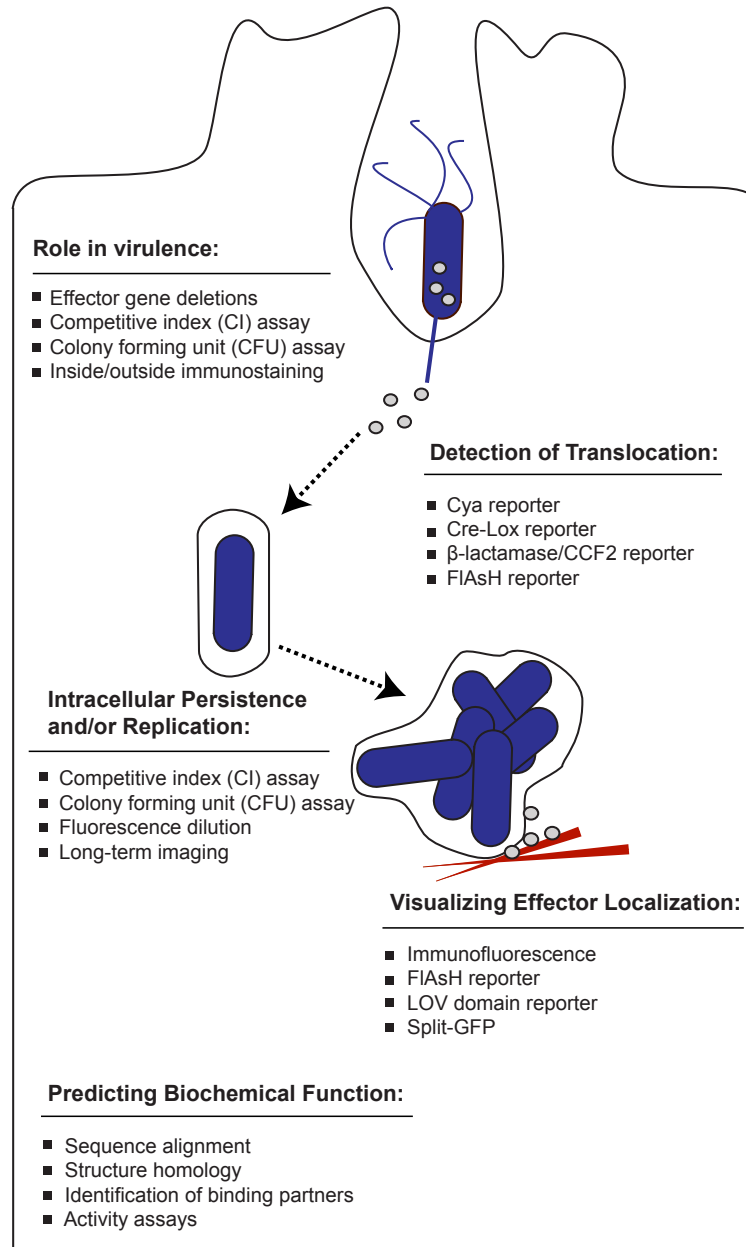


**Figure 1.4. Outline of methods used to study effector protein roles in infection**

The techniques discussed in this chapter for assessing effector protein roles in infection are listed under the different method category headings. *Salmonella* are shown as dark blue rods and effector proteins are shown as small grey circles. The red lines represent actin nests localized to the mature SCV.

### **Split-GFP labeling**

Split-GFP is composed of two fragments of the GFP  $\beta$ -barrel that were engineered to be stable, soluble and non-fluorescent in isolation and to combine spontaneously and irreversibly to form the GFP chromophore and recapitulate GFP fluorescence (GFP<sub>comp</sub>)<sup>140</sup> (Figure 1.5). To exploit the split GFP system for effector protein tagging, the small 13-amino-acid 11th strand of the GFP  $\beta$ -barrel (GFP11) is genetically fused to *Salmonella* effector proteins. The complementary strands of GFP (GFP1–10) are expressed *in trans* in the host cell prior to infection and upon challenge with *Salmonella* and T3SS effector translocation, spontaneous complementation of the two split-GFP fragments results in fluorescent tagging and visualization of the effector population within the host cell<sup>103</sup>.

The split-GFP labeling system is best suited for visualization of effector proteins at later time points post infection (from 2 hrs to 24+ hrs) due to the time required for fluorescence complementation<sup>141</sup>. The original split-GFP system was therefore adapted for labeling T3SS-2 effectors. This approach enabled the visualization of *Salmonella* effector proteins SteA, SteC and PipB2 in epithelial cells, and PipB2 in the macrophage cell line RAW264.7, illustrating the usefulness of split-GFP in tagging diverse T3SS effectors and tracking effector populations in live host cells over time<sup>103</sup>.

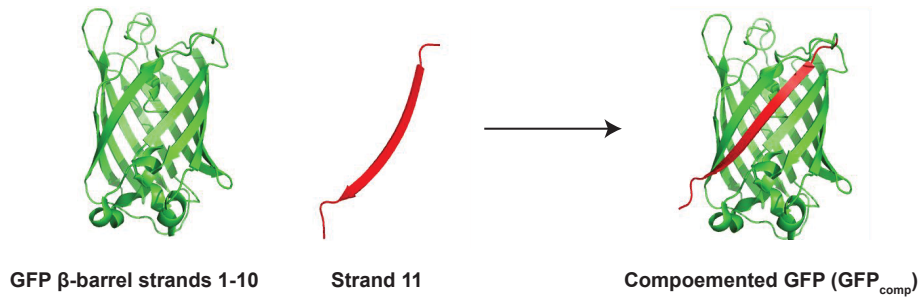


### Figure 1.5. The split-GFP system

The split-GFP system is composed of GFP β-barrel strands 1-10 and GFP β-barrel strand 11 which are not fluorescent. When the two split components are introduced they are able to combine and form a complemented version of the full fluorescent GFP protein (GFP<sub>comp</sub>).

However, we encountered limitations with this original system when we were unable to detect a number of new effector proteins, including SopA, SseF, SseG and SlrP, under their endogenous promoters. There are a number of possible explanations for the failure of the split-GFP system in detection of these effectors. For example, some effector protein promoter regions are not well defined and the boundaries are difficult to predict. This is especially true for effector proteins encoded within operons, such as SseG and SseF. Therefore, the attempted expression of any of our new effector targets may have been under incorrectly selected promoter regions. Alternatively, the endogenous promoters could have been too weak to express detectable levels of labeled effectors within the host cell using split-GFP. We could not easily determine whether this issue was due to low expression and low fluorescence signal verses another issue such as inability to undergo fluorescence complementation in the host cytosol, or rapid protein turnover in the host cell.

## 1.6 DEVELOPMENT OF A NEW MODULAR SPLIT-GFP LABELING PLATFORM

This thesis work was focused on expanding the utility of the split-GFP labeling system<sup>103</sup> for visualizing translocated *Salmonella* effector proteins during the infection of live cells. A new modular labeling platform was developed to facilitate facile tagging and evaluation of split-GFP complementation signal intensities for different effector proteins using a suite of expression approaches. This new platform enables amplification of split-GFP complementation signals by driving the expression of labeled effector proteins under the control of a generic promoter or by multimerizing the GFP11 tag. In addition, I developed a new assay to test the expression and split-GFP complementation efficiencies of labeled effector proteins in bacteria prior to carrying out invasions of host cells. With these techniques to verify and amplify signal split-GFP, I was able to visualize three effector proteins, SseF, SseG and SlrP, during live infections for the first time. These results revealed that the localization of SseG is influenced by the presence of SseF and that the C-terminus of SlrP is absent in the ER but maintained in the cytosol of the host cell throughout infection. Finally, this new labeling system was applied to primary bone marrow derived macrophages (BMDMs) from immunocompetent mice and demonstrated visualization of effector proteins in this model of infection for the first time.

## CHAPTER 2

### FLUORESCENCE COMPLEMENTATION PLATFORM FOR VISUALIZING *SALMONELLA* EFFECTOR PROTEINS BY LIVE CELL MICROSCOPY

Alexandra M. Young, Michael Minson, Sarah E. McQuate, Amy E. Palmer

Department of Chemistry and Biochemistry, BioFrontiers Institute,  
UCB 596, University of Colorado Boulder

#### 2.1 INTRODUCTION

Visualizing the host-pathogen interface between *Salmonella* and infected mammalian cells is a key step in unraveling the complex dynamics of infection biology. *Salmonella* is a food born Gram-negative bacterial pathogen that consists of multiple subspecies and over 2,400 serovars<sup>142</sup>. *Salmonella enterica* serovar Typhimurium (*S. Typhimurium*) infects a range of animal hosts, including humans, and is a major cause of enteric illness. *S. Typhimurium* is equipped with complex nanomachines, called Type III Secretion Systems (T3SSs) that function as injectisomes, spanning both bacterial membranes and penetrating the membrane of a host cell to inject bacterial proteins, also called effector proteins, directly into the host cytosol<sup>143-146</sup>. The cocktail of translocated bacterial effector proteins provides *S. Typhimurium* with a powerful virulence mechanism that interrupts and manipulates host-signaling cascades to influence host cellular processes for the benefit of the bacteria. These processes include regulating actin dynamics to facilitate bacterial internalization, manipulating molecular motors, commandeering endocytic trafficking to establish and maintain an intracellular replicative niche called the *Salmonella* containing vacuole (SCV), evading phagosomal-lysosomal fusion, controlling apoptotic pathways, and manipulating host cell immune signaling (Reviewed in<sup>19,21,28,147-149</sup>). *S. Typhimurium* has two distinct T3SSs called T3SS-1 and T3SS-2. T3SS-1 is expressed upon

contact with epithelial host cells and T3SS-1 translocated effector proteins are important for bacterial internalization and establishing the SCV<sup>150,151</sup>. T3SS-2 is expressed at later stages of the infection process and T3SS-2 translocated effector proteins are important for the maturation and maintenance of the SCV as well as for interfering with host cell immune responses<sup>152,153</sup>. The coordinated activity of effector proteins is crucial to bacterial survival, replication and dissemination within a host organism. However, the distinct functions of many effector proteins necessary for *Salmonella* infection are not yet fully understood. Defining the localization of effector proteins within the host cell at different stages of infection is important for elucidating how the pathogen manipulates host cell processes in different subcellular regions. Spatiotemporal information about an effector protein's localization in the context of infection can highlight that protein's role in the infection process. We therefore set out to expand upon the tools available for visualizing *S. Typhimurium* effector proteins in living host cells.

Live cell imaging is important for defining the dynamic interface between a pathogen and a host. Cell fixation has been shown to significantly alter infection phenotypes, such as the integrity of membrane tubules that emanate from the SCV<sup>132</sup>. Static snap shots of dynamic processes can fail to capture or misrepresent phenotypes. An example of this is the dispersion and coalescence of the SCV at different stages of infection<sup>126</sup>. Moreover, *Salmonella* infections display heterogeneity at the single cell level. For example, *Salmonella* can use different mechanisms to invade individual epithelial cells, employing either a T3SS-1 effector protein mediated trigger mechanism, or an outer membrane protein facilitated zipper mechanism, which activate different host cell signaling pathways to facilitate bacterial entry<sup>43,44,50,154-160</sup>. Additionally, *Salmonella* has been shown to have a bimodal lifestyle in epithelial cells, where bacteria can survive and replicate in the vacuolar environment of the SCV or can escape and hyper-replicate in the cytosol<sup>70,126,129,160-165</sup>. The two bacterial populations differentially express the genes that code for T3SS-1, T3SS-2 and flagella<sup>129,166</sup>. Collectively, these cell-to-cell variations in infection phenotypes are likely due, at least in part, to the differential presence and

function of effector proteins<sup>19</sup>, driving efforts to develop techniques that capture and highlight effector protein localization and infection phenotypes, while preserving single cell heterogeneity.

While live cell imaging approaches are widely sought after, monitoring bacterial effector proteins during live cell infections is technically challenging due to the mechanism of T3SS translocation. Effector proteins must be unfolded by chaperones in the bacterial cytosol, threaded through the needle-like T3SS, and refolded upon translocation into the host<sup>133,134,144,167</sup>. The threading method of translocation is incompatible with fluorescent protein (FP) tagging due to the large size and high thermodynamic stability of FPs<sup>135</sup>. Therefore, techniques geared toward visualizing T3SS translocated bacterial effector proteins during live cell infections must use alternate approaches. The techniques currently established have used fluorescence complementation where small affinity tags that label an effector protein within bacteria are coupled with complementary components that are either introduced to the bacteria or to a host cell to generate a fluorescent label when the two components join together.

Different methods have been developed to facilitate visualization of different aspects of the infection process, including detection of effectors within bacteria prior to and throughout the process of translocation, identification of the appearance of bacterial effectors in the host cytosol, and visualization of effector protein localization within the host cell. Fluorescence based techniques to visualize the presence of effector proteins in bacteria and translocation into host cells include a  $\beta$ -lactamase/CCF2 reporter system<sup>117,168</sup> and the FIAsh/tetracysteine system<sup>26,130</sup>. The  $\beta$ -lactamase/CCF2 reporter system involves fusion of  $\beta$ -lactamase to an effector protein of interest and introduction of a freely diffusing dye (CCF2) that undergoes a color-change upon cleavage by  $\beta$ -lactamase. If CCF2 is delivered to the mammalian cell, the system reports on the delivery of effector proteins to the host cytosol, although it doesn't permit identification of effector localization because the dye is not physically tethered to the effector protein. The FIAsh/tetracysteine labeling system uses the fluorescein-based biarsenical dye

(FIAsH) that binds a 15 amino acid tetracysteine-motif appended to an effector protein to detect labeled effector proteins. The system was used visualize effector translocation into host cells by monitoring the depleting bacterial population and presence of effector proteins within fixed host cells<sup>26,130</sup>, but poor signal to noise prevented visualization of effector dynamics within host cells.

Currently, the fluorescent reporters capable of monitoring the fate of translocated effector proteins within living host cells during infection are limited to a light-oxygen-voltage-sensing (LOV) domain reporter system that binds to cellular flavin mononucleotides to produce a fluorescent label and a split-GFP system. The LOV-domain technology has been used to monitor real time effector protein expression, translocation and host cell localization<sup>136,137</sup>, however the fluorescence signal was found to be low compared to split-GFP<sup>103</sup>.

In this study we expanded the utility of split-GFP labeling<sup>103</sup> by developing a platform that permits facile tagging and evaluation of complementation signal intensities of different effector proteins using a suite of expression approaches. This platform enables amplification of split-GFP complementation signals by driving their expression with a generic promoter or multimerizing the GFP11 tag. Using this platform we visualized SseF, SseG and SlrP during live infections for the first time, revealing that the localization of SseG is influenced by the presence of SseF and that the C-terminus of SlrP is absent in the ER but is maintained in the cytosol of the host cell throughout infection. Finally, we applied this system to primary bone marrow derived macrophages (BMDMs) from immunocompetent mice demonstrating visualization of effector proteins in this niche for the first time.

## 2.2 RESULTS

### Split-GFP labeling platform to visualize translocated effector proteins in live host cells

To facilitate visualization of *Salmonella* effector proteins during infection of live cells a modular expression platform was generated. The plasmid-based platform features an exchangeable promoter region, effector, and a GFP11 tag as well as a constitutively expressed fluorescent protein (FP) that serves as a bacterial marker (Fig. 2.1A). Each feature of the platform can be exchanged by standard molecular cloning techniques (Fig. 2). The pACYC177 plasmid was chosen as the backbone because unlike pAYCY184, pWSK29 or plasmids derived from pBR322, it doesn't interfere with growth or pathogenicity when expressed in *Salmonella*<sup>169,170</sup>. For each effector tested, a pair of plasmids was created, one that expressed the effector under the control of its endogenous promoter, and another that used a generic promoter. The promoter for the *Salmonella* effector protein *steA* was chosen as a generic promoter because SteA was previously shown to express at a level sufficient for visualization with split-GFP<sup>103</sup>. Additionally, SteA is expressed and translocated under both SPI-1 and SPI-2 inducing conditions, suggesting that its regulatory region would be useful in visualizing T3SS-1 or T3SS-2 translocated effectors. The use of a generic promoter was prompted by the fact that promoter boundaries of uncharacterized effector proteins may be difficult to accurately predict and some effector proteins are expressed at low levels, limiting visualization with split-GFP.

### Measuring effector protein expression and split-GFP complementation in bacteria

We developed a method to test effector protein expression and split-GFP complementation within bacteria as an early test for new targets of our labeling system (Fig. 2.3A). This assay enables comparison of effector protein expression levels under a variety of different conditions to identify the best approach for visualization of effectors in the context of infection. For example, we can compare the intensity of the complementation signal for an effector that is expressed under control of the generic *steA* promoter versus plasmid-based expression under

its endogenous promoter versus expression from its endogenous locus upon integration of the tag into the chromosome. Once complemented, mature GFP is unable to translocate through the T3SS apparatus<sup>135</sup> and therefore remains within the bacteria, prohibiting the fluorescence signal decay from effector translocation and providing a consistent signal representing the accumulating effector protein population within the bacteria. For the bacterial expression assay, all *Salmonella* strains expressing an effector tagged with GFP11 were co-transformed with GFP1-10 produced from a separate plasmid. Transformants were selected with chloramphenicol and GFP1-10 presence was verified by colony PCR for all strains. Arabinose induced GFP1-10 expression and split-GFP complementation within *Salmonella* was compared to SteA-GFP11 as a positive control. The GFP<sub>comp</sub> signal intensity was quantified in individual bacteria and used as a measure of effector protein expression and split-GFP complementation prior to application with host cell infections (Fig. 2.3B).

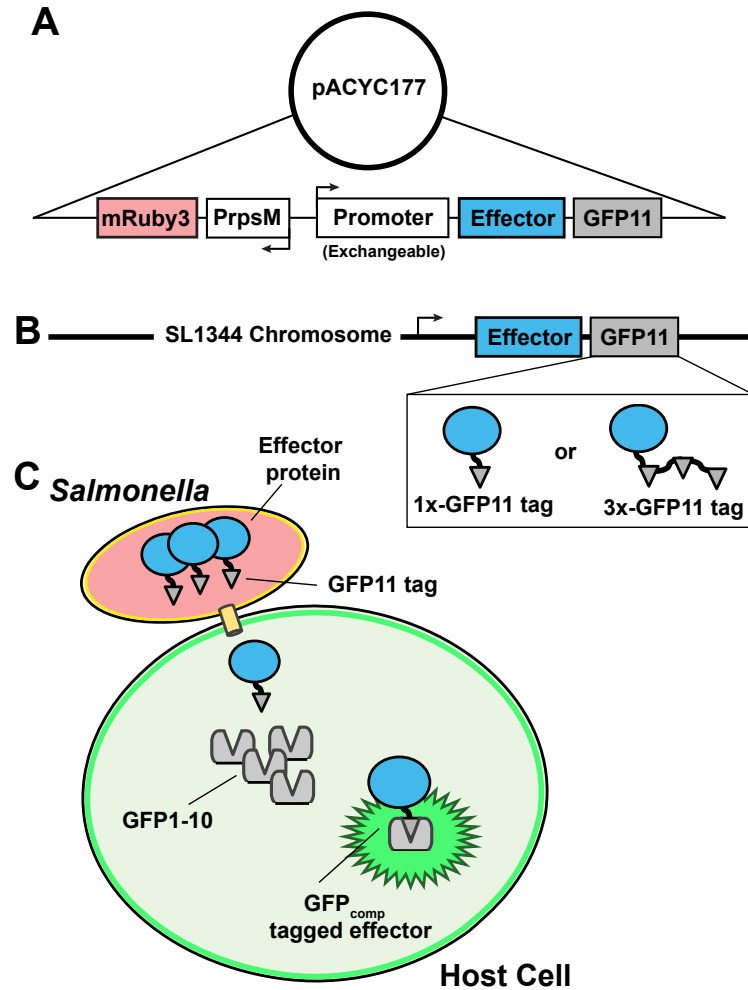


**Figure 2.1. Platforms for labeling *Salmonella* effector proteins with split-GFP**

(A) The plasmid based effector protein-labeling platform with exchangeable promoters, effectors, and tags including a constitutive mRuby bacterial marker. (B) Chromosomally integrated effector-labeling using 1X-GFP11 or 3X-GFP11 tags. (C) Split-GFP effector protein-labeling to fluorescently tag and visualize effector proteins during infections of live host cells.

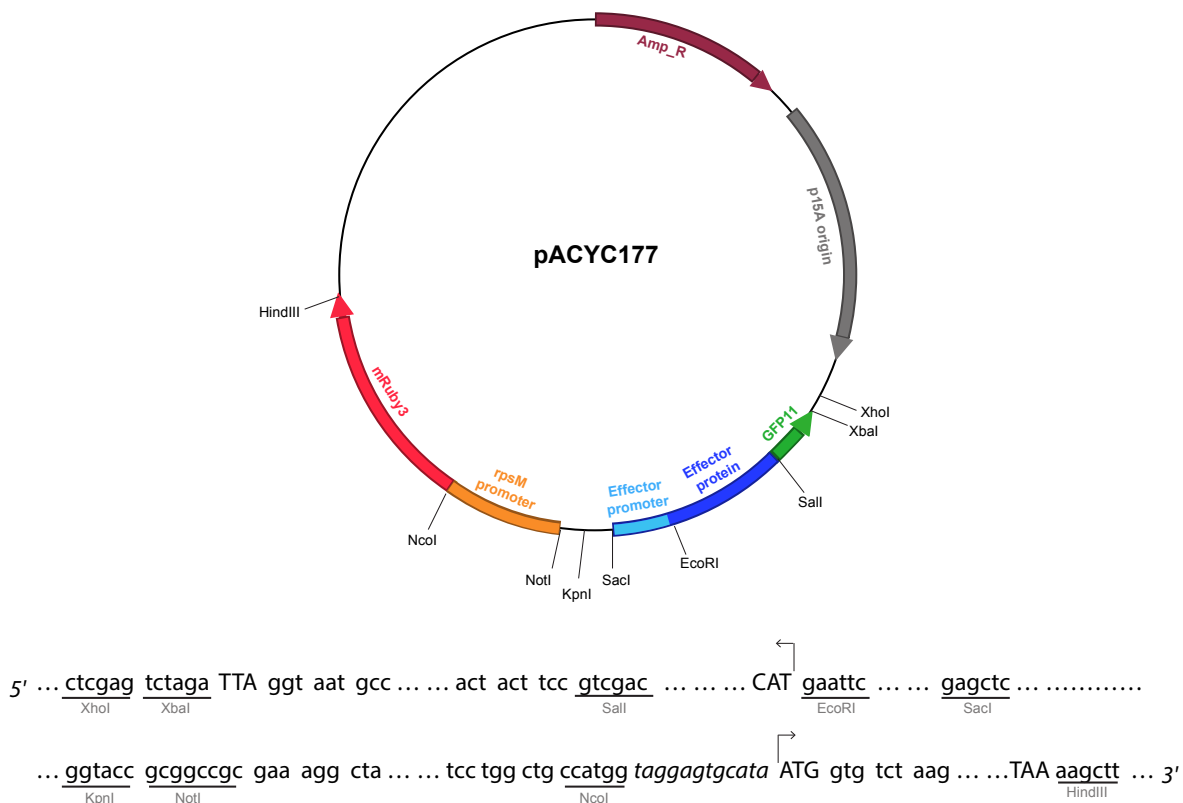


**Figure 2.2. Cloning layout of the pACYC plasmid based GFP11 effector protein labeling platform**

The plasmid-based effector protein labeling platform with exchangeable promoters, effectors, and tags including a constitutively expressed mRuby3 bacterial marker was made modular with restriction cloning sites. Encoded on the reverse complement strand, the effector protein promoter region is flanked by *SacI* and *EcoRI*, immediately followed by the effector protein region, and finally the in frame GFP11 tag which is flanked by *Sall* and *XbaI*. Driven by the *rpsM* promoter, the mRuby3 bacterial marker is encoded in the forward direction flanked by *NcoI* and *HindIII*. The reading frame context for cloning sites are depicted below the plasmid map, shown in the 5' to 3' direction. Restriction cloning sites are underlined and labeled, the initiation and termination codons are capitalized for easy detection, and the Shine-Dalgarno sequence used for mRuby3 expression is shown in italics.

Growth and expression conditions routinely used for SPI-1 and SPI-2 induction were adapted for use with split-GFP complementation as described in Experimental Methods. Induced bacteria were imaged at early stationary phase ( $OD_{600}$  0.5-0.6) and analyzed using ICY. Briefly, an automated region of interest (ROI) detector, guided by size and signal boundaries, was used to select and measure the fluorescence signal within individual bacteria. Each ROI represents a single bacterium. A negative control consisting of GFP1-10 alone, lacking the presence of GFP11, was used to define the signal intensity of positive GFP<sub>comp</sub> signals (Fig. 3C,D). Histograms of the GFP<sub>comp</sub> signal were used to define the intensity distributions for *Salmonella* populations expressing different effector proteins (Fig. 2.3, Fig. 2.4, Table 2.1).

We observed split-GFP complementation in bacteria for SteA, SlrP, SseF, SseG, and SopA when these effectors were expressed from a plasmid under control of the generic *steA* promoter (Figure 2.3C, Table 2.1). SteA has been tagged previously<sup>103</sup>, while the other four effectors have never been tagged with the split-GFP system and represent new targets for visualization during live cell infection. SteA, SlrP, SseF, and SseG all gave significantly higher split-GFP complementation signals when expressed under the *steA* promoter compared to endogenous promoters, suggesting that the *steA* promoter may be stronger than their endogenous promoters. Consistent with this notion, a previous study that used a firefly luciferase reporter system to quantitatively compare effector protein expression levels within bacteria as well as within infected host cells showed that SseG and SlrP express at very low levels compared to a handful of other SPI-2 encoded effectors<sup>139</sup>. SopA showed high split-GFP complementation signals that were comparable between endogenous and the *steA* promoter.

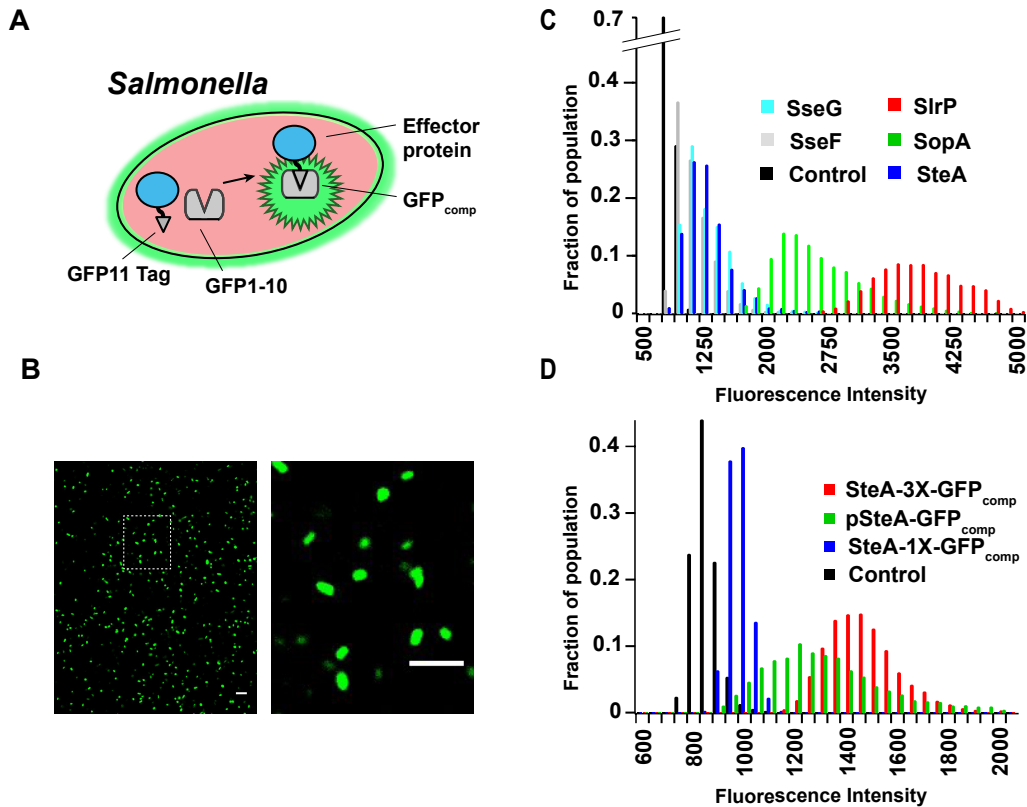


**Figure 2.3. Bacterial expression assay to validate effector protein expression and split-GFP complementation efficiencies**

(A) Chromosomally integrated or plasmid-based expression of GFP11-tagged effectors are expressed in bacteria alongside GFP1-10. The GFP<sub>comp</sub> fluorescence signal is used to report on effector protein expression efficiency. (B) Representative image of GFP<sub>comp</sub> fluorescence signal within bacteria used for automated ROI selection and analysis. Right image is a zoom in of box indicated by dashed line. (C) Representative effector protein expression and GFP-complementation levels for select bacterial strains using the plasmid based labeling platform. (D) The expression and GFP-complementation levels for SteA using chromosomal versus plasmid based labeling platforms. Results represent the pooled total of 3 biological replicates, including 4 technical replicates per condition,  $n_{\text{total}} \geq 1000$  bacteria (ROI) per condition.

Different effector proteins expressed under the *steA* promoter displayed a range of GFP<sub>comp</sub> signal intensities (Fig. 2.3C, Table 2.1). For example, SlrP-GFP<sub>comp</sub> signal intensities were three fold higher than SteA-GFP<sub>comp</sub>, suggesting that SlrP is produced at higher levels than SteA under the same promoter. It has been shown that different proteins expressed from the same promoter containing the same ribosomal binding site and 5' untranslated region may be expressed at different levels<sup>171-173</sup> as the mRNA secondary structure impacts mRNA stability and translation initiation rates due to accessibility of the ribosomal binding site<sup>174</sup>. Additionally, the nature and identity of codons at the N-terminus can alter the rate of translation, where rare codons are correlated with decreased structure and high expression levels<sup>175,176</sup>. According to RNA structural predictions using KineFold<sup>177</sup>, *slrP*, which gave the highest expression in our assay, has a less structured N-terminal coding region than the other effectors expressed under the *steA* promoter. Therefore, the variability in expression for different effector proteins under the *steA* promoter may result from a combination of codon bias and mRNA structure in the context of the *steA* regulatory region.

The intensity of the fluorescence signal varied based on whether the effector was expressed from a plasmid or the GFP11 tag was chromosomally integrated (Fig 2.3D, Table 2.1). As expected, for all effectors, split-GFP signal intensities were higher for plasmid-based expression. Fig 3D shows the data for plasmid-based expression of SteA (pSteA-GFP<sub>comp</sub>) versus chromosomal expression (SteA-1X-GFP<sub>comp</sub>). The data for other effectors are presented in Supplementary Figure 3. The intensity of the fluorescence signal could also be increased by including a 3-fold repeat of the GFP11 tag (Fig 2.2D, Table 2.1). The 3X-GFP11 tag was generated using synonymous codons and a 15 amino acid flexible linker as described in Kamiyama *et al.* 2016. All effectors showed an increase in complementation signal intensity for the 3X-GFP11 tag compared to 1X-GFP11 (Fig. 2.4). However, with the exception of SteA, the average signal for chromosomal expression with 1X-GFP<sub>comp</sub> was only slightly above background, which limited our ability to quantify the fold increase in signal upon GFP11

multimerization. SteA showed an increase in signal intensity that was approximately 3 fold, indicating near stoichiometric complementation.

<b>PLASMID EXPRESSION UNDER <i>steA</i> PROMOTER</b>			
<b>Promoter</b>	<b>Effector Protein</b>	<b>Expression</b>	<b>Visualization in Host Cell</b>
<i>steA</i>	SteA	++	Y
	SlrP	+++++	Y
	SseF	+	Y
	SseG	++	Y
	SopA	++++	N
<b>PLASMID EXPRESSION UNDER ENDOGENOUS PROMOTERS</b>			
<b>Promoter</b>	<b>Effector Protein</b>	<b>Expression</b>	<b>Visualization in Host Cell</b>
<i>slrP</i>	SlrP	+	N
<i>sseA</i>	SseF	+	Y
<i>sseA</i>	SseG	-	N
<i>sopA</i>	SopA	+++	N
<b>CHROMOSOMAL EXPRESSION</b>			
<b>Effector Protein</b>	<b>Tag</b>	<b>Expression</b>	<b>Visualization in Host Cell</b>
SteA	1x-GFP11	+	Y
	3x-GFP11	++++	Y
SlrP	1x-GFP11	-	N
	3x-GFP11	+	N
SseF	1x-GFP11	-	N
	3x-GFP11	-	N
SseG	1x-GFP11	-	N
	3x-GFP11	-	N

**Table 2.1. Comparison of bacterial expression assay and split-GFP complementation in infected host cells**

The bacterial expression assay from Figure 2D was quantified as follows: - represents no detection of fluorescence signal above the negative control, + is the major peak of fluorescence signal within a population is within 1 standard deviation of the negative control, +++ is within 3 standard deviations of the negative control and so on. Visualization within infected host cells was assessed for each condition between 4-24 hrs post infection, where Y indicates that effector-GFP<sub>comp</sub> signal was detectable above background, N indicates no detectable GFP<sub>comp</sub> signal.

## Visualization of effector proteins in live host cells

Visualization of effector proteins in the context of infection in host cells using the split-GFP system is influenced by a number of factors including effector protein expression level, T3SS translocation efficiency, the rate of effector protein turnover within the host cell, and accessibility of the C-terminal GFP11 tag to the host cytosol where GFP1-10 is localized. The bacterial expression assay allowed us to identify conditions for robust expression of effectors, with the highest expression generally observed for plasmid expression from the generic *steA* promoter. To visualize effectors in host cells upon infection we generated *Salmonella* strains expressing the mRuby3<sup>178</sup> fluorescent protein marker under control of the *rpsM* promoter, and harboring an isogenic deletion of the target effector protein. These strains were complemented by plasmid-based expression of a GFP11 tagged version of the effector. Growth of bacteria *in vitro* expressing effectors and the mRuby3 marker was not significantly different from wild type (Fig. 2.5).

Based on the bacterial expression assay, we anticipated being able to visualize SteA, SlrP, SseF, SseG, and SopA when expressed from a plasmid under control of the SteA promoter. Indeed, we observed all of these effectors except SopA upon live cell infection of HeLa cells (Table 2.1, Fig 2.6A). Cells were imaged beginning at 4 hours post infection, however the labeled effector proteins were not observed until approximately 7 hours post infection. SseF and SseG both localized to the SCV and associated filaments in live HeLa cells for the duration of 7-28 hours post infection, in agreement with previous immunofluorescence-based studies<sup>65,64</sup>. SseF and SseG containing filaments were highly dynamic and displayed an increase in effector-GFP<sub>comp</sub> signal over time, suggesting these effectors accumulate in the host cell over time (Fig. 2.7). SlrP was observed from 9-28 hours post infection and appeared diffuse in the cytosol of the host cell. This result agrees with a 2009 study that identified the cytosolic host cell protein thioredoxin as an interaction partner for SlrP<sup>109</sup>. Expressed under the *steA* promoter, SlrP-GFP<sub>comp</sub> signal appeared to increase in the host cell cytosol over time (Fig. 2.7).

To our knowledge, this is the first time that these three effector proteins have been visualized live, over time, in the context of infection.

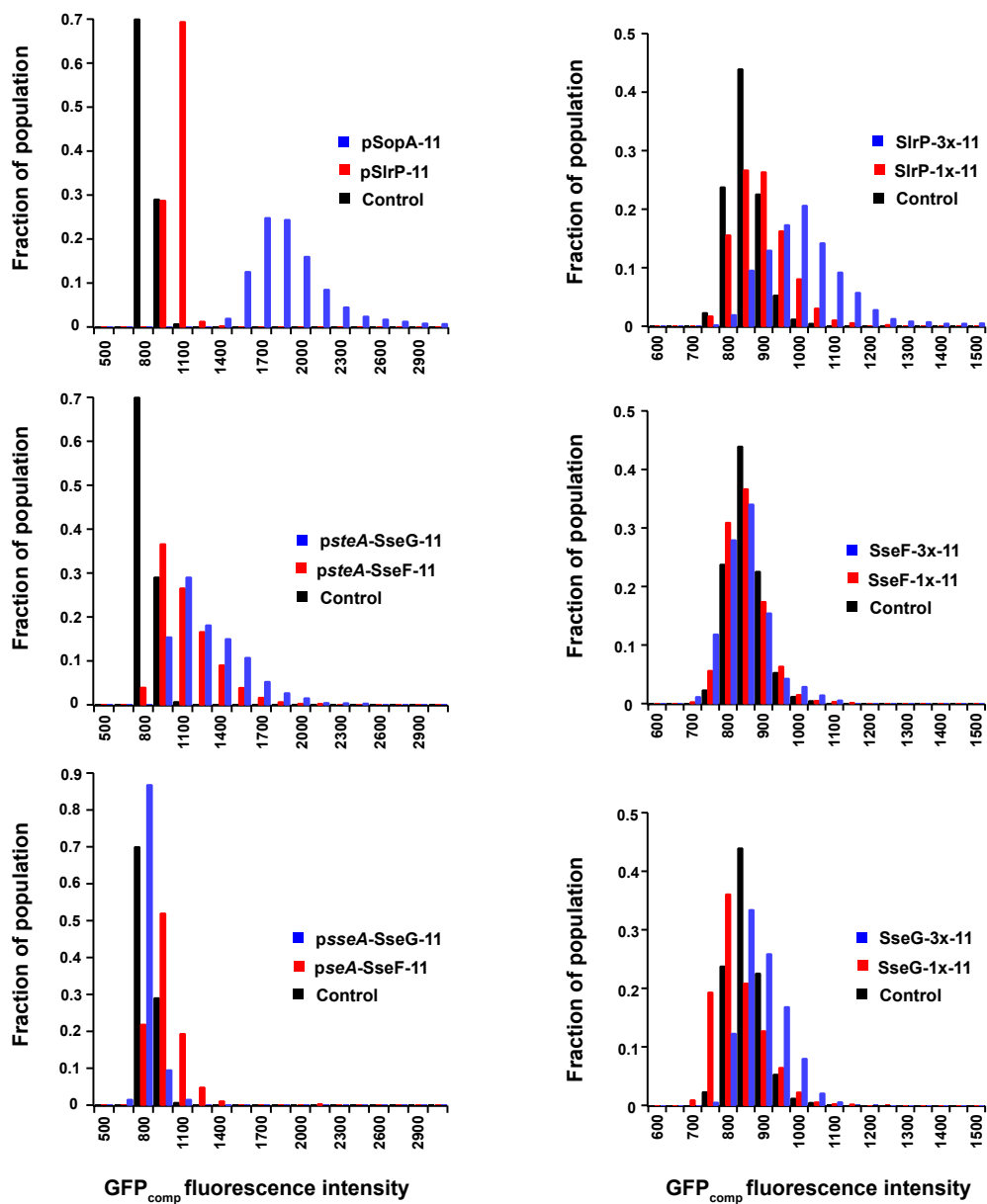


**Figure 2.4. GFP<sub>comp</sub> intensity profiles for effector proteins tested with the bacterial expression assay**

Comparison of the GFP<sub>comp</sub> signal intensity in individual bacteria for different expression paradigms to compare expression efficiency and complementation. Plasmid-based (left hand side) and chromosomally-integrated (right hand side) GFP11-tagged effectors are expressed alongside GFP1-10, which is expressed on a separate plasmid, within bacteria. SPI-1 or SPI-2 induction and bacterial imaging were accomplished as defined in Experimental Methods. All effector proteins were expressed under SPI-2 conditions, except for SopA, which is exclusively translocated through T3SS-1 and induced under SPI-1 conditions. Results represent the pooled total of 3 biological replicates, including 4 technical replicates each, per condition,  $n \geq 1000$  bacteria (ROI) per condition.

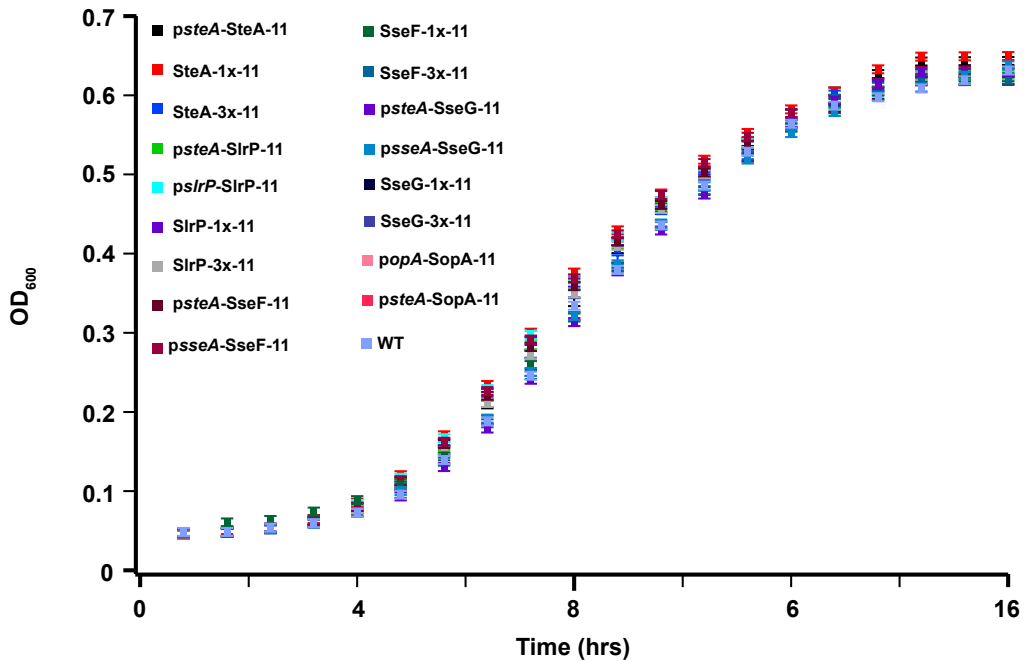


**Figure 2.5. In vitro growth curves of *Salmonella* strains used in this study**

*Salmonella* expressing GFP11-labeled effector proteins have no significant growth defects compared to WT *Salmonella* grown in LB. *Salmonella* strains were grown overnight in LB and then diluted 1:100 into fresh LB prior to measuring the OD600 value at time point 0. Values are the mean  $\pm$  the standard error of the mean ( $n = 3$  for all four different strains at each time point).

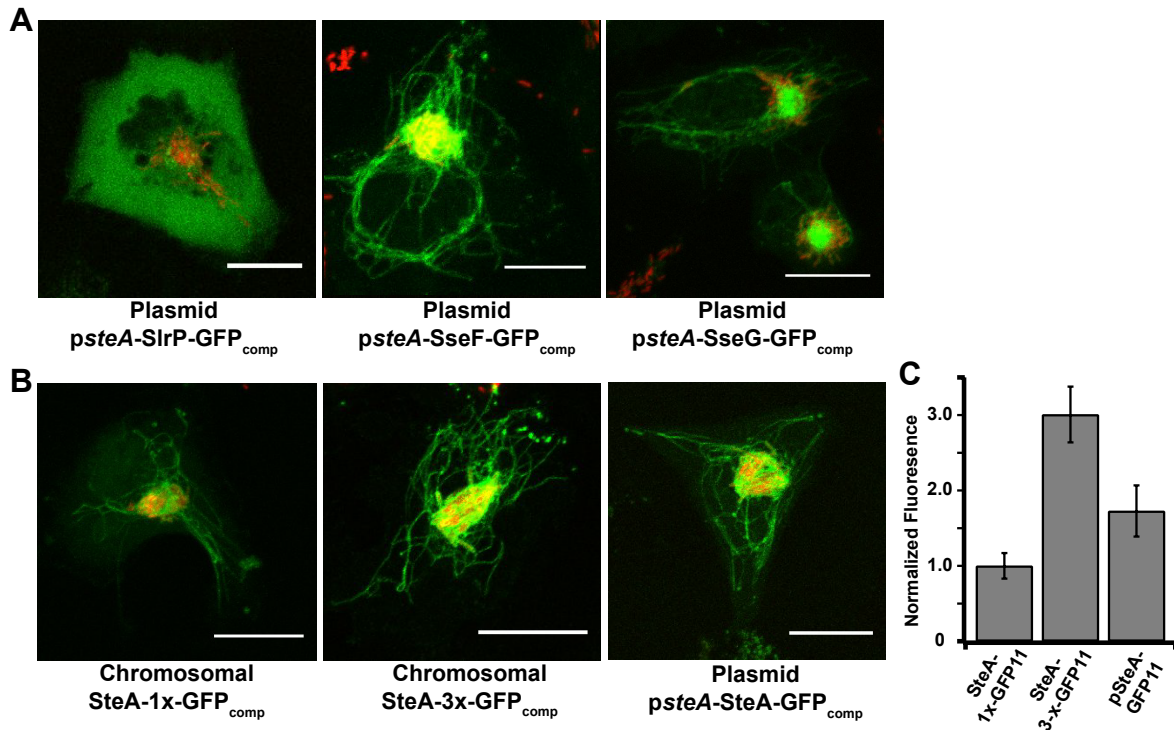


**Figure 2.6. Visualizing translocated effector proteins inside live host cells**

(A) The effector proteins SteA, SlrP, SseF, and SseG were expressed under the *steA* promoter for visualization in HeLa cells 16-20hrs post infection. Green is GFP<sub>comp</sub> labeled effectors and red is *Salmonella* constitutively expressing mRuby3. Scale bars represent 20µm. (B) Plasmid and chromosomal based expression of SteA-GFP<sub>comp</sub> or SteA-3xGFP<sub>comp</sub> is visualized in HeLa cells 18hr post infection. GFP fluorescence was acquired for all images using identical settings and all images are scaled to the same intensity. Scale bars represent 20µm. (C) Average fluorescence intensities of SCV localized SteA-GFP<sub>comp</sub> are compared for the plasmid based labeling platform for SteA-GFP11 versus chromosomal expression of SteA-1X-GFP11 and SteA-3X-GFP11. Fluorescence signal intensities are normalized to chromosomal SteA-1xGFP<sub>comp</sub>. n = 20 per condition. Error bars are SD.

SopA was the only effector that we readily visualized via the bacterial expression assay but were unable to observe in infected host cells between 4 and 28 hours post infection. The inability to detect translocated SopA could result from inefficient T3SS translocation of exogenously expressed SopA-GFP11, rapid turnover of SopA inside the host cell, or an unavailable C-terminal-GFP11 tag in the host cytosol for complementation with GFP1-10. Epitope-tagged SopA has been shown to localize to mitochondria<sup>46</sup> in fixed cells, but it has not yet been determined whether SopA associates with or resides within mitochondria.

As predicted from the bacterial expression assay, only SteA and SseF were detected when expressed from a plasmid with their endogenous promoters. SseF localization was consistent between endogenous or *steA* driven expression, with an increase in the detectable GFP<sub>comp</sub> signal for *steA* driven expression. The bacterial expression assay also allowed us to predict that the only effector likely to be observed under native transcriptional and translational regulation upon chromosomal integration of the GFP11 tag was SteA. Consistent with this prediction, SteA was the only chromosomally labeled effector protein successfully visualized within infected host cells. SseF, SseG and SirP are likely expressed too low under endogenous conditions for visualization within infected host cells with split-GFP. We found that multimerizing the GFP11 tag boosted the fluorescence signal in mammalian cells (Fig 2.6B,C). Finally, although chromosomal expression of SirP-3X-GFP<sub>comp</sub> and SteA-1X-GFP<sub>comp</sub> gave comparable split-GFP complementation efficiencies in the bacterial expression assay, we were not able to detect SirP-3X-GFP<sub>comp</sub> in infected cells. We speculate that this could result from the fact that SteA protein is concentrated on the SCV, while SirP is diffuse in the cytosol, leading to less contrast over the background fluorescence of cells.

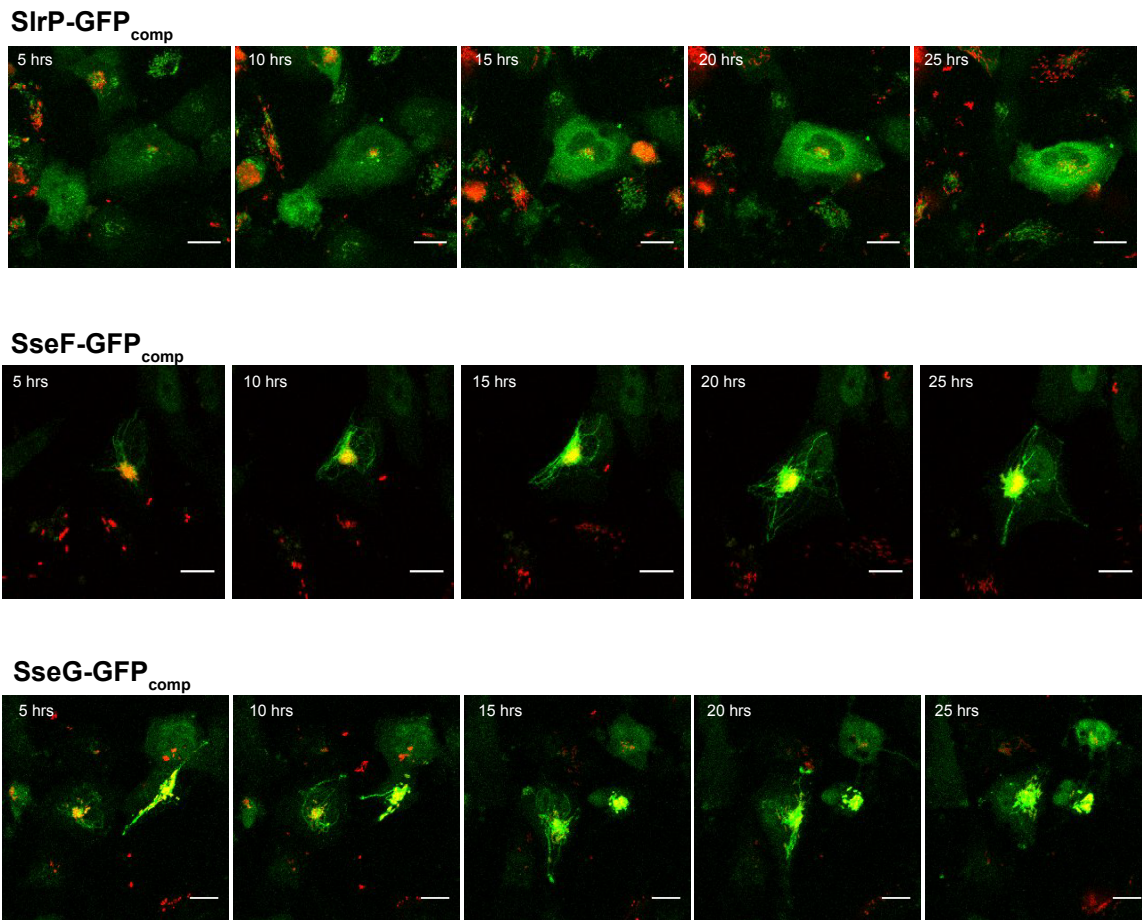


**Figure 2.7. Time course images for GFP<sub>comp</sub>-labeled effector proteins in infected HeLa cells**

Snap shots at distinct time points from long term imaging of live infections are represented to show the development of GFP<sub>comp</sub> signal for different labeled effector proteins over time. Images are overlay of red fluorescence (*Salmonella*) and green fluorescence (effector-GFP<sub>comp</sub>). All images for a given experiment are scaled to the same intensity range to permit direct comparison of relative brightness. Scale bars are 20  $\mu$ m.

## **SseG localization is mediated by SseF**

Given our ability to visualize SseG in live host cells, we set out to examine how the localization of SseG depends on SseF. SseF and SseG have been shown to physically and functionally interact to coordinate SCV localization and maintenance<sup>64,66,84,85,179,180</sup>. These proteins have been suggested to tether the SCV to the Golgi by jointly interacting with the host Golgi network associated protein ACBD3<sup>85</sup>. SseF and SseG have also been shown to associate with endocytic membranes and microtubules<sup>64,83</sup> and are hypothesized to redirect host exocytic traffic from the Golgi<sup>66</sup> by recruiting dynein to the SCV<sup>181</sup>. Transfected SseG showed a scattered distribution in a majority of cells (80%) that was globular in appearance and co-localized with the trans-Golgi network marker TGN46<sup>83</sup>. In a minority of cells, transfected SseG was filamentous, co-localized with microtubules, and appeared similar to translocated SseG localization during infection<sup>83</sup>, suggesting differential localization when SseG is expressed alone versus translocated with the rest of the effector cohort. Given these observations, we set out to determine whether the difference in localization was due to the mode of delivery (transfection versus T3SS-mediated translocation) or the absence of SseF.

To examine the localization of SseG in the absence of SseF during infections, we generated a *Salmonella* strain containing an isogenic *sseF/sseG* deletion while expressing SseG-GFP11 under the control of the *steA* promoter on our plasmid based platform. SseG localized to the SCV in the presence and absence of SseF (Fig 8A). However, in the absence of SseF there was a globular population of SseG at the host cell periphery (Fig 2.8A) in approximately 70% of cells (n = 65), whereas less than 10% of cells display peripheral SseG in the presence of SseF (n = 73) (Fig 2.8B). Thus, in the absence of SseF, T3SS translocated SseG displays a localization pattern similar to transfected SseG, suggesting that SseF is required for proper SseG localization. There was also a change in the morphology of filaments emanating from the SCV in the absence of SseF, where SseG containing filaments appeared either punctate or thinner than in WT infections (Fig 2.9). Thin LAMP1-associated filaments

have been observed for infections using *Salmonella* strains lacking either SseF or SseG<sup>132</sup>. Additionally, Kreiger *et al.* 2014 showed that a subset of SCV associated filaments are composed of double membranes that enclose portions of host cell cytosol and cytoskeletal filaments within its inner lumen and that the formation of these double membranes requires the function of SseF and SseG<sup>62</sup>. Our results are consistent with the observation that SseF and SseG are involved in acquiring and redirecting host cell endosomal compartments and exocytic traffic to maintain the SCV and associated filaments<sup>64,182</sup>, and that they physically interact with one another<sup>84,85</sup>.

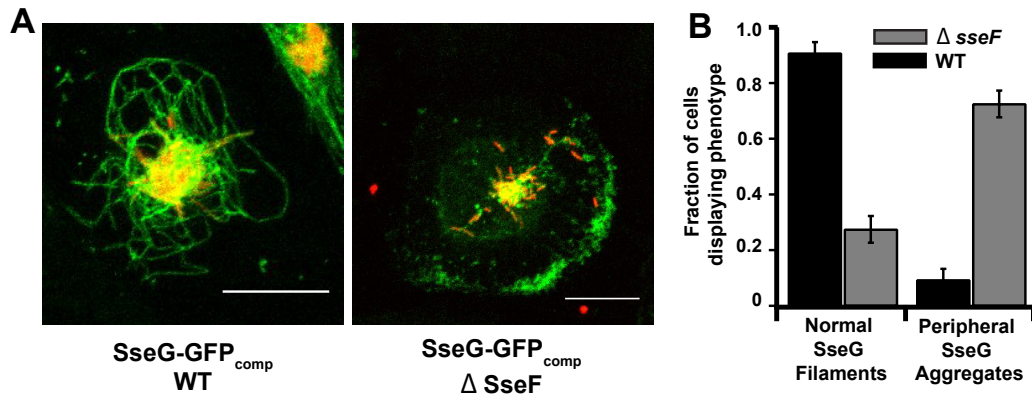


**Figure 2.8. SseG gathers at the host cell periphery in the absence of SseF**

(A) Representative images of infected HeLa cells at 14hrs post infection displaying localization of SseG-GFP<sub>comp</sub> in the presence of SseF (WT, Left) and the absence of SseF ( $\Delta sseF$ , Right). (B) Average fraction of infected cells that display SseG-GFP<sub>comp</sub> uniformly distributed across filaments compared to cells that contain SseG-GFP<sub>comp</sub> aggregates at the host cell periphery.  $n_{total} = 65$  cells ( $\Delta sseF$ ), 73 cells (WT). Error bars are SD across 3 separate infection experiments.

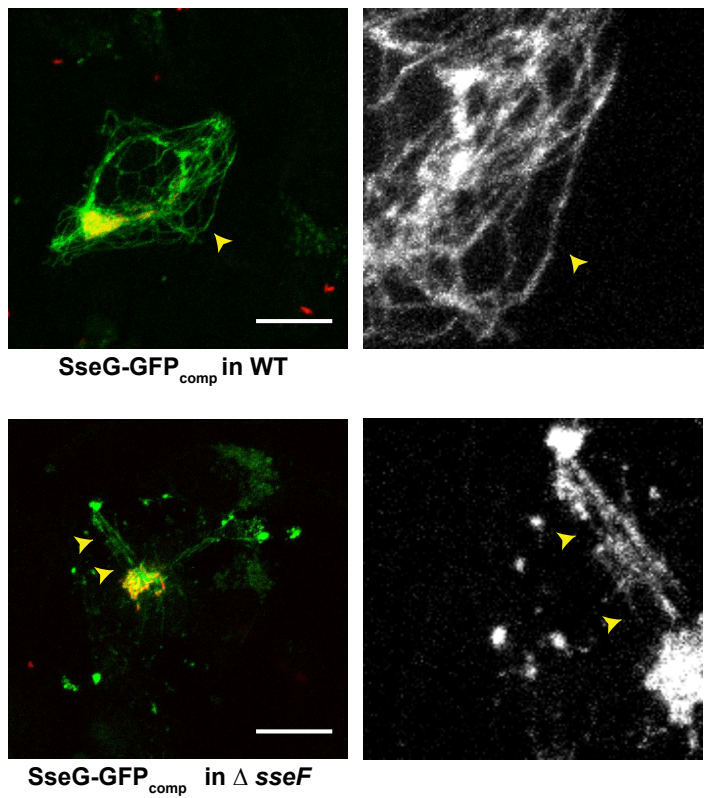


**Figure 2.9. SseG filaments are thin and punctate in the absence of SseF**

HeLa cells expressing GFP1-10 were infected with *Salmonella* strains expressing mRuby3 and SseG-GFP11, in the presence or absence of SseF. Representative images of complementation from 16 hours post infection are shown for SseG-GFP<sub>comp</sub> filaments in the presence of SseF (left) and in the absence of SseF (right). Red is *Salmonella* and Green is SseG-GFP<sub>comp</sub>. The arrows indicate a select SseG associated filament. Scale bars are 20  $\mu$ m.

## SlrP is localized to the cytosol in infected host cells

One advantage of the split-GFP system is the ability to target the GFP1-10 to subcellular compartments in the host cell to address questions about the specific localization of effector proteins. By comparing fluorescence complementation signals from split-GFP where the GFP1-10 fragment is directed to the cytosol with a version targeted to an organelle, we can distinguish whether an effector protein resides inside an organelle versus associated at the cytosolic face of the organelle. Additionally, if an effector protein changes localization at different stages of infection, as has been demonstrated for SopB<sup>145</sup>, these dynamic changes in localization can be visualized over time.

SlrP was used as a model to establish our system within host cell organelles because SlrP has been suggested to have dual localization within the host, with populations of SlrP residing in the cytosol and the ER lumen<sup>110</sup>. Motivated by the possibility of dual localization proposed by Bernal-Bayard *et al.* 2010, we aimed to distinguish two distinct populations of SlrP, one cytosolic and one ER localized, as opposed to a dynamic population that changes localization at different stages of the infection process. To assess these scenarios, we carried out long-term imaging of live cells infected with *Salmonella* expressing SlrP-GFP11, from 4-28 hours post infection. To exclusively visualize ER populations of SlrP, we used an ER lumen localized version of GFP1-10 (ER-GFP1-10)<sup>183</sup>. Using ER-GFP1-10 together with the ER luminal protein disulfide isomerase tagged to GFP11<sup>183</sup> we first verified that split-GFP localized to the ER is able to recombine and recapitulate robust fluorescence in the environment of the ER lumen (Fig. 5A). We were unable to detect signal for SlrP-GFP<sub>comp</sub> in the ER lumen at any time 4-28 hours post infection (Fig. 5C), but we consistently observed cytosolic complementation beginning at 7 hours post infection and continuing for the duration imaged (Fig. 10B). These results were observed for plasmid based expression of SlrP-GFP11 under the *steA* promoter as well as chromosomal expression of SlrP-1X-GFP11 and SlrP-3X-GFP11. Our results indicate that SlrP maintains a cytosolic C-terminus throughout 7-28 hours post infection.

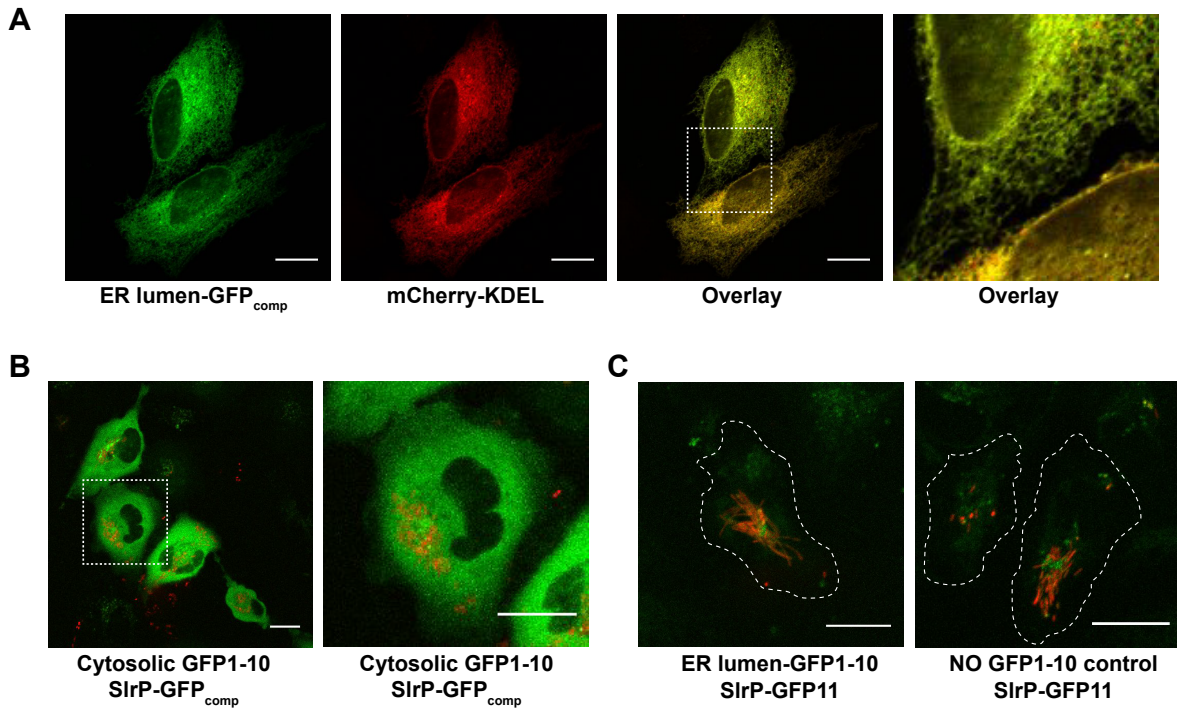


**Figure 2.10. Defining subcellular localization of SirP during live cell infections**

(A) Split-GFP components were localized to the ER lumen for complementation and fluorescence signal verification. (B,C) Host cells expressing cytosolic GFP1-10 (B) or ER localized GFP1-10 (C) were infected with *Salmonella* expressing SirP-GFP11. (B) Representative infected cells transiently expressing cytosolic GFP1-10. Second panel shows a zoomed in perspective. (C) Representative infected cells with and without transient expression of ER localized GFP1-10. GFP fluorescence was acquired for all images using identical settings and all images are scaled to the same intensity. Scale bars represent 20 $\mu$ m.

## Visualization of effector proteins in primary macrophage cells using split-GFP

*Salmonella* target both epithelial cells and macrophages during infection of a host organism and these niches give rise to very different host-pathogen interfaces (reviewed in <sup>19,28,148,184</sup>). For example, infected macrophages produce high levels of reactive oxygen species<sup>150</sup> as well as reactive nitrogen species<sup>152</sup> that require the expression of SPI-2 effectors and maintenance of the SCV to confer protection to intracellular *Salmonella* and enable the bacteria to survive and replicate. Alternatively, in epithelial cells *Salmonella* display a bimodal lifestyle with a SPI-1 dependent population that is able to replicate to a greater extent in the cytosol compared to the SPI-2 dependent population that resides in the SCV (reviewed in <sup>164</sup>). In fact the mode of *Salmonella* internalization, the strategies used for intracellular survival as well as the fate of the infected host cell varies based on cell type and depends on the temporal expression of *Salmonella* secretion systems<sup>184</sup>. For instance, macrophage cells take up bacteria through phagocytosis (reviewed in <sup>185</sup>), whereas epithelial cells are forcibly modified by the action of SPI-1 translocated effector proteins in order to facilitate bacterial engulfment through macropinocytosis. In the intracellular milieu, the role of *Salmonella* SPI-1 expression differs for different host cell types. SPI-1 expression was shown to elicit innate immune responses in epithelial cells through mitogen-activated protein (MAP) kinase and NF-κB signaling<sup>155</sup>, while inducing the opposite effect in macrophage cells by suppressing levels of select chemokines and RhoA to reduce the host innate response<sup>157</sup>. Furthermore, SPI-1 expression delays apoptosis in epithelial cells through suppression of the c-Jun N-terminal Kinase (JNK) apoptotic pathway<sup>43</sup> and concomitant activation of Akt, a kinase that can exert prosurvival effects<sup>44</sup>. However, SPI-1 expression was shown to stimulate rapid cell death by Caspase-1 dependent pyroptosis in macrophages<sup>50,162</sup>. Collectively, these studies underscore the importance of visualizing effector proteins in live cell infection models for both epithelial cells and macrophages in order to define differences in the discrete roles effector proteins play in manipulating the host to establish distinct niches in different types of host cells.

In this study, we set out to develop approaches for applying the split-GFP effector labeling platform in primary BMDMs from immunocompetent mice to visualize effector proteins for the first time in living primary immune cells. Although effector proteins have been visualized in macrophage-like cell lines such as Raw264.7 cells from immune-compromised mice, studies indicate the intracellular niche may be significantly different in cell lines versus primary cells. For example, Helaine et al measured different replication kinetics and different requirement for SPI-2 effectors in Raw264.7 cells compared to primary BMDMs<sup>125</sup>, suggesting differential need for effector proteins in promoting replication in these different cell types. BMDMs are notoriously challenging to transfect because they are highly differentiated, have decreased proliferation rates, and can be readily activated or undergo cell death upon exposure to foreign DNA<sup>161,186,187</sup>. To overcome this limitation, we used Nucleofector™ Technology to express the GFP1-10 in primary BMDMs<sup>167,188</sup>. To further facilitate visualization, we incorporated a blue nuclear marker (NLS-mTagBFP2) downstream of the gene encoding GFP1-10, and separated by an internal ribosomal entry site (IRES). This construct facilitated identification of transfected cells since the GFP1-10 is non-fluorescent in the absence of complementation with GFP11. Nucleofection of GFP1-10-IRES-NLS-mTagBFP led to identification of transfected cells via visualization of blue nuclear fluorescence and confirmation of split-GFP complementation via co-transfection of an ERK-GFP11 positive control (Fig 11).

We successfully visualized SlrP, SteA, PipB2, and SseF in primary BMDMs. To visualize these effector proteins during infection of primary BMDMs, a plasmid containing GFP1-10 was nucleofected into BMDM cells 6 days post isolation and differentiation, followed by plating and infection with *Salmonella* expressing the GFP11 tagged effector (Fig 6). SlrP generates robust split-GFP fluorescence when translocated into HeLa cells and has previously been shown to translocate into RAW264.7 cells from 8-16 hours post infection<sup>189</sup>. SlrP-GFP<sub>comp</sub> signal appeared diffusely cytosolic, indicating that localization in BMDMs is consistent with localization seen in HeLa cells for SlrP-GFP<sub>comp</sub> at 16 hours post infection. SteA, PipB2, and SseF don't display

diffuse fluorescence and instead appear to localize to intracellular membranes, consistent with their localization in epithelial cells and the macrophage-like cell line, Raw264.7<sup>65,103</sup>. However, we observed distinct differences in SteA and PipB2 localization compared to Raw cells. We previously found that SteA and PipB2 accumulated on the SCV and membrane tubules in both HeLa and Raw cells<sup>103</sup> (Fig 13). In the primary BMDMs used in this study, effectors generally colocalized with internalized bacteria, but the pattern of effector localization was more spread out on intracellular membranes. This is consistent with our observations that primary BMDMs often lack a compact SCV, and instead internalized bacteria are more commonly spread throughout the cell<sup>126</sup>(Fig 13), as was observed previously in infection of human monocyte-derived macrophages<sup>190</sup>. Finally, we examined the localization of the host cell marker LAMP1, which is routinely used to mark the compact SCV, and found the pattern of LAMP1 localization to be similar to effector localization and very different from what is observed in HeLa or Raw cells (Fig 13). These results reveal different phenotypes, suggesting different niches, in different kinds of cells and demonstrate that the split-GFP effector protein labeling platform can be used in multiple cell types to study effector protein localization under different model infection conditions.

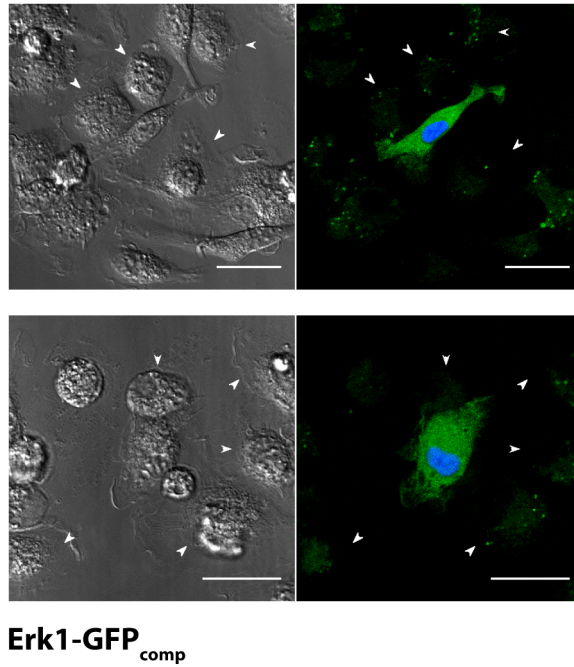


**Figure 2.11. Fluorescence images demonstrating split-GFP fluorescence complementation in cells nucleofected with GFP1-10-IRES-NLS-mTagBFP2**

Fluorescence images show blue nuclear marker (NLS-mTagBFP2) and green split-GFP complementation (GFP1-10 complemented with co-transfected Erk1-GFP11). Importantly cells without blue nuclear marker show decreased/no fluorescence signal in the green channel. Images are scaled to the same intensity range to allow for direct comparison of relative intensity of fluorescence signal. Scale bar represents 20  $\mu\text{m}$ . Image acquired by Mike Minson.

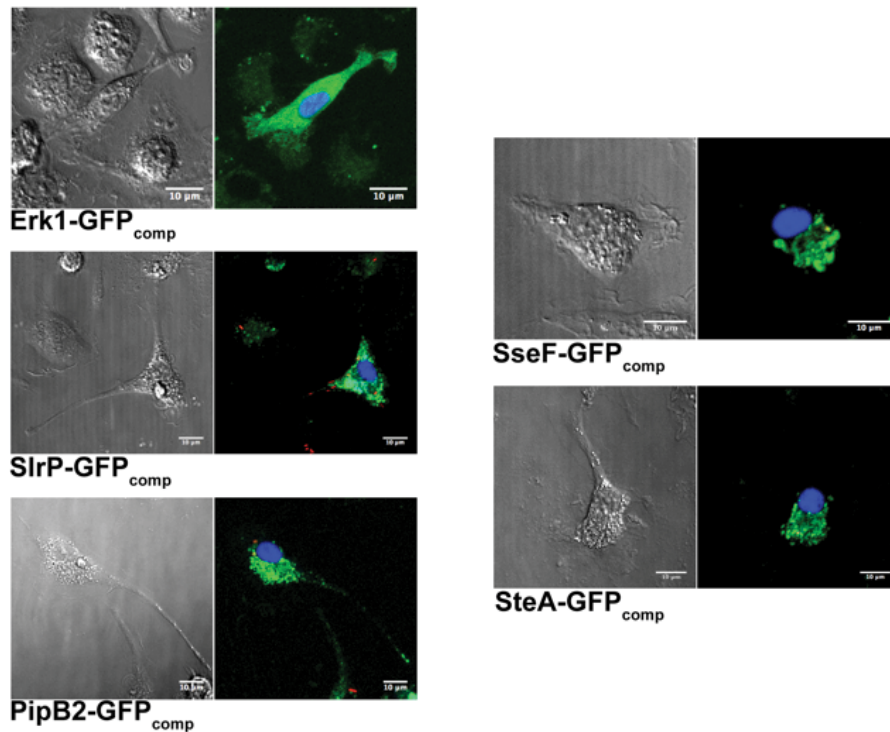


**Figure 2.12. Fluorescence images demonstrating split-GFP fluorescence complementation in BMDMs nucleofected with GFP1-10-IRES-NLS-mTagBFP**

DIC (left) and fluorescence overlay (right; blue NLS-mTagBFP2, green GFP<sub>comp</sub>, red mRuby3 in *Salmonella*) images of bone marrow derived macrophages expressing GFP1-10-IRES-NLS-mTagBFP2. In the top row cells were co-transfected with ERK-GFP11 as a positive control. Remaining rows represent cells nucleofected with GFP1-10-IRES-NLS-mTagBFP2 and infected with *Salmonella* strains expressing mRuby3 and the specified effector tagged with GFP-11. Representative images collected from 12-14 hours post infection are shown. Images acquired by Mike Minson.

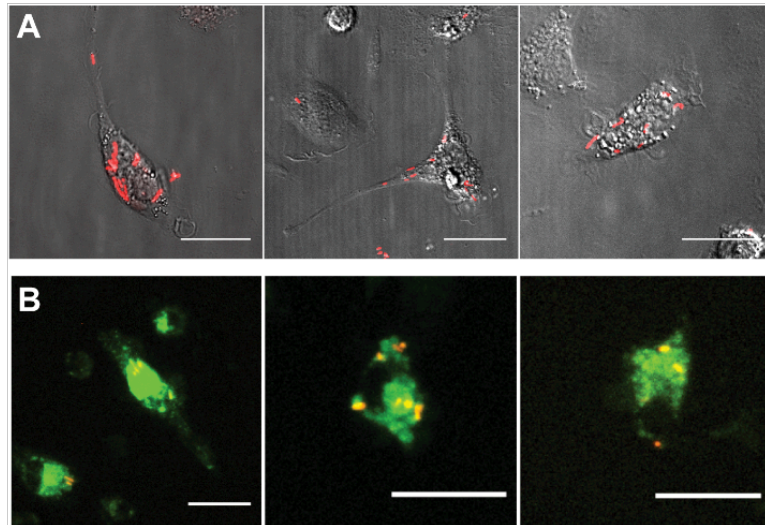


**Figure 2.13. Images of infected primary BMDMs illustrating dispersed as opposed to compact bacteria**

A) Overlay images showing primary BMDMs (DIC images) and bacteria (Salmonella, red). Images reveal that in primary BMDMs bacteria often don't cluster in a massive compact SCV but are more dispersed. B) Overlay of LAMP1-GFP (green) and bacteria (Salmonella, red) showing that in infected primary BMDM cells LAMP1 doesn't cluster in a massive SCV but is more dispersed throughout cytosol.

## 2.3 DISCUSSION

Due to the capability to invade and survive in multiple types of eukaryotic host cells with different environments, the intracellular life of *Salmonella* is reliant on its ability to establish a versatile niche within host cells. The coordinated action of translocated effector proteins enables *Salmonella* and similar intracellular pathogens to modulate and adapt host cell signaling and transport processes to generate this protective niche, resulting in a highly dynamic interplay between the bacteria and the host cell. Unraveling the elements of this complex interplay and elucidating the roles of individual effector proteins in establishing *Salmonella*'s niche requires techniques that monitor bacteria together with translocated effector proteins within the different types of infected host cells, as the different modes of infection and different intracellular environments may require different subsets of effector proteins.

The development of innovative imaging approaches and fluorescence-based tools has enormous potential for defining the intracellular phenotypes of *Salmonella* infection at the single cell level. Because methods based on fixation and immuno-staining infected host cells are limited by the fact that the fate of intracellular bacteria, and the localization of effector proteins within the host cell cannot be followed over time throughout the course of infection, we have focused on developing approaches for live cell imaging. Current approaches developed by us and others have addressed the challenge that tagged effectors must be compatible with translocation through the narrow T3SS<sup>26,103,130,136,137</sup>, and in this work we further tackle the necessity for a versatile tool capable of illuminating effectors that are expressed at low levels.

The original split-GFP system adapted for labeling SPI-2 effectors exclusively used endogenous promoters and enabled the visualization of *Salmonella* effector proteins SteA, SteC and PipB2 in epithelial and Raw264.7 macrophage-like cell lines, illustrating its utility in tagging diverse T3SS effectors and tracking effector populations in live host cells. However, we encountered limitations with this original system when we were unable to detect a number of new effector proteins, including SseF, SseG and SlrP, under their endogenous promoters and

could not determine whether this issue was due to low expression, poor complementation due to steric constraints, perturbation of translocation, or rapid protein turnover in the host cell. The development of the bacterial effector expression assay assisted in differentiating problems with low expression and/or complementation versus translocation and residence time within host cells.

The modular platform for split-GFP labeling developed in this work enables the amplification of fluorescent signals by tuning effector protein expression level or by multimerizing the tag. Additionally, we generated a platform for expression of GFP1-10 along with a blue nuclear marker that serves to reveal GFP1-10 expressing host cells and aid in the verification of low complementation signals. Using these new tools, we visualized a number of different translocated effector proteins in living cells upon infection. Importantly, we demonstrate the ability of this tool to illuminate the intracellular niche in both epithelial cells and primary macrophages. A number of these effectors (SseF, SseG and SlrP) were visualized during live infection for the first time. We discovered that SlrP localizes to the host cell cytosol in epithelial cells at all times during infection, shedding light on two conflicting studies regarding SlrP's localization and potential functions within host cells. Transfected SlrP had been found to localize to the cytosol, where it was suggested to function as an E3 ubiquitin ligase with thioredoxin as a binding partner<sup>109</sup>. But, a later study identified the ER luminal chaperone ERdj3 as a potential binding partner, and suggested that transfected SlrP could localize to the ER<sup>110</sup>. Our findings are consistent with SlrP functioning exclusively in the cytosol during infection of epithelial cells.

There is ample evidence that *Salmonella* infection of epithelial cells and macrophages gives rise to substantially different host-pathogen interfaces and divergent outcomes. Different pathogenicity islands, and their associated effectors have been implicated in setting up different niches in these cell types. But far less attention has been paid to possible differences in the roles effectors may play between macrophage-like cell lines such as Raw264.7 cells and primary macrophages from different mouse models. Yet, the role of pathogenicity islands and

the ability of *Salmonella* to replicate in Raw cells versus primary mouse macrophages versus human monocyte-derived macrophages in different activations states differs significantly<sup>125,190</sup>. In this work, we examine primary BMDMs from immunocompetent mice (SV129S6), as a model for systemic infection. SV129S6 mice contain a functional NRAMP1 metal transport protein and *Salmonella* can persist within macrophages of *Nramp1*<sup>+/+</sup> mice for up to 1 year, establishing this system as a model for chronic infection<sup>13,191,192</sup>. In contrast, RAW264.7 cells are derived from immunocompromised NRAMP1<sup>-/-</sup> mice and are commonly used as a model for acute infection. RAW264.7 cells have been shown to differ significantly from primary BMDMs in proteomics and phagosome maturation<sup>166</sup>, as well as in their ability to promote intracellular replication<sup>125</sup>. By examining effector localization and tracking internalized *Salmonella* in primary BMDMs, we discovered that bacteria don't cluster in a compact SCV the way they do in epithelial cells or Raw264.7 cells. Additionally, effector proteins such as SteA, PipB2, and SseG localize to intracellular membranes as they do in Raw and epithelial cells, but they don't accumulate around bacteria, and *Salmonella*-induced tubules or filaments are not readily apparent. These results suggest that effectors may play substantially different roles in different niches. The tools developed here open up the possibility of comparing localization, dynamics and lifetime of effector proteins in different types of infected host cells to identify the different roles these effector proteins play in different infection models.

## 2.4 METHODS

### Bacterial strains and plasmids generated in this study

All strains used in this study were isogenic derivatives of *Salmonella enterica* serovar Typhimurium SL1344 constitutively expressing mRuby3 from a plasmid (parent pACYC177) under the *rpsM* ribosomal gene promoter. *Salmonella* effector gene deletion strains ( $\Delta steA$ ,  $\Delta sseF$ ,  $\Delta sseG$ ,  $\Delta slrP$ ,  $\Delta sopA$ ,  $\Delta steB$ ,  $\Delta gtgE$ ) and chromosomal integration of the GFP11 or 3xGFP11 were generated as described previously<sup>193-195</sup> using lambda Red recombination. Table S1 in Supporting Information lists all strains and plasmids developed in this study.

Transient cytosolic over-expression of GFP1-10 in HeLa or BMDM cells was accomplished using either pGFP1-10<sub>mamopt</sub> (Plasmid pCMV-mGFP1-10 encoding the GFP1-10 fragment with mammalian-optimized codons,<sup>141</sup> or pGFP1-10-IRES-NLS-mTagBFP2. Localization of GFP1-10 to the ER lumen was accomplished using pER-GFP1-10 (GFP1-10 containing an N-terminal ER localization sequence and a C-terminal retention sequence, a kind gift from Bernard Moss (Hyun *et al.*, 2015)). To verify split-GFP expression, complementation and fluorescence efficiency within the ER, the ER luminal Protein Disulfide Isomerase fused to GFP11 (a kind gift from Bernard Moss (Hyun *et al.*, 2015)), subcloned into pcDNA3.1 and transfected along with pER-GFP1-10.

A stable HeLa cell line expressing GFP1-10 and NLS-mTagBFP2 was generated using the PiggyBac<sup>TM</sup> Transposon Vector System. HeLa cells were co-transfected using *TransIT-LT1* (Mirus) transfection reagent with 1000 ng of pGFP1-10-IRES-NLS-mtagBFP2 in PB510B-1 vector backbone and 500 ng Super PiggyBac<sup>TM</sup> transposase. Stable transformants were selected with 2  $\mu$ g/ml puromycin in DMEM (Gibco) supplemented with 10% FBS (Gibco).

## **Bacterial cell culture and growth curves**

### *Growth curves*

*Salmonella* strains were grown with aeration at 37°C to saturation in LB (EMD) media supplemented with antibiotics as required. Cultures were then diluted 1:100 into fresh LB (EMD) media supplemented with appropriate antibiotics and the OD<sub>600</sub> was measured every 30 minutes for a duration of 16 hours using a Tecan Safire II monochromator-based plate reader.

### *Growth for infections*

For infection of HeLa cells, *Salmonella* strains were grown in LB (EMD) supplemented with 300 mM NaCl (Fisher Scientific) and 25 mM MOPS (Sigma) at pH 7.6 and appropriate antibiotics at 37°C for 16 hours without aeration. Prior to infection, bacteria were diluted 1:33 in 3 ml of SPI-1 media, with appropriate antibiotics for 4 hours at 37 °C without aeration. For infection of primary BMDMs, bacteria were grown to stationary phase in LB, with appropriate antibiotics at 37 °C with aeration. Prior to infection of BMDMs, bacteria were opsonized in a 1:1 solution of mouse serum (Sigma) and cell culture media (Gibco) for 30 min at 37 °C.

### *Growth under SPI-2 inducing conditions for the bacterial effector expression assay*

For SPI-2 induction, *Salmonella* strains were grown in defined media consisting of 5mM KCl, 7.5mM (NH<sub>4</sub>)<sub>2</sub>SO<sub>4</sub>, 38mM glycerol (0.3% v/v), 0.1% casamino acids, 0.5mM K<sub>2</sub>SO<sub>4</sub>, 8μM MgCl<sub>2</sub>, 337μM PO<sub>4</sub><sup>-3</sup> (K<sub>3</sub>PO<sub>4</sub>), 80mM MES, pH 6.5 with aeration. The pH conditions for SPI-2 induction are often 5.4, however we modified these growth conditions to pH 6.5 for simultaneous expression of SPI-2 and split-GFP recombination (Fig S7). Cultures were grown to early stationary phase and used for the bacterial expression assay.

## **Mammalian cell culture and infections**

HeLa cells were maintained in DMEM (Gibco) supplemented with 10% FBS (Gibco), 100 Units/mL penicillin G sodium (Gibco), and 100 µg/mL streptomycin sulfate (Gibco) at 37°C with 5% CO<sub>2</sub>. Primary BMDMs were isolated, as previously described (<sup>196</sup>). Briefly, marrow was flushed from the femurs and tibias of 2 to 3-month-old SV129S6 mice (Taconic Laboratories, Hudson, NY, USA). The cells were resuspended in DMEM (Sigma-Aldrich, St. Louis, MO, USA) supplemented with FBS (20%), L-glutamine (2 mM), sodium pyruvate (1 mM), beta-mercaptoethanol (50 µM), HEPES (10 mM) and penicillin-streptomycin (50 IU/ml of penicillin and 50 µg/ml of streptomycin). The cells were overlaid onto an equal volume of Histopaque-1083 (Sigma-Aldrich, St. Louis, MO, USA) and centrifuged at 500g for 25 min. Monocytes at the interface were harvested and incubated for 6 to 7 days at 37 °C in 5% CO<sub>2</sub> in supplemented DMEM that also contained 30% macrophage colony stimulating factor obtained from NIH/3T3 cells (acquired from Jeffery Cox, University of California, San Francisco, USA) to promote monocyte differentiation into macrophages.

### *Transfections:*

HeLa cells between a passage number of 2-10 were seeded into 35 mm glass-bottom dishes and allowed to proliferate for 24 hours. Transfection of pGFP1-10<sub>mamopt</sub> was achieved using *TransIT-LT1* (Mirus) transfection reagent and conditions recommended by the manufacturer for 3 µg of DNA. Transfected cells were incubated at 37°C with 5% CO<sub>2</sub> for 48 hours prior to imaging. Differentiated primary macrophage at 6-7 days post isolation were lifted by scraping and cells were subjected to nucleofection using 2.5 µg of DNA and reaction conditions recommended by the manufacturer for Nucleofector® Program Y-001. Nucleofected cells were seeded into 35 mm glass-bottom dishes and incubated at 37°C with 5% CO<sub>2</sub> for 6 - 24 hours prior to imaging.

### *Infections:*

HeLa cells expressing GFP1-10 were challenged with *Salmonella* grown under SPI-1 inducing conditions at a multiplicity of infection (MOI) of 50. Macrophage cells expressing GFP1-10 were infected with opsonized *Salmonella* at an MOI of 20. Infections were allowed to proceed for 35 minutes at 37°C and 5% CO<sub>2</sub> before a gentamicin protection was carried out, where the *Salmonella*-containing media was exchanged with phenol red free DMEM containing 10% FBS (HeLa cells) or 20% FBS (macrophages) and 100 µg/mL gentamicin, to eliminate any non-internalized bacteria. After incubating for 45 minutes in a high concentration of gentamicin at 37°C and 5% CO<sub>2</sub>, the media was replaced with phenol red free DMEM containing 10%FBS and a low concentration (10 µg/mL) gentamicin to limit extracellular bacteria for the remainder of the experiment.

### **Live cell imaging of infected mammalian cells:**

All imaging work was performed at the BioFrontiers Institute Advanced Light Microscopy Core. Laser scanning confocal microscopy was performed on a Nikon A1R microscope acquired by the generous support of the NIST-CU Cooperative Agreement award number 70NANB15H226. Spinning disc confocal microscopy was performed on Nikon Ti-E microscope acquired through partial support from the Howard Hughes Medical Institute.

*Salmonella* infections of HeLa cells with the split-GFP effector labeling system were imaged on a Nikon A1R laser scanning confocal microscope equipped with the Nikon Elements software platform, Ti-E Perfect Focus system, a motorized XY stage with a Ti Z drive and an environmental chamber (Pathology Devices) to maintain cells at 37°C, 5% CO<sub>2</sub> and 70% humidity. Images were acquired using a 40x oil objective (NA 1.30) and the following channels: red (561 nm laser line, PMT gain: 100, emission filter: 600/50 nm), green (488 nm laser line, PMT gain: 120, emission filter: 525/50 nm), and bright field DIC. All imaging was performed with the channel series function engaged to prevent bleedthrough between fluorescence channels

and all fields of view were imaged with a pixel dwell time of 2  $\mu$ s. Long-term imaging of infected cells was done between 5-25 hours post infection, acquiring images every 15 minutes. The motorized XY stage was used to select and store the locations of multiple fields of view in order to follow the fates of many infected cells over the course of the experiment. The Z drive was used to generate z slices that stack to encompass the entirety of the cells within each field of view, thus ensuring the complete detection of any bacteria and effector-GFP<sub>comp</sub> signal present. Select images were acquired with a digital zoom, sampling at Nyquist resolution to capture effector-GFP<sub>comp</sub> signal in detail. All images were processed using Fiji to merge individual fluorescence channels and to flatten Z stacks using the Maximum z Projection algorithm into a single image per time point and per field of view. Background was subtracted using the rolling ball background correction algorithm with a radius set to 100 pixels. Fluorescence signal intensities were false colored and brightness and contrast were held to equivalent values per channel between images.

### **Bacterial expression assay:**

#### *Growth and GFP1-10 induction:*

*Salmonella* strains expressing GFP11-tagged effectors were transformed with GFP1-10 (pBAD18-Cmr) and tested for effector expression efficiency using GFP<sub>comp</sub> signal. Transformants were selected with 25 $\mu$ g/mL chloramphenicol and verified by colony PCR. Strains were grown in SPI-1 inducing (high osmolarity and low aeration) or SPI-2 inducing (low pH and low Mg<sup>2+</sup>) conditions corresponding to the endogenous effector gene, and GFP1-10 expression was induced with 0.2% arabinose. SPI-2 induction conditions were verified using an mKate2 reporter expressed under the SseA promoter (Fig S7). Bacteria at early stationary phase were rinsed with PBS and seeded into 96 well glass bottom dishes (MatriPlate MGB096-1-2-LG-L) pre-treated with 0.1 mg/mL poly-L-lysine (Sigma), incubated for 1-2 hours for adherence and imaged as described below.

*Imaging split-GFP complementation within bacteria:*

*Salmonella* were imaged on a Nikon Ti-E microscope fitted with a Yokogawa CSU-X1 spinning disc head and equipped with the Nikon Elements High Content Analysis (HCA) software platform, Ti-E Perfect Focus system, a motorized XY stage with a Ti Z drive and a fully enclosed environmental chamber (Okolabs) to maintain cells at 37°C, 5% CO<sub>2</sub> and 70% humidity. Images were acquired using a 40x air objective (NA 0.95) and the following channels: red (mRuby3: 561 nm laser line, emission filter: 620/60 nm; mCherry: 594 nm laser line, emission filter: 645/75 nm), green (488 nm laser line, emission filter: 525/50 nm), and bright field DIC (HBO arc lamp) detected with an iXon Ultra 888 EMCCD camera (Andor). Fluorescence channels were acquired with a readout mode of 10MHz at 16 bit and an EM gain of 300.

*ICY analysis of GFP<sub>comp</sub> signals in bacteria:*

GFP<sub>comp</sub> images acquired using the NIKON ELEMENTS software platform were exported as Tiff files and imported into the image analysis software ICY (version 1.8.6.0)<sup>(197)</sup> for processing and analysis. The Spot Detector plugin was used to perform automated selection and intensity assessment of GFP<sub>comp</sub> signals in bacteria. Each region of interest (ROI) detected and analyzed represents a single bacterium. Spot Detector settings were as follows: USWTWavelet Detector set to detect bright spots over a dark background with a sensitivity set at 75 for Scale 3 (~7 pixels) and a size filter range of 10-300 pixels. Processed images were exported with ROI labels and the binary versions were assessed by eye to verify that selected ROIs analyzed for signal intensity resemble the shape of bacteria. The fluorescence intensity data generated from ICY was exported in XLS file format, background subtracted and further analyzed. Histograms displaying split-GFP signal intensities for the bacterial expression assay were produced from the total pooled results of 3 replicate experiments and the fluorescence intensity values used are the average signal intensity in an ROI. Pooled ROI intensity values were binned (by 50 or 150) to identify the frequency of ROIs in different intensity ranges. Binned

values were then divided by the total number of ROIs (bacteria) to generate the fraction of the bacterial population represented by each bin in order to normalize for differences in population size between conditions.

## SUPPLEMENTARY EFFECTOR PROTEINS

The modular platform for split-GFP effector labeling described in CH2 was designed to facilitate facile labeling of new effector protein targets as well as to enable amplification of fluorescent signals by tuning effector protein expression level or by multimerizing the GFP11 tag. We targeted several effector proteins in addition to those described in CH2, however, we were unsuccessful in detecting this set of supplementary effector proteins during live cell infections (Table S.1). These effector proteins include CigR, GtgA, GtgE, SteB, and SseK2, which were excluded from the study described in CH2 because they have yet to be screened for expression and split-GFP complementation efficiencies under endogenous promoters or by using multimerized tags. In addition, we studied the effector protein SopD2 and discovered that the expression and complementation of this effector protein under its endogenous promoter is affected by the presence of a restriction site upstream of the initiation codon.

Expressed under the *steA* promoter in the modular plasmid based platform, SteB and GtgE produced split-GFP complementation signals that were comparable to background (Table S.1, Figure S.1). We therefore hypothesize that the reason for the lack of detection of these effector proteins during live cell infections is related to expression efficiency. It would be important to test these effectors under their endogenous promoters and potentially under other generic promoters as well as with a multimerized GFP11 tag in order to further investigate our observations of low expression and complementation. On the other hand, GtgA and SseK2 showed expression and complementation signals that were above background when expressed under the *steA* promoter. CigR showed very strong expression and complementation signals when expressed under the *steA* promoter (Table S.1, Figure S.1). However, we were unable to visualize the complementation of GtgA or SseK2 within infected host cells at any time from 4-25 hours post infection. It is possible that GtgA and SseK2 are expressed at a level below the threshold of detection for split-GFP within a host cell, even though the expression assay

indicated levels above background. Alternatively, this issue may be due to the inability of the effector proteins, especially in the case of CigR-GFP11, to complement with GFP1-10 in the host cytosol, either because the C-terminal tag is unavailable due to alternate localization within the host or because the effector has a binding interface that occludes split-GFP complementation. Alternatively, populations of the tagged effector could be rapidly degraded within the host. It would be important to probe these scenarios further using complementary methods such as immunofluorescence and Western blotting to assess localization and timing of residence within the host cell for these effector proteins.

<b>PLASMID EXPRESSION UNDER <i>steA</i> PROMOTER</b>			
<b>Promoter</b>	<b>Effector Protein</b>	<b>Expression</b>	<b>Visualization in Host Cell</b>
<i>steA</i>	SteB	-	<i>N</i>
	GtgA	+	<i>N</i>
	GtgE	-	<i>N</i>
	SseK2	+	<i>N</i>
	CigR	+++++++	<i>N</i>

**Table S.1. Comparison of bacterial expression assay and split-GFP complementation in infected host cells for supplementary effector proteins**

The bacterial expression assay from Figure 2.2D was quantified as follows: - represents no detection of fluorescence signal above the negative control, + is the major peak of fluorescence signal within a population is within 1 standard deviation of the negative control, +++ is within 3 standard deviations of the negative control and so on. Visualization within infected host cells was assessed for each condition between 4-24 hrs post infection, where Y indicates that effector-GFP<sub>comp</sub> signal was detectable above background, N indicates no detectable GFP<sub>comp</sub> signal.

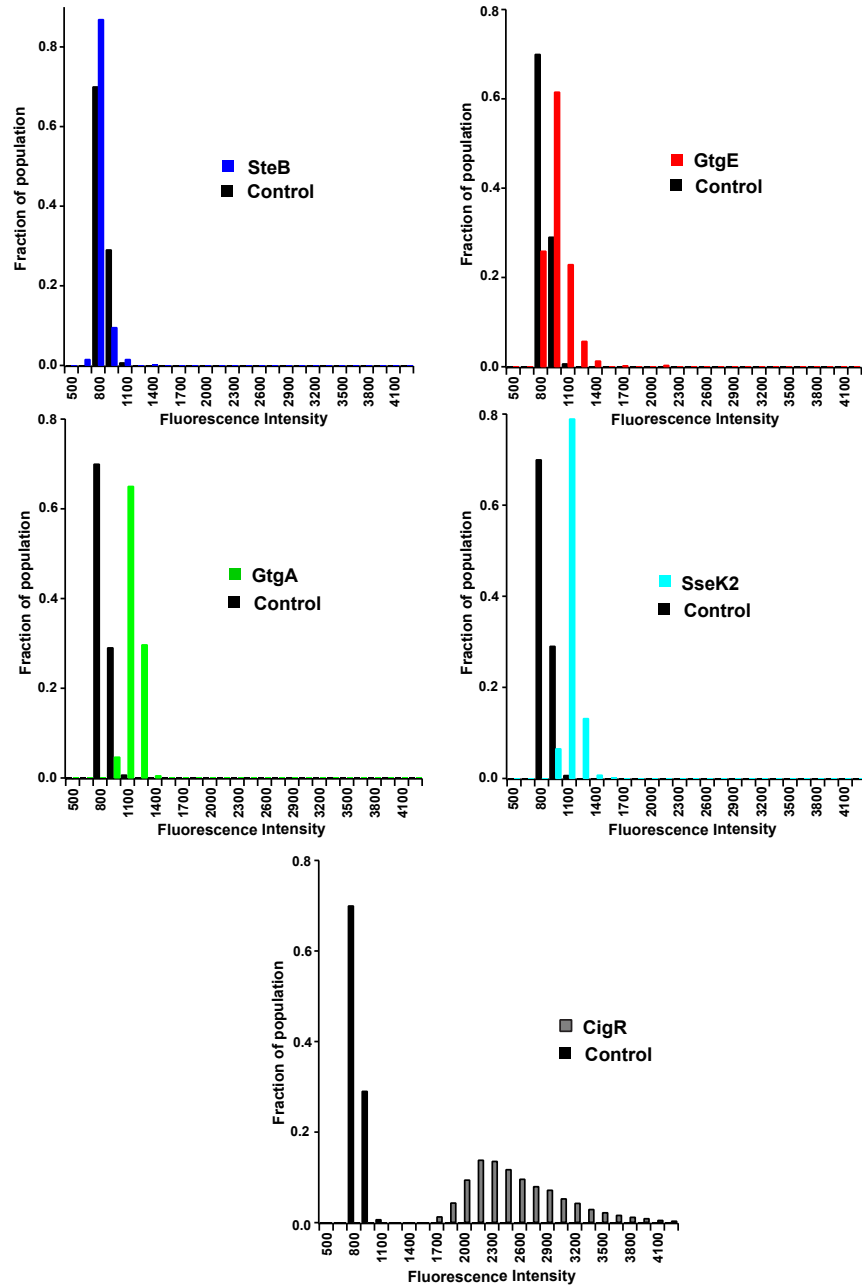


**Figure S.1. GFP<sub>comp</sub> intensity profiles for supplementary effector proteins tested with the bacterial expression assay**

Comparison of the GFP<sub>comp</sub> signal intensity in individual bacteria for different supplementary effectors. Plasmid-based GFP11-tagged effectors are expressed under the *steA* promoter alongside GFP1-10, which is expressed on a separate plasmid, within bacteria. SPI-2 induction and bacterial imaging were accomplished as defined in Experimental Methods. Results represent the pooled total of 3 biological replicates, including 4 technical replicates each, per condition,  $n \geq 1000$  bacteria (ROI) per condition.

The effector protein SopD2 had been expressed and visualized during infections previously in the Palmer lab using the original effector labeling platform depicted in Figure S.2.A. Because it is exclusively a T3SS-2 translocated effector protein that had been established to express at a level that showed strong split-GFP complementation signals, we attempted to use its promoter region to drive the expression of new T3SS-2 effector targets in place of the *steA* promoter. However, upon cloning the promoter region into the new modular platform that includes the restriction site EcoRI upstream of the initiation codon in place of the spacer that follows the Shine-Dalgarno sequence (Figure S.2.B), we discovered that SopD2 expression and split-GFP complementation was hampered (Table S.2, Figure S.3). To investigate whether this issue was due to a feature of the new expression platform versus interference with protein production because of the presence of the EcoRI restriction site, we generated a plasmid using the new expression platform that removed this restriction site (Figure S.2.C). We then used the bacterial expression assay to test for protein production and split-GFP complementation (Figure S.3) and discovered that the presence of EcoRI in place of the Shine-Dalgarno sequence spacer did indeed interfere with SopD2 expression.

Based on our observation that modifying the upstream regulatory region of SopD2 interfered with effector expression, we hypothesize that the regulatory region in context with the 5' coding region of effector protein is sensitive to sequence-related structural architecture at the mRNA level. For example, the sequence of mRNA can dictate the secondary structural elements that form which in turn dictate the availability of the ribosomal binding site and subsequent protein translation<sup>172,198,199</sup>. In addition to this scenario, altering the length of the spacer between the ribosomal binding site and the initiation codon could have an added effect on protein expression because this distance has been shown to impact translation efficiency<sup>172</sup>. These observations underscore the usefulness of the effector expression assay in determining appropriate promoter-effector combinations for optimal expression. It is possible that the

effectors that produce low or background level signals could be expressed under a different promoter to achieve more efficient protein production and split-GFP complementation.



<b>PLASMID EXPRESSION UNDER ENDOGENOUS SopD2 PROMOTER +/- RESTRICTION SITES</b>			
<b>Promoter and restriction site context</b>	<b>Effector Protein</b>	<b>Expression</b>	<b>Visualization in Host Cell</b>
<i>sopD2</i> promoter Original platform with no restriction sites	SopD2	++	Y
<i>sopD2</i> promoter New platform with restriction sites surrounding each component	SopD2	-	N
<i>SopD2</i> promoter New platform with EcoRI removed	SopD2	++	Y

**Table S.2. Comparison of bacterial expression assay and split-GFP complementation in infected host cells for SopD2 expressed in different plasmid layouts**

The bacterial expression assay from Figure 2D was quantified as follows: - represents no detection of fluorescence signal above the negative control, + is the major peak of fluorescence signal within a population is within 1 standard deviation of the negative control, +++ is within 3 standard deviations of the negative control and so on. Visualization within infected host cells was assessed for each condition between 4-24 hrs post infection, where Y indicates that effector-GFP<sub>comp</sub> signal was detectable above background, N indicates no detectable GFP<sub>comp</sub> signal.

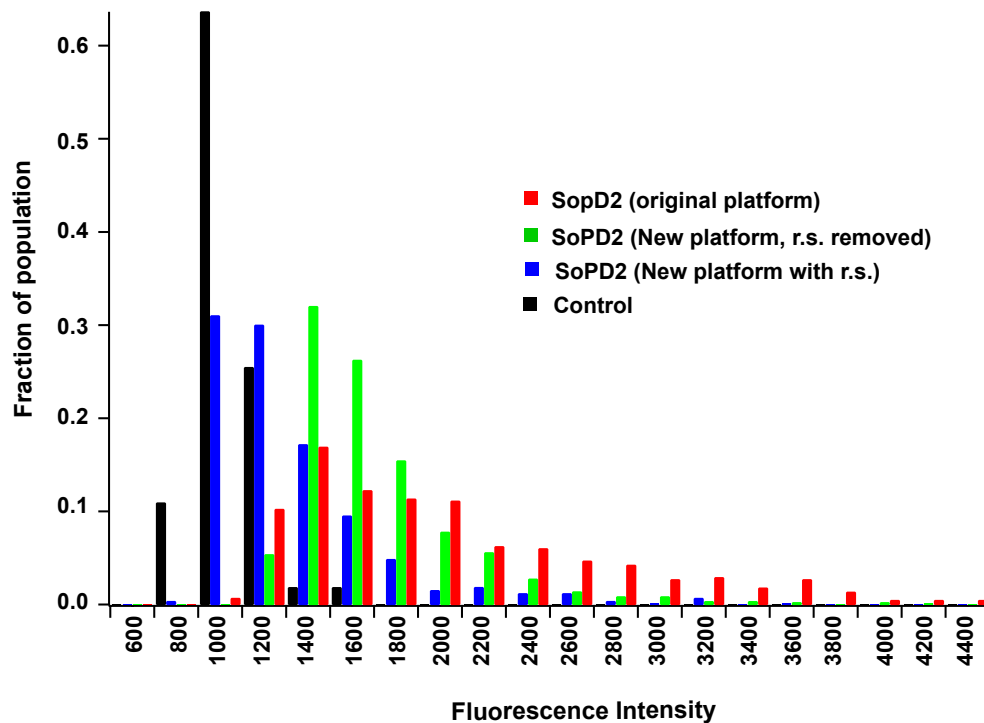


**Figure S.3. The presence of the EcoRI restriction site between the promoter and the initiation codon effects the expression of SopD2**

Comparison of the GFP<sub>comp</sub> signal intensity in individual bacteria for SopD2 expressed under the different platform layouts shown in Figure A.2. Plasmid-based GFP11-tagged SopD2 is expressed under the endogenous *sopD2* promoter in the presence or absence of an EcoRI restriction site (r.s.) alongside GFP1-10, which is expressed on a separate plasmid, within bacteria. SPI-2 induction and bacterial imaging were accomplished as defined in Experimental Methods. Results represent the pooled total of 3 biological replicates, including 4 technical replicates each, per condition, n ≥ 1000 bacteria (ROI) per condition. (r.s. = restriction site = EcoRI).

## CHAPTER 3

### FUTURE DIRECTIONS

*Salmonella* infection of host cells is a complex dynamic process controlled by the presence and function of effector proteins. Pathogen survival is dictated by the ability to overcome specific challenges posed by the host cell environment, including survival within epithelial and macrophage cells that have mechanisms to detect and eliminate foreign bodies. In order to investigate the specific roles and contributions of individual effector proteins in different host cell environments it is important to be able to visualize the effector proteins themselves throughout the infection processes. Tracking the localization dynamics of an effector protein population within the host offers spatial and temporal information that can be used to map the presence of bacterial proteins in relation to host cell factors. Details regarding the stage of infection that an effector protein is present and its lifetime within a host cell coupled with where it localizes and how this relates to host cell processes can shed light onto the effectors' role in infection. In addition, methods that monitor the perturbations of the host cell during infection can be coupled with mechanistic studies that will reveal insight into an effector protein's essential mechanism of action.

#### **Optimizing the expression of tagged effector proteins**

In this thesis work I sought to develop a versatile tool capable of illuminating effector proteins that are expressed at low levels throughout the infection process while preserving the complexity of different infection models and maintaining the ability to track the evolution of infection phenotypes over time. In Chapter Two, I developed a modular *Salmonella* effector protein labeling platform that improved our ability to monitor specific effector protein localization within the host cell. A key feature of this system was the addition of the bacterial effector expression assay, which assisted in differentiating problems with low effector expression and/or

complementation versus translocation and residence time within host cells. This method could be expanded to test the expression and split-GFP complementation of a broader set of effector proteins in the future, including different effector promoter regions for use as generic promoters to further tune effector expression levels. Based on our observation that several effector proteins did not express and complement well under the *steA* promoter, including GtgA, GtgE, SteB, and SseK2, we hypothesize that the regulatory region in context with the 5' coding region of effector proteins is sensitive to sequence related structural architecture at the mRNA level. For example, because the effector proteins expressed under the *steA* promoter all share the same regulatory region, their level of transcription is expected to be comparable. Therefore, the range of split-GFP complementation levels observed for different effectors under the *steA* promoter is likely a result of mRNA structural elements that affect protein translation. More specifically, by exchanging the 5' untranslated region of an effector protein with *steA*'s 5' untranslated region, there is some likelihood of either introducing or interrupting important secondary structural elements that either stabilize or destabilize the mRNA to affect translation initiation. This observation suggests that different promoter regions will need to be matched to certain effector proteins for robust protein expression. This effect can be tested along with promoter strength as a streamlined screening approach to obtain optimal expression and complementation conditions for visualizing different effector proteins. The modular platform for split-GFP labeling developed in this work enables the amplification of fluorescent signals by tuning effector protein expression level or by multimerizing the tag. These techniques could be used in the future in combination to amplify very low signals. Alternatively, the extent of multimerization of the GFP11 tag could be increased from 3x up to 7x for increasing signals of chromosomally tagged effectors<sup>200</sup>.

### **Further defining effector protein localization with split-GFP**

A strong feature of the split-GFP labeling system is that it is composed of genetically encodable elements and therefore can be adapted to address nuanced questions about localization by genetically targeting GFP1-10 to different regions of the host cell. With our system, we discovered that SlrP localizes to the host cell cytosol in epithelial cells at all times during infection, shedding light on two conflicting studies regarding SlrP's localization and potential functions within host cells. We could investigate this further by performing a thorough study of truncated versions of the SlrP protein and our ER localized GFP1-10 to verify whether or not any portion of SlrP gets delivered to the ER. Additionally, this technique could be applied to other effector proteins including SopA, which has been shown to localize to the mitochondria when transiently transfected but was unable to be detected using our system. SopA could be present in the mitochondrial matrix, explaining why cytosolic GFP1-10 was unable to show complementation. We could address this question of localization with our labeling system by expressing a mitochondrial targeted version of GFP1-10 during *Salmonella* infections.

### **Characterizing effector protein localization in primary BMDMs**

In this work, we examined primary BMDMs from immunocompetent mice (SV129S6), as a model for systemic infection. Because *S. Typhimurium* elicits a systemic typhoid-like disease in mice<sup>9</sup> and macrophage cells serve as a reservoir for persisting bacteria<sup>13</sup>, primary murine BMDM cells represent an ideal model to study chronic infection at the single cell level. It is becoming more evident that different modes of infection, such as acute infection (modeled by epithelial cells) versus chronic infection (modeled here in BMDM cells), require different responses from *Salmonella* to maintain intracellular survival and these differences may arise through differential presence and function of effector proteins<sup>19,126</sup>.

By examining effector localization and tracking internalized *Salmonella* in primary BMDMs, we discovered that bacteria don't cluster in a compact SCV the way they do in

epithelial cells or Raw264.7 cells. Additionally, effector proteins such as SteA, PipB2, and SseG localize to intracellular membranes as they do in Raw and epithelial cells, but they don't accumulate around bacteria, and *Salmonella*-induced tubules or filaments are not readily apparent. These results suggest that effectors may play substantially different roles in different niches and demonstrate the importance of studying effector protein localization in multiple infection models. It will be important to further investigate the repertoire of effector proteins in the BMDM model of infection in the future. Even though expression of exogenous material in BMDMs is challenging, with our system we were able to visualize split-GFP complementation as well as the nuclear BFP marker simultaneously. We could adapt this setup to accommodate an FP that localizes to an infection related feature or region in the host (such as GalT or LAMP-1 which often mark the SCV) as opposed to the nucleus and monitor co-localization of effector proteins tagged with split-GFP in real time. In addition, we could use fluorophore conjugated dextran to mark the SCV<sup>126</sup>, while tracking effector proteins with split-GFP. These experiments would allow us to further compare effector protein localization phenotypes between epithelial cell infection and BMDM infection in order to begin addressing whether different effector proteins serve different roles during the evolution of infection in different model systems.

### **Dual labeling to visualize multiple effector proteins**

The tools developed here open up the possibility of comparing the presence, localization, and dynamics of effector proteins in different types of infected host cells to identify the different roles these effector proteins play in different infection models. If the development of orthogonal imaging systems were pursued, we would be able to achieve visualizing multiple *Salmonella* effector proteins simultaneously. For example, the split-GFP system could be used to label one effector protein and another orthogonal tag to label another effector protein. One candidate system for this would be split-mCherry<sup>200</sup>, though the complementation signal efficiency would need to undergo further optimization prior to use with lowly abundant

*Salmonella* effector proteins. Another possible system is the Halo tag technology, which uses a modified bacterial haloalkane dehalogenase tag designed to covalently bind synthetic ligands such as fluorescent dyes<sup>201</sup>. Additionally, the Antigen-binding fragment (Fab)<sup>202,203</sup> system linked to a fluorophore could be recruited against a small epitope tag such as FLAG-labeled effector proteins. With dual labeling systems, we could use long-term imaging approaches to track multiple effector proteins over the course of infection. This setup could allow for the differentiation of the functions between two tightly linked effector proteins including SseG and SseF, which are hypothesized to work together throughout the infection process and have no known distinguishing features<sup>66,84,180,204</sup>.

## APPENDIX

### DEVELOPMENT OF FLUORESCENCE MICROSCOPY ASSAYS TO EXAMINE HOST CELL $\text{Ca}^{2+}$ TRANSIENTS DURING *SALMONELLA* INVASION OF HELA CELLS

#### A.1 INTRODUCTION

*Salmonella* is able to infect non-phagocytic epithelial cells through the use of T3SS-1 translocated effector proteins. Once present inside the host cell, T3SS-1 effector proteins hijack intracellular signaling pathways to initiate actin polymerization, leading to a dramatic rearrangement of the membrane and engulfment of *Salmonella* by macropinocytosis<sup>36</sup>. This event forms the SCV and has been linked to modulations in host intracellular concentrations of  $\text{Ca}^{2+}$ , an important and vital signaling ion in cells. Because  $\text{Ca}^{2+}$  signals impact a number of cellular pathways there has been interest in determining the mechanisms by which *Salmonella* invasion may induce these signals, and what consequences  $\text{Ca}^{2+}$  transients may have for infection.

Maintaining cellular  $\text{Ca}^{2+}$  homeostasis is a highly coordinated and tightly regulated process. Steady-state levels of  $\text{Ca}^{2+}$  are maintained through the activity of a number of receptors and channels within the plasma and organelle membranes<sup>205</sup>. During a signaling event, these receptors initiate  $\text{Ca}^{2+}$  release from intracellular stores or the extracellular environment to activate downstream processes including gene transcription, actin polymerization, and endocytosis. Given the importance of  $\text{Ca}^{2+}$  in multiple pathways, it is possible that *Salmonella* could manipulate and utilize host cell  $\text{Ca}^{2+}$  signaling during invasion. In fact, *Salmonella* effectors are able to modulate the levels and distribution of cell phosphoinositides<sup>206,207</sup>, the precursors to second messengers including diacylglycerol (DAG) and inositol-1,4,5-trisphosphate ( $\text{IP}_3$ ), which in turn impact host cell  $\text{Ca}^{2+}$ . Effector modulation of phosphoinositides is essential for the actin rearrangement that causes membrane ruffling upon

invasion and subsequent SCV biogenesis<sup>35,208</sup>. Therefore, modulation of  $\text{Ca}^{2+}$  signaling has the potential to affect the *Salmonella* invasion process. *Salmonella* invasion has been shown to correlate with  $\text{Ca}^{2+}$  transients in the host cytosol<sup>209</sup>. In addition, influx of  $\text{Ca}^{2+}$  from *Salmonella*-induced membrane injury enabled membrane repair in CHO cells<sup>210</sup>, while depletion of intracellular  $\text{Ca}^{2+}$  impaired bacterial uptake in HeLa cells<sup>206</sup>. However, there are discrepancies in the literature regarding the source of  $\text{Ca}^{2+}$ , its significance in bacterial uptake, and the correlation between  $\text{Ca}^{2+}$  dynamics and immune responses<sup>206,211,212</sup>. Many of the differences observed for invasion-associated  $\text{Ca}^{2+}$  dynamics are due to the fact that different tools and model systems were used across studies limiting the ability to directly compare results.

To define the origin and nature of infection-associated  $\text{Ca}^{2+}$  elevation, we examined *Salmonella* invasion of HeLa cells at the single cell level. This work was performed in collaboration with a former graduate student in the lab, Janet McCombs, who initiated the project. My contribution focused on developing new live cell fluorescence microscopy assays to study the host cell  $\text{Ca}^{2+}$  response in the context of infection. Initial studies performed by Janet used the ratiometric  $\text{Ca}^{2+}$  selective dye Fura2 to track *Salmonella* induced  $\text{Ca}^{2+}$  transients at the site of membrane ruffling in HeLa cells. This system proved to be useful for correlating host cell  $\text{Ca}^{2+}$  responses at ruffling sites when paired with differential interference contrast (DIC), which allowed identification of infected cells. Because the dye is membrane permeable, it labels every cell in a field of view, enabling visualization of potential  $\text{Ca}^{2+}$  dynamics for every infected cell in a field of view.

Unfortunately, there were some limitations of the Fura2/DIC experiments that limited reproducibility of long-term experiments. First, Fura2 has an excitation maximum in the UV, requiring cells to be exposed to high energy light, limiting the duration of imaging experiments due to phototoxicity-induced cell death or photobleaching of the dye. Additionally, the optical requirements for imaging Fura2 restricted experiments to a microscope that was not equipped with an environmental chamber or perfect-focus system, meaning we could not control factors

such as temperature and couldn't image over long time periods. I found that *Salmonella* induced  $\text{Ca}^{2+}$  transients were temperature dependent in that they directly correlated with invasion efficiency which is highly temperature sensitive (optimal at 37°C). Day-to-day fluctuations in ambient room temperature proved to be too difficult for obtaining reproducible infection assays. This discovery motivated the development of new approaches for investigating host cell  $\text{Ca}^{2+}$  perturbations during *Salmonella* invasion.

## **A.2 RESULTS AND DISCUSSION**

The original Fura2 data acquired by Janet using a Zeiss axiovert 200M widefield microscope in the Palmer Lab imaging room in the Cristol Chemistry building showed that approximately 80% of infected cells gave a detectable  $\text{Ca}^{2+}$  response. However, in the environment of the new imaging core facility in JSCBB, using the same microscope and imaging set up, we were unable to reproduce this result and instead observed only approximately 30% of infected cells gave a  $\text{Ca}^{2+}$  response. To investigate the origin of this difference, I looked into the effects of experimental parameters including multiplicity of infection (MOI), duration of imaging and the rate of image acquisition. MOI had a direct effect on the numbers of internalized bacteria but did not alter the percent of infected cells showing  $\text{Ca}^{2+}$  transients. However, imaging for a longer duration and acquiring images more rapidly, every 4 seconds as opposed to every 15 seconds, did indeed capture a higher percent of invaded cells showing  $\text{Ca}^{2+}$  transients (Figure A.1).

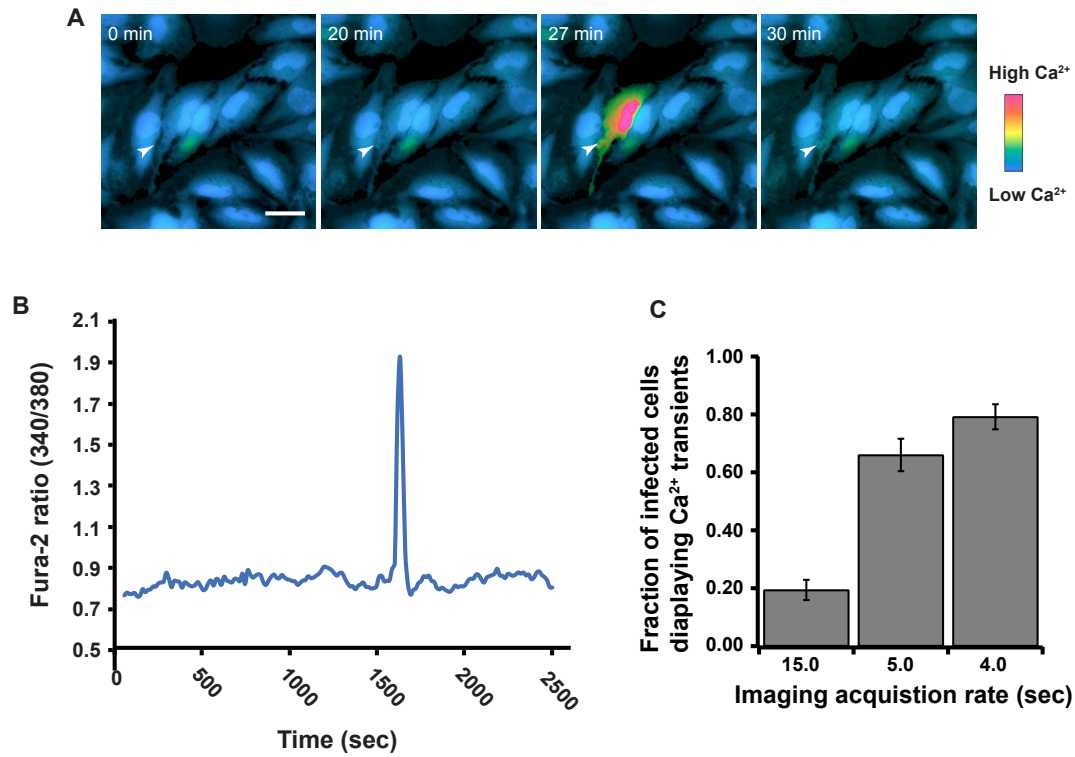


**Figure A.1. Image acquisition rate impacts visualization of Ca<sup>2+</sup> transients with Fura-2**

HeLa cells treated with Fura-2 were exposed to *Salmonella* and imaged immediately to capture bacterial induced host cell Ca<sup>2+</sup> responses. (A) Representative time-lapse images of a cell undergoing infection and displaying a *Salmonella* induced Ca<sup>2+</sup> transient. The arrow indicates the bacterial invasion site represented by plasma membrane ruffling. Shown are pseudo-colored ratio images of Fura-2 excitation (340/380 nm) that increases in the presence of Ca<sup>2+</sup>. Blue designates regions of lower Ca<sup>2+</sup>, where red indicates high levels of Ca<sup>2+</sup>. Scale bar = 20 μm (B) Time-trace of Fura-2 ratio (340nm/380nm) for the cell shown in (A). The region-of-interest measured encompasses the whole cell. (C) The average fraction of infected cells displaying a Ca<sup>2+</sup> transient was measured using 15 sec, 5 sec, and 4 sec imaging acquisition rates to assess whether rapid acquisition would capture more *Salmonella* induced Ca<sup>2+</sup> transients. n = 379 cells (15 sec), 104 cells (5 sec), and 121 cells (4 sec). Infected cells were identified by the presence of membrane ruffling events Error bars are the standard deviation between three replicates.

As mentioned previously, we were unable to directly investigate the role of temperature using Fura-2 due to restrictions of the microscope as the optics required for Fura2 were only available on a microscope that was not equipped with an environment chamber. To assess whether  $\text{Ca}^{2+}$  transients depended on temperature, we used the  $\text{Ca}^{2+}$ -sensitive intensimetric indicator Fluo-4<sup>211</sup> to track host cell  $\text{Ca}^{2+}$  responses during invasion and a microscope equipped with an environmental chamber that allowed us to regulate temperature, humidity and  $\text{CO}_2$ . These experiments revealed that there is a direct correlation with temperature and invasion efficiency, which was quantified by visualizing the number of ruffling events in Fluo-4 treated cells exposed to *Salmonella* at 25°C or 37°C (Fig A.2). Additionally, I found that invasions occurred more rapidly at 37°C than at 25°C, where the first observable ruffling events at 37°C occurred around 3 minutes, as opposed to 15 minutes at 25°C. I was unable to determine whether  $\text{Ca}^{2+}$  transients varied at the different temperatures due to the large discrepancy in invasion efficiencies. These results indicate that it is important to regulate temperature while studying *Salmonella* infection and further motivated us to establish a new assay that maintains the benefit of a ratiometric sensor, like Fura-2 but overcomes the limitations of Fura-2 mentioned previously.

A ratiometric sensor is preferable to an intensimetric one because it accounts for the issue of accumulating fluorophore at the gathering membrane during ruffling events. An increase in fluorophore population due to membrane gathering will yield an increase in fluorescence signal at the site of invasion. But, it wouldn't be possible to distinguish whether the fluorescence increase is due to accumulated fluorophore versus an increase in  $\text{Ca}^{2+}$ . Ratiometric sensors circumvent this issue because they indicate the presence of  $\text{Ca}^{2+}$  by a shift in excitation or emission wavelength, and the ratio of the different wavelengths will not be affected by sensor accumulation. Therefore, to visualize  $\text{Ca}^{2+}$  in HeLa cells during live infections I used the genetically encodable ratiometric  $\text{Ca}^{2+}$  responsive FRET sensor lynD3CPV (Fig A.3).

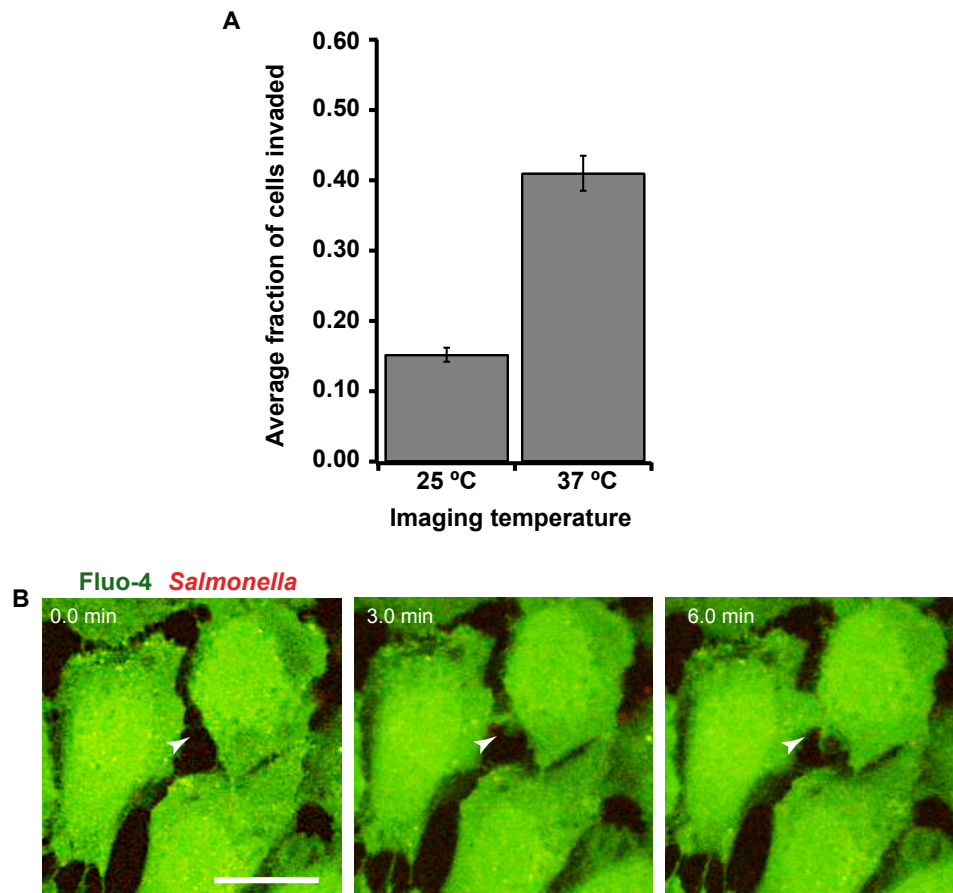


**Figure A.2. *Salmonella* infection efficiency is temperature dependent**

HeLa cells treated with Fluo-4 were exposed to *Salmonella* and imaged immediately to capture bacterial internalization, evident by host plasma membrane ruffling, and bacterial-induced host cell  $\text{Ca}^{2+}$  responses. (A) The average fraction of cells displaying membrane ruffling within 30 minutes post exposure to bacteria was measured at 25°C and 37°C. These data represent the number of cells in a field of view that had a visible ruffling event divided by the total number of cells in the field of view. (B) Representative fluorescence image of a cell undergoing infection and displaying plasma membrane ruffling. Fluo-4 fluorescence signal represented in green and *Salmonella* in red. Scale bar = 20  $\mu\text{m}$ .

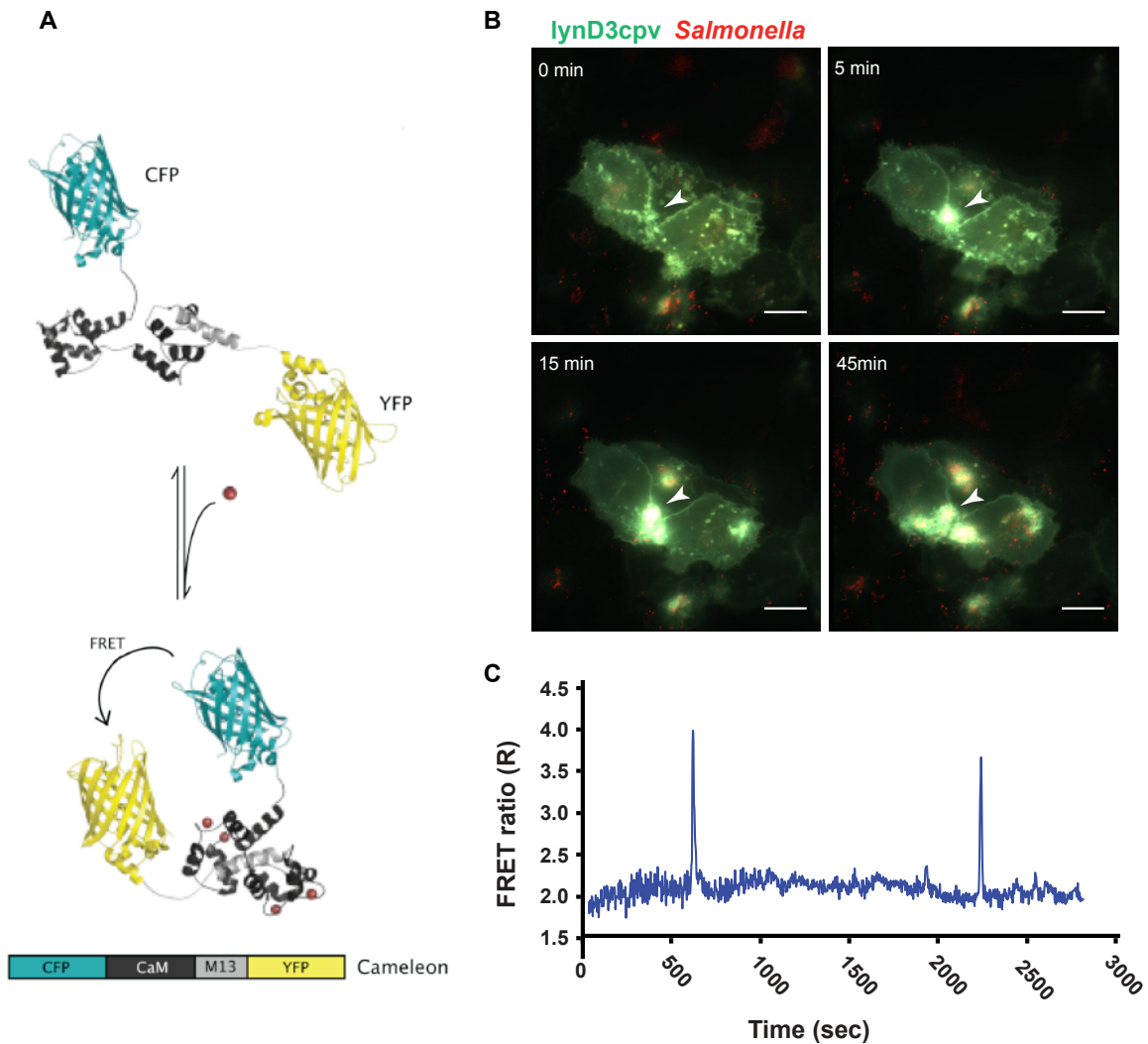


**Figure A.3. Host cell  $\text{Ca}^{2+}$  responses to *Salmonella* internalization measured with the genetically encodable FRET sensor *lynD3cpv***

HeLa cells expressing the membrane localized  $\text{Ca}^{2+}$  sensor *lynD3cpv* were exposed to *Salmonella* and imaged immediately to capture bacterial internalization, evident by host plasma membrane ruffling, and bacterial-induced host cell  $\text{Ca}^{2+}$  responses. (A) The genetically encodable FRET sensor D3cpv, derived from the Cameleon family of sensors, responds to labile  $\text{Ca}^{2+}$  by undergoing a conformation change that increases FRET between CFP and YFP (cpVenus). D3cpv is localized to the plasma membrane with the addition of an N-terminal myristoylation-palmitoylation sequence derived from Lyn kinase (Figure adapted from McCombs and Palmer, 2008)<sup>213</sup>. (B) Representative fluorescence overlay image of cells undergoing infection. Red is *Salmonella* and yellow is *lynD3cpv* FRET. The arrow designates one ruffling event over time, the FRET ratio of which is plotted in (C). (C) FRET ratio trace representing local  $\text{Ca}^{2+}$  transients at the designated ruffling site for the total of 45 minutes post exposure to bacteria. Scale bar = 20  $\mu\text{m}$ .

The optical requirements of lynD3cpv enabled the use of a widefield fluorescence microscope equipped with an environmental chamber, where I was able to regulate temperature for reproducible infections and could carry out longer term imaging experiments. Additionally, the lynD3CPV sensor is localized to the host cell membrane, which allowed for visualization of membrane ruffling concurrent with local cytosolic  $\text{Ca}^{2+}$  responses. This feature eliminated the need to pair with DIC and enabled faster acquisitions in order to capture more rapid  $\text{Ca}^{2+}$  transients.

Using the new experimental conditions along with pharmacological host cell treatments and *Salmonella* strains carrying specific genetic deletions, I probed the source of the  $\text{Ca}^{2+}$  transients (Fig A.4). Additionally, I investigated whether the presence of the T3SS-1 translocon and the effector protein SopB was important for the  $\text{Ca}^{2+}$  transients. Finally, I asked whether the presence of  $\text{Ca}^{2+}$  transients impacted infection efficiency (Fig A.4). Cells were imaged in the absence of bacteria and in the presence of heat killed bacteria as controls. Both of these conditions generated very little  $\text{Ca}^{2+}$  response (Fig A.4.A).

A *Salmonella* strain harboring the deletion of *invA* ( $\Delta invA$ ) and unable to assemble the T3SS-1 translocon was used to assess whether the translocon and associated T3SS-1 translocated effector proteins played a role in generating host cell  $\text{Ca}^{2+}$  transients. *Salmonella* that were unable to introduce effector proteins elicited a much lower  $\text{Ca}^{2+}$  response, however the presence of transients were not abolished (Fig A.4.A). This result indicates that the T3SS-1 and translocated effector proteins have an impact on invasion-associated  $\text{Ca}^{2+}$  transients. The fact that some transients were observed in the absence of the effector proteins necessary for *Salmonella* internalization is consistent with the presence of alternate invasion pathways being used by the bacteria, such as the zipper mode of entry mediated by the outer membrane protein Rck<sup>148,158</sup>.

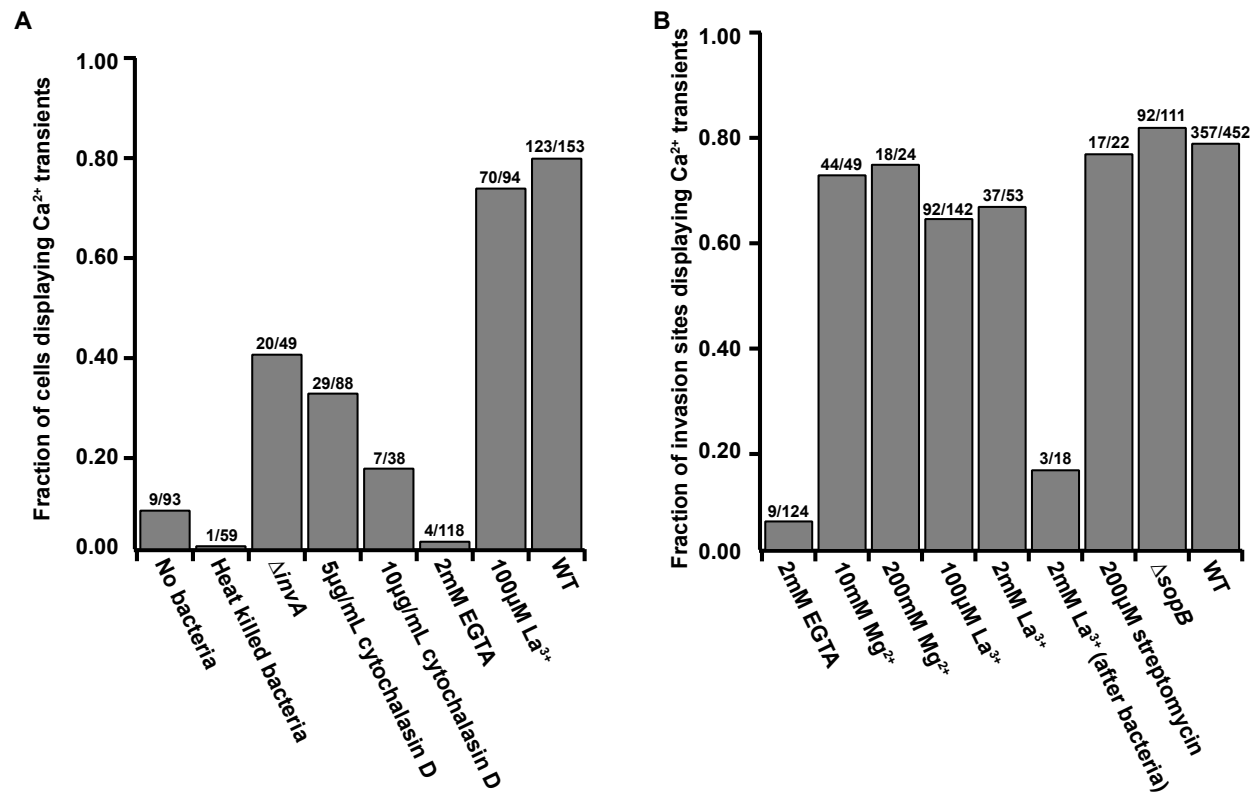


**Figure A.4. Ca<sup>2+</sup> transients near the plasma membrane of infected host cells are dependent on extracellular Ca<sup>2+</sup>**

HeLa cells expressing the membrane localized Ca<sup>2+</sup> sensor lynD3cpv were exposed to *Salmonella* and imaged immediately to capture bacterial induced host cell Ca<sup>2+</sup> responses. (A) Whole cell regions were assessed for Ca<sup>2+</sup> responses and the fraction of HeLa cells that showed visible Ca<sup>2+</sup> transients via increased lynD3cpv FRET ratios are reported. The number of cells quantified for each treatment or condition is indicated above the bar (B) Regions of interest localized to host membrane ruffling events were assessed for Ca<sup>2+</sup> responses via lynD3cpv FRET ratios. The fraction of invasion sites (indicated by ruffling events) showing transient increases in lynD3cpv FRET ratios is quantified for each treatment or condition and is indicated above the bar. All results indicated are within 60 minutes of exposure to *Salmonella*.

To investigate whether  $\text{Ca}^{2+}$  transients were upstream of effector protein mediated actin assembly and membrane ruffling; HeLa cells were treated with the mycotoxin cytochalasin D to prevent invasion induced actin polymerization. Infections with cytochalasin D-treated HeLa cells showed a dose dependent effect of the inhibitor, which decreased the presence of  $\text{Ca}^{2+}$  transients (Fig A.4.A). This indicates that *Salmonella*-induced actin polymerization and associated membrane ruffling play a role in the observed  $\text{Ca}^{2+}$  response.

The activity of the effector protein SopB has been implicated in modulating the levels and distribution of host cell phosphoinositides<sup>206,207</sup>, the precursors to second messengers including diacylglycerol (DAG) and inositol-1,4,5-trisphosphate ( $\text{IP}_3$ ), which in turn impact host cell  $\text{Ca}^{2+}$ . This modulation of phosphoinositides is essential for the actin rearrangement that causes membrane ruffling upon invasion and subsequent SCV biogenesis<sup>35,208</sup>. Because membrane ruffling seems to play a role in the observed  $\text{Ca}^{2+}$  transients upon invasion, we investigated whether the activity of the effector protein SopB was involved. However, carrying out infections with a strain of *Salmonella* lacking SopB ( $\Delta\text{sopB}$ ) did not alter the occurrence of  $\text{Ca}^{2+}$  transients compared to wild type (Fig A.4.B).

Pharmacological perturbations that did not interfere with membrane ruffling were carried out and infections were analyzed for  $\text{Ca}^{2+}$  transients local to membrane ruffling sites. These perturbations were used to assess the source of  $\text{Ca}^{2+}$  and the mode by which it was introduced to the cytosol. Cells were treated with  $\text{Ca}^{2+}$  free media containing 2mM EGTA (ethylene glycol-bis( $\beta$ -aminoethyl ether)-N,N,N',N'-tetraacetic acid) to remove  $\text{Ca}^{2+}$  from the extracellular environment and investigate whether the source of  $\text{Ca}^{2+}$  transients was extracellular influx. Infections in the absence of extracellular  $\text{Ca}^{2+}$  showed very little host cell  $\text{Ca}^{2+}$  response indicating that the source of  $\text{Ca}^{2+}$  was largely extracellular. To further probe the mode of  $\text{Ca}^{2+}$  influx and differentiate between entry through a channel or a plasma membrane pore, lanthanum (III) chloride was used to block membrane channels. However,  $\text{La}^{3+}$  salts precipitate rapidly upon exposure to phosphates and even with phosphate free media, the presence of  $\text{La}^{3+}$

formed a white precipitate on the surface of HeLa cells. This phenomenon limited our ability to assess infection results because we could not accurately determine how much  $\text{La}^{3+}$  remained soluble to function as a  $\text{Ca}^{2+}$  channel inhibitor. The results of these experiments indicated that  $\text{La}^{3+}$  treatment in our phosphate free imaging buffer did not alter  $\text{Ca}^{2+}$  transients significantly compared to wild type (Fig A.4.A). Different concentrations of the  $\text{Ca}^{2+}$  channel blockers streptomycin,  $\text{Mg}^{2+}$  and  $\text{La}^{3+}$  were used to further assess the role of  $\text{Ca}^{2+}$  channels in the observed influx (Fig A.4.B). These treatments had little effect, with the exception of 2mM  $\text{La}^{3+}$  when introduced immediately following addition of bacteria to HeLa cells. However, this version of  $\text{La}^{3+}$  treatment resulted in the abolishment of invasion events in two out of three of the dishes tested, and the results are therefore difficult to interpret.

Based on the lack of effect of  $\text{Ca}^{2+}$  channel inhibitors, we asked whether the *Salmonella* T3SS translocon generated pores in the plasma membrane (Fig A.5.A). To assess the presence of *Salmonella* induced membrane punctures or pores we used a cell membrane permeability assay with the impermeable dye GelRed. GelRed, like ethidium bromide, intercalates into DNA marks the nucleus if the plasma membrane is compromised. HeLa cells were treated with GelRed and imaged in the presence and absence of digitonin, a detergent used to permeabilize membranes (Fig A.5.B). Only cells exposed to digitonin showed GelRed labeled nuclei. When GelRed treated cells were subjected to *Salmonella* and imaged for 60 min, the only infected cells that demonstrated GelRed labeled nuclei had undergone visible death (Fig A.5.C), suggesting that *Salmonella* does not generate a large pore that would allow  $\text{Ca}^{2+}$  to enter the host cytosol from the extracellular milieu. However, one caveat of this interpretation is that  $\text{Ca}^{2+}$  is much smaller than GelRed so a small pore made by the T3SS couldn't be ruled out. To test this possibility, we used the  $\text{Zn}^{2+}$  responsive FRET sensor ZapCV2 and infected cells in the presence of 20  $\mu\text{M}$  extracellular  $\text{Zn}^{2+}$ . However, we did not detect  $\text{Zn}^{2+}$  influx upon invasion (results not shown).

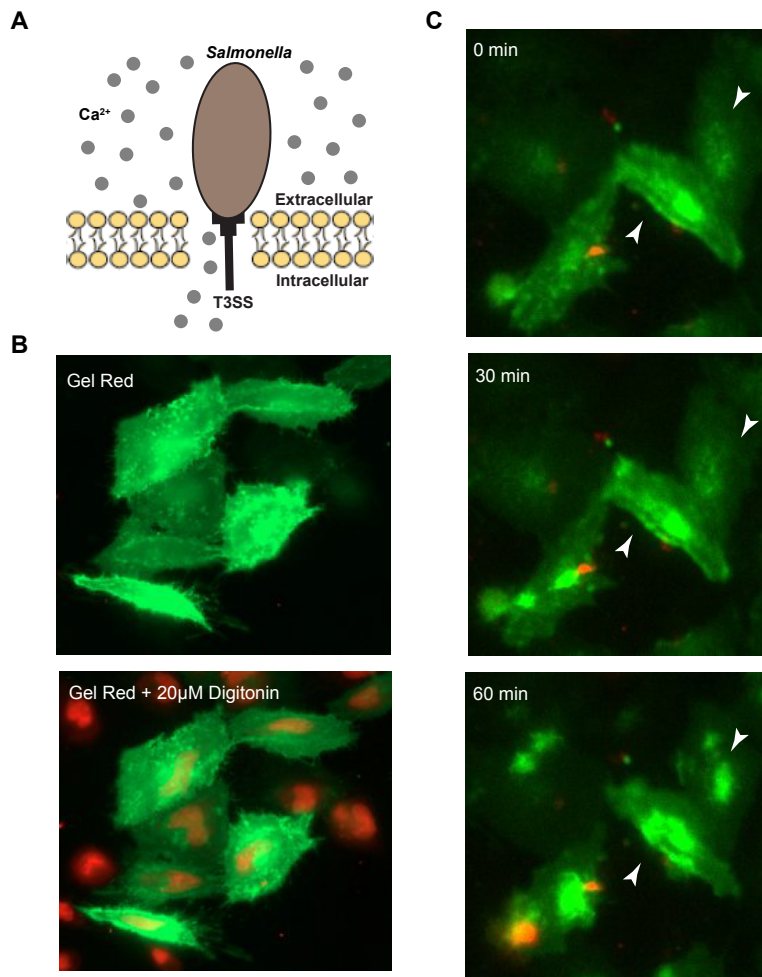


**Figure A.5. *Salmonella* infection does not create large host cell membrane pores**

HeLa cells expressing lymD3cpv were treated with 1  $\mu\text{g}/\text{mL}$  GelRed and tested for *Salmonella* induced membrane pores or punctures. (A) Host cell membrane pores or punctures created by the *Salmonella* T3SS injectisome as it penetrates the membrane could allow  $\text{Ca}^{2+}$  and other small extracellular material, like GelRed, to seep into the host cytoplasm. (B) GelRed treated HeLa cells before (above) and after (below) membrane permeabilization by 20  $\mu\text{M}$  digitonin. Green is lymD3cpv marking the cell membrane and red is GelRed localized to nuclei. (C) GelRed treated HeLa cells were infected with *Salmonella* and imaged for 90 min to identify cells with infection induced compromised plasma membranes via GelRed labeled nuclei. The arrows indicate infection sites marked by a ruffling event to designate the cell as infected. The designated infected cells do not display GelRed labeled nuclei. The cells that do display GelRed labeled nuclei have undergone cell death.

We next explored how the  $\text{Ca}^{2+}$  responses observed during *Salmonella* invasion differed between cells and invasion sites. This approach was used to investigate whether different types of  $\text{Ca}^{2+}$  responses could be correlated to some signaling event or infection phenotype. A FRET trace analysis was developed to analyze  $\text{Ca}^{2+}$  transients localized at membrane ruffling sites (Fig A.6). The trace analysis quantified the number of transients at a ruffling site, the size of each signal and the timing of each signal in order to identify whether or not any patterns existed. We were able to identify eight different trace phenotypes (Fig A.6.A-H) and we found that 80% of ruffling sites corresponded to some type of  $\text{Ca}^{2+}$  transient (Fig A.6.I). Based on this analysis we found that the majority of  $\text{Ca}^{2+}$  transients occur early after exposure to *Salmonella* (within 10 min). However, the traces most indicative of signaling, oscillations and large plateaus, occurred rarely indicating that these phenotypes are not correlated to routine infection signaling events (Fig A.6.J).

To determine whether  $\text{Ca}^{2+}$  influx was important to the infection process, we performed a CFU assay and replication assay to test whether removal of the  $\text{Ca}^{2+}$  signal by depleting extracellular  $\text{Ca}^{2+}$  altered infection or replication properties. The CFU assay was performed using gentamycin protection at early time points post challenge with *Salmonella* to investigate the significance of  $\text{Ca}^{2+}$  influx on *Salmonella* uptake (Fig A.7). The replication assay allowed infections to proceed for 16 hours in order to visualize and enumerate the internalized replicating bacterial population in fixed infected cells (Fig A.8). The results of these experiments suggested that the presence of extracellular  $\text{Ca}^{2+}$  had little effect on *Salmonella*'s ability to invade and replicate within HeLa cells. It is important to note that the CFU assay is a bulk population study that does not provide enough resolution to reveal cell-to-cell variations in infection phenotypes. Additionally, the invasion assay is a static technique that lacks the ability to capture dynamic infection phenotypes. It is therefore possible that  $\text{Ca}^{2+}$  has some role in different modes of infection; however, we were unable to detect this using CFU and invasion assays.

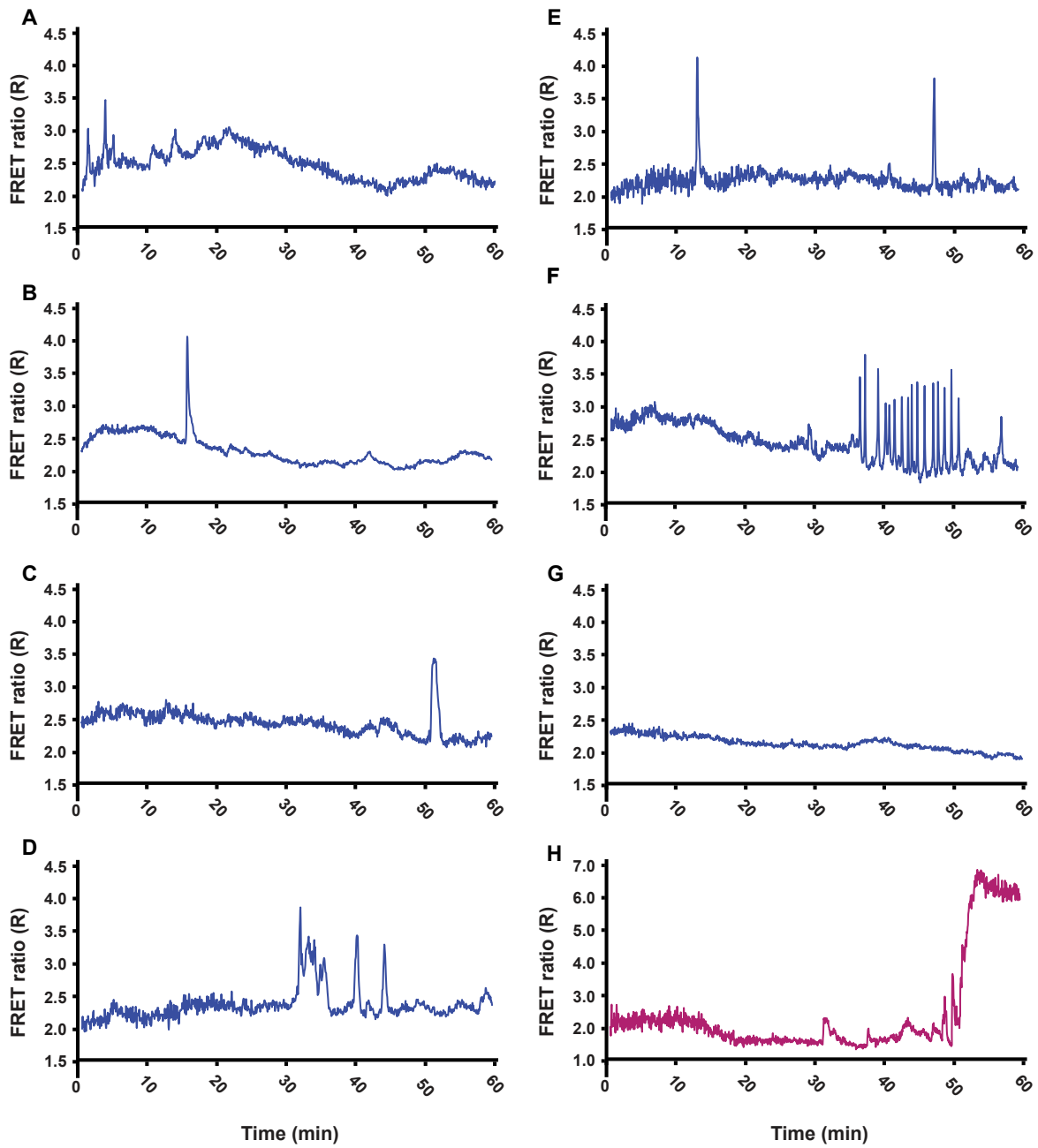
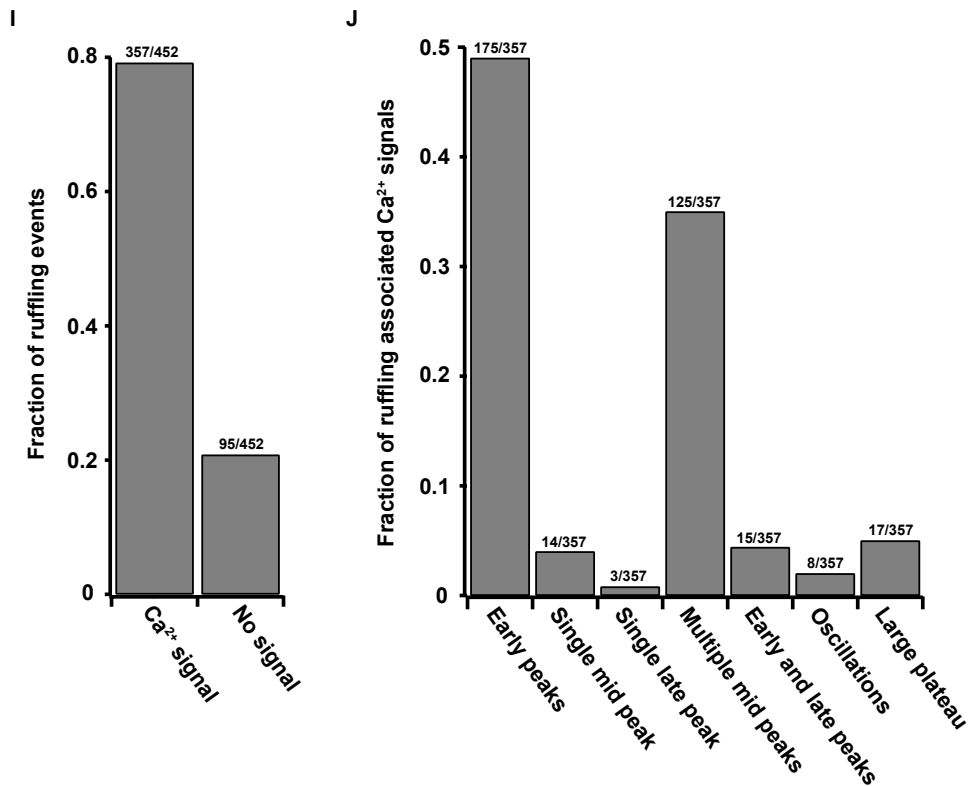
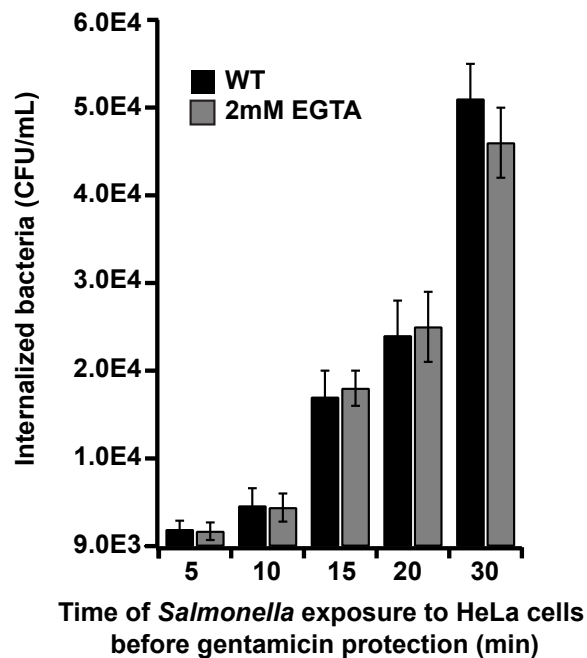


Figure A.6. *Salmonella* induced host cell  $Ca^{2+}$  transients have multiple phenotypes



**Figure A.6 (continued). *Salmonella* induced host cell Ca<sup>2+</sup> transients have multiple phenotypes**

We explored different types of Ca<sup>2+</sup> responses based on an analysis of lynD3cpv FRET signal traces (A-H) during wild type infection to investigate potential signaling implications. HeLa cells expressing lynD3cpv were imaged during exposure to *Salmonella* for the duration of 1hr. (A-H) Representative FRET traces of individual membrane ruffling sites demonstrating Ca<sup>2+</sup> transients show multiple trace phenotypes. The resulting trace phenotypes were categorized as follows (A) early peaks (within 10 min of *Salmonella* exposure) (B) a single mid range peak (between 10-30 min post *Salmonella* exposure) (C) a single late peak (after 40 min) (D) multiple mid range peaks (E) individual early and late peaks (F) oscillations (G) no peaks (H) late large plateau. (I) The fraction of ruffling events showing detectable local Ca<sup>2+</sup> signals was quantified. (J) The ruffling events that did show Ca<sup>2+</sup> signals were analyzed and categorized by trace phenotype to indicate the regularity of each phenotype.



**Figure A.7. Extracellular  $\text{Ca}^{2+}$  is not essential for *Salmonella* internalization in HeLa cells**

HeLa cells seeded into 12-well dishes pre-treated with poly-L-lysine were challenged with *Salmonella* and subjected to gentamicin protection (100 $\mu\text{g}/\text{mL}$ ) at 5, 10, 15, 20, or 30 minutes post exposure to bacteria. All infections were allowed to proceed for the total of 1 hour before cells were permeabilized and assayed for colony forming units (CFUs). The average internalized bacteria (CFU/mL) are shown for the different exposure times prior to gentamicin protection. Error bars are the standard deviation between 3 replicates.

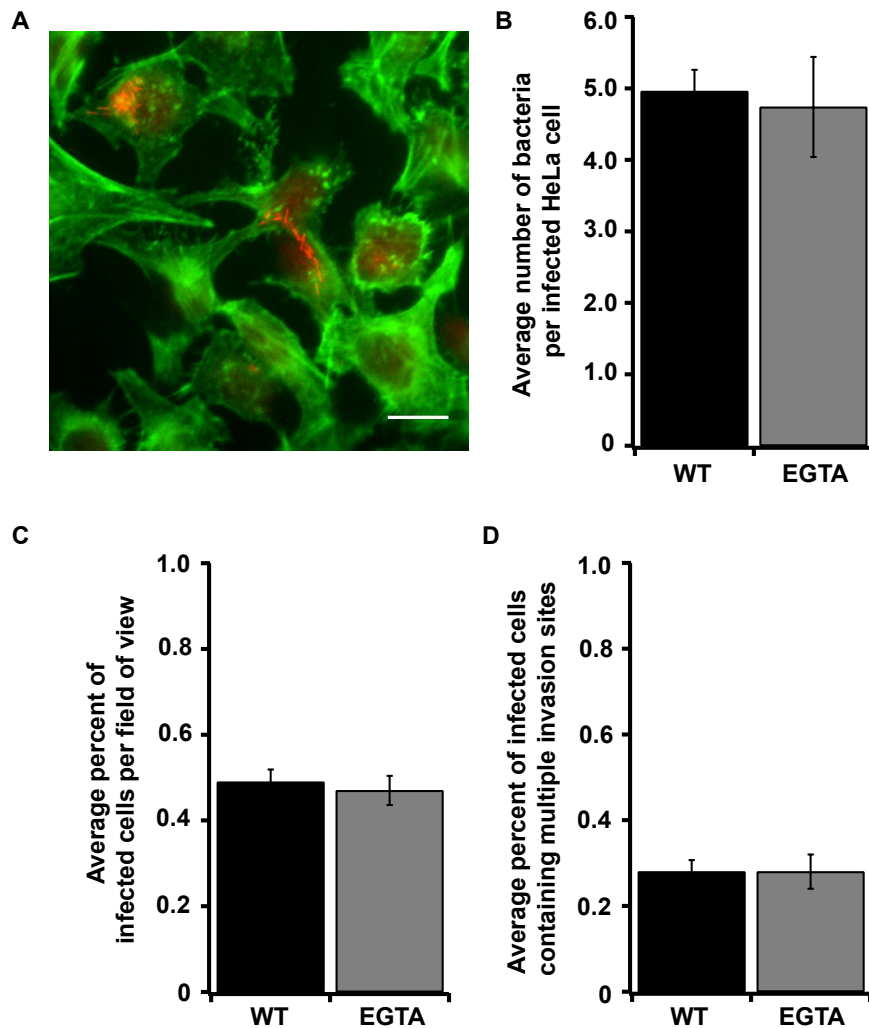


**Figure A.8. Extracellular  $\text{Ca}^{2+}$  is not essential for *Salmonella* infection or replication in HeLa cells**

HeLa cells seeded onto coverslips pre-treated with poly-L-lysine were infected with *Salmonella* and were subsequently fixed and stained at 16hr p.i. (A) A representative image of *Salmonella* infected HeLa cells. Green = phalloidin, Red = *Salmonella* expressing mCherry. (B-D) The infection efficiency for untreated cells (WT) or cells treated with 2mM EGTA to remove extracellular  $\text{Ca}^{2+}$  (EGTA) was quantified as follows: (B) The average number of internalized bacteria per infected cell, (C) the average percent of cells in a field of view that are infected with *Salmonella*, and (D) the average percent of cells containing more than one invasion site. n = 452 cells (WT) and 490 cells (EGTA). Error bars are the standard deviation between 3 slides. For the invasion assay, percent of cells infected: WT =  $0.47 \pm 0.034$ , EGTA =  $0.49 \pm 0.029$ , Average salmonella per cell: WT =  $4.96 \pm 0.3$ , EGTA =  $4.74 \pm 0.7$ , cells with multiple invasion sites: WT =  $0.28 \pm 0.04$ , EGTA =  $0.28 \pm 0.027$

## Conclusion

Ultimately, I found that the presence of extracellular  $\text{Ca}^{2+}$  was necessary for the occurrence of cytosolic  $\text{Ca}^{2+}$  transients in the host cell during infection; however, extracellular  $\text{Ca}^{2+}$  had no detectable impact on membrane ruffling or invasion efficiency. Deletion of T3SS1 decreased the fraction of cells exhibiting transients but did not abolish the transients altogether, this could be due to the presence of alternate invasion mechanisms used by *Salmonella*. Because *Salmonella* is known to use both a trigger and zipper mechanism to invade epithelial cells, removing the ability for *Salmonella* to use the trigger mechanism decreases the amount of internalized bacteria but does not prevent infection<sup>158</sup>. These results suggest that  $\text{Ca}^{2+}$  transients reliably occur during the endocytosis of *Salmonella* by HeLa cells but that  $\text{Ca}^{2+}$  signals are not required for successful internalization (there is no difference in the fraction of cells with bacterial colonies at 16 hours post infection in the absence of extracellular  $\text{Ca}^{2+}$ ). One hypothesis consistent with literature on endocytosis is that extracellular fluid containing high concentrations of  $\text{Ca}^{2+}$  is encapsulated upon macropinosome formation and then  $\text{Ca}^{2+}$  is evacuated along with other ions as an important step in endosomal maturation. The cytosolic signal could be a consequence of clearing  $\text{Ca}^{2+}$  from the vacuole. This scenario is consistent with the observation that eliminating extracellular  $\text{Ca}^{2+}$  diminishes visible cytosolic transients but does not impede internalization of *Salmonella* according to the invasion assay. However, because the host cell  $\text{Ca}^{2+}$  response was shown to have no detectable effect on the infection process, at least for the assays used in this study, we have decided not to pursue publication on this project.

## **METHODS**

### **Bacterial strains**

All strains used in this study were isogenic derivatives of *Salmonella enterica* serovar Typhimurium SL1344 constitutively expressing mCherry from a plasmid (parent pACYC177) under the *rpsM* ribosomal gene promoter. *Salmonella* gene deletion strains ( $\Delta invA$ ,  $\Delta sopB$ ) were generated as described previously<sup>193-195</sup> using lambda Red recombination.

#### *Growth for infections:*

For infection of HeLa cells, *Salmonella* strains were grown in LB (EMD) supplemented with 300 mM NaCl (Fisher Scientific) and 25 mM MOPS (Sigma) at pH 7.6 and appropriate antibiotics at 37°C for 16 hours without aeration. Prior to infection, bacteria were diluted 1:33 in 3 ml of SPI-1 media, with appropriate antibiotics for 4 hours at 37 °C without aeration.

#### *Heat killed bacteria:*

Cultures of *Salmonella* prepared for infection were aliquoted into Eppendorf tubes and boiled at 95°C for 20 min. Tubes were cooled to room temperature prior to using the heat killed cultures in experiments.

### **Mammalian cell culture and infection**

HeLa cells were maintained in DMEM (Gibco) supplemented with 10% FBS (Gibco), 100 Units/mL penicillin G sodium (Gibco), and 100 µg/mL streptomycin sulfate (Gibco) at 37°C with 5% CO<sub>2</sub>.

#### *Transfections:*

HeLa cells between a passage number of 2-10 were seeded into 35 mm glass-bottom dishes and allowed to proliferate for 24 hours. Transfection of pcDNA3-lynD3cpv was achieved using

*TransIT-LT1* (Mirus) transfection reagent and conditions recommended by the manufacturer for 0.5 µg of DNA. Transfected cells were incubated at 37°C with 5% CO<sub>2</sub> for 48 hours prior to

*Infections:*

HeLa cells expressing lynD3cpv or HeLa cells treated with Fura-2 or Fluo-4 dye were challenged with *Salmonella* grown under SPI-1 inducing conditions at a multiplicity of infection (MOI) of 50-100. Infections were allowed to proceed for 30 minutes at 37°C and 5% CO<sub>2</sub> before a gentamicin protection was carried out, where the *Salmonella*-containing media was exchanged with phenol red free DMEM containing 10% FBS (HeLa cells) or 20% FBS (macrophages) and 100 µg/mL gentamicin, to eliminate any non-internalized bacteria. After incubating for 45 minutes in a high concentration of gentamicin at 37°C and 5% CO<sub>2</sub>, the media was replaced with phenol red free DMEM containing 10%FBS and a low concentration (10 µg/mL) gentamicin to limit extracellular bacteria for the remainder of the experiment.

*Invasion assay:*

HeLa cells seeded into 12 well dishes containing sterilized coverslips were washed with HHBSS and infected as described previously. Following invasion and gentamycin protection, cells were washed with PBS and fixed with 3.7% paraformaldehyde in PBS for 10min at room temperature. Cells are then washed twice with PBS and incubated briefly with 20mM ammonium chloride to quench the paraformaldehyde and permeablized with 0.1% Triton. The fixed and permeabilized cells are then stained with 50µg/mL coumarin labeled phalloidin.

*CFU assay:*

HeLa cells were seeded into 12-well cell culture plates maintained in antibiotic-free DMEM supplemented with 10% FBS and were held at 37 °C with 5% CO<sub>2</sub> throughout the infection process. Infections with *Salmonella* strains were carried out as described above. At 5, 10, 15,

and 30 minute time points post exposure to *Salmonella* cells were treated with 100µg/mL gentamicin to eliminate non-internalized bacteria, and infections were allowed to proceed with gentamicin protection for the duration of an hour. The infected cells were then rinsed twice with PBS and incubated with 0.1% Triton in PBS at room temperature for 5 min. A series of dilutions in PBS were generated and plated in quadruplicate on appropriate antibiotic containing LB–Agar plates. After growth overnight, the CFUs were calculated for each infection condition.

### **Fluorescence imaging:**

All infection imaging was performed in replicates of 3 or more, and imaged on either a Nikon Ti-E wide-field or a Zeiss Axiovert 200M wide-field microscope. The Nikon Ti-E wide-field microscope was equipped with the NIKON ELEMENTS software platform, Ti-E Perfect Focus system, a motorized XY stage with a Ti Z drive and an environmental chamber (Pathology Devices) to maintain the cells at 37°C, 5% CO<sub>2</sub> and 70% humidity. Images acquired on this microscope used a 20x air objective (NA 0.5) or a 60x oil objective (NA 1.40), an iXon3 897 EMCCD camera (Andor) and a xenon-arc lamp to image mCherry *Salmonella* (excitation: 560/40 nm, emission: 630/75 nm, dichroic: 585 nm) Fluo-4 (excitation: 427/30 nm, emission: 520/40 nm, dichroic: 490 nm), and lynD3cpv FRET (donor excitation: 434/17 nm, donor emission: 474/23 nm, dichroic: 458 nm; acceptor excitation: 500/20 nm, acceptor emission: 535/30 nm, dichroic: 515 nm; FRET excitation 434/17 nm, FRET emission: 535/30 nm, FRET dichroic: 515 nm). The Zeiss Axiovert 200M wide-field microscope was equipped with a Lambda 10-3 filter changer (Sutter Instruments) and Cascade 512B camera (Photometrics). Images were acquired at room temperature using METAFLUOR software (Universal Imaging). Experiments were performed using a 40x oil objective (1.3 NA) using either 1X or 1.6X optovar to image Fura-2 (excitation: 340/26 nm, 380/10 nm, emission: 535/40 nm, dichroic: 455 nm), GFP (excitation: 480/20 nm, emission: 510/20 nm, dichroic: 495 nm), and mCherry *Salmonella* (excitation: 577/20 nm, emission: 630/60 nm, dichroic: 595 nm).

*Imaging live infections:*

For live imaging of *Salmonella* internalization, HeLa cells expressing lynD3cpv or HeLa cells treated with Fura-2 or Fluo-4 that had been seeded into 3.5 cm glass bottom dishes were washed and placed in Hank's Balanced Salt Solution with HEPES (20mM HEPES, 1X HBSS (Gibco), and 2g/L D-glucose, pH 7.2) or Ca<sup>2+</sup>-free HHBSS (20mM HEPES, 1X HBSS without Ca<sup>2+</sup>, Mg<sup>2+</sup>, or sodium bicarbonate, 2g/L D-glucose, 490mM MgCl<sub>2</sub>, 450mM MgSO<sub>4</sub>, pH 7.2). Following treatment, dishes were positioned on the microscope and a field of view was selected. Bacteria were added to the cells at an MOI of 50-100 after acquiring several frames. The infections were then allowed to proceed for up to 60 min capturing fluorescence images as rapidly as possible using the acquisition setting "no delay" in Nikon Elements

*FRET trace analysis:*

The NIKON ELEMENTS software platform was used to generate fluorescence intensity traces corresponding to Ca<sup>2+</sup> transients at localized invasion sites. Regions of interest were selected around individual invasion sites, indicated by membrane ruffling events that were visible due to the membrane-localized fluorescence of lynD3cpv. NIKON ELEMENT traces of measured fluorescence signal intensities within each ROI were all exported in excel format. These included intensity information from: CFP, CFP-YFP FRET and the FRET ratio channels. An automated MATLAB-based analysis (script written by Kyle Carter) was then used to further analyze the FRET traces by enabling automated background correction and conversion of quantified signal data into graphical traces of FRET ratio over time for characterization of the observed Ca<sup>2+</sup> transients.

## REFERENCES

1. Barlow, M. & Hall, B. G. Origin and Evolution of the AmpC-Lactamases of *Citrobacter freundii*. *Antimicrob. Agents Chemother.* **46**, 1190–1198 (2002).
2. Schikora, A. *et al.* Conservation of *Salmonella* Infection Mechanisms in Plants and Animals. *PLoS ONE* **6**, e24112 (2011).
3. Eng, S.-K. *et al.* *Salmonella*: A review on pathogenesis, epidemiology and antibiotic resistance. 1–11 (2015). doi:10.1080/21553769.2015.1051243
4. Crump, J. A., Luby, S. P. & Mintz, E. D. The global burden of typhoid fever. *Bulletin of the World Health Organization* **82**, 346–353 (2004).
5. Majowicz, S. E. *et al.* The Global Burden of Nontyphoidal *Salmonella* Gastroenteritis. *CLIN INFECT DIS* **50**, 882–889 (2010).
6. Reeves, M. W., Evins, G. M., Heiba, A. A., Plikaytis, B. D. & Farmer, J. J., III. Clonal Nature of *Salmonella typhi* and Its Genetic Relatedness to Other *Salmonellae* as Shown by Multilocus Enzyme Electrophoresis, and Proposal of *Salmonella bongori* comb. nov. *Journal of Clinical Microbiology* **27**, 313–320 (1989).
7. Brenner, F. W., Villar, R. G., Angulo, F. J., Tauxe, R. & Swaminathan, B. *Salmonella* Nomenclature. *Journal of Clinical Microbiology* **38**, 2465–2467 (2000).
8. Gal-Mor, O., Boyle, E. C. & Grassl, G. A. Same species, different diseases: how and why typhoidal and non-typhoidal *Salmonella enterica* serovars differ. *Front. Microbio.* **5**, 1–10 (2014).
9. Steele-Mortimer, O. The *Salmonella*-containing vacuole—Moving with the times. *Current Opinion in Microbiology* **11**, 38–45 (2008).
10. Haraga, A., Ohlson, M. B. & Miller, S. I. *Salmonellae* interplay with host cells. *Nat Rev Micro* **6**, 53–66 (2008).
11. McCormick, B. A. *et al.* Surface Attachment of *Salmonella typhimurium* to Intestinal Epithelia Imprints the Subepithelial Matrix with Gradients Chemotactic for Neutrophils. *The Journal of Cell Biology* **131**, 1599–1608 (1995).
12. Santos, R. L. *et al.* Life in the inflamed intestine, *Salmonella* style. *Trends in Microbiology* **17**, 498–506 (2009).
13. Monack, D. M., Bouley, D. M. & Falkow, S. *Salmonella typhimurium* Persists within Macrophages in the Mesenteric Lymph Nodes of Chronically Infected Nrampl1+/+ Mice and Can Be Reactivated by IFN $\gamma$  Neutralization. *Journal of Experimental Medicine* **199**, 231–241 (2004).
14. Ruby, T., McLaughlin, L., Gopinath, S. & Monack, D. *Salmonella*'s long-term relationship with its host. *FEMS Microbiology Reviews* **36**, 600–615 (2012).
15. Bakowski, M. A., Braun, V. & Brumell, J. H. *Salmonella*-Containing Vacuoles: Directing Traffic and Nesting to Grow. *Traffic* **9**, 2022–2031 (2008).
16. Moest, T. P. & Méresse, S. *Salmonella* T3SSs: successful mission of the secret(ion) agents. *Current Opinion in Microbiology* **16**, 38–44 (2013).
17. Marlovits, T. C. & Stebbins, C. E. Type III secretion systems shape up as they ship out. *Current Opinion in Microbiology* **13**, 47–52 (2010).
18. McClelland, M. M. *et al.* Complete genome sequence of *Salmonella enterica* serovar Typhimurium LT2. *Nature* **413**, 852–856 (2001).
19. LaRock, D. L., Chaudhary, A. & Miller, S. I. *Salmonellae* interactions with host processes. *Nat Rev Micro* **13**, 191–205 (2015).
20. McGhie, E. J., Brawn, L. C., Hume, P. J., Humphreys, D. & Koronakis, V. *Salmonella* takes control: effector-driven manipulation of the host. *Current Opinion in Microbiology* **12**, 117–124 (2009).

21. Agbor, T. A. & McCormick, B. A. *Salmonella* effectors: important players modulating host cell function during infection. *Cell Microbiol* **13**, 1858–1869 (2011).
22. Lawley, T. D. *et al.* Genome-Wide Screen for *Salmonella* Genes Required for Long-Term Systemic Infection of the Mouse. *PLoS Pathog* **2**, e11 (2006).
23. Kumar, Y. & Valdivia, R. H. Leading a Sheltered Life: Intracellular Pathogens and Maintenance of Vacuolar Compartments. *Cell Host and Microbe* **5**, 593–601 (2009).
24. Creasey, E. A. & Isberg, R. R. Maintenance of Vacuole Integrity by Bacterial Pathogens. *Current Opinion in Microbiology* **17**, 46–52 (2014).
25. Ellermeier, J. R. & Slauch, J. M. Adaptation to the host environment: regulation of the SPI1 type III secretion system in *Salmonella enterica* serovar Typhimurium. *Current Opinion in Microbiology* **10**, 24–29 (2007).
26. Vanengelenburg, S. B. & Palmer, A. E. Quantification of Real-Time *Salmonella* Effector Type III Secretion Kinetics Reveals Differential Secretion Rates for SopE2 and SptP. *Chemistry & Biology* **15**, 619–628 (2008).
27. Altier, C. Genetic and Environmental Control of *Salmonella* Invasion. *The Journal of Microbiology* **43**, 85–92 (2005).
28. Ramos-Morales, F. Impact of *Salmonella enterica* Type III Secretion System Effectors on the Eukaryotic Host Cell. *ISRN Cell Biology* **2012**, 1–36 (2012).
29. Raffatellu, M. *et al.* SipA, SopA, SopB, SopD, and SopE2 Contribute to *Salmonella enterica* Serotype Typhimurium Invasion of Epithelial Cells. *Infection and Immunity* **73**, 146–154 (2004).
30. Schlumberger, M. C. & Hardt, W.-D. *Salmonella* type III secretion effectors: pulling the host cell's strings. *Current Opinion in Microbiology* **9**, 46–54 (2006).
31. Hayward, R. D. & Koronakis, V. Direct nucleation and bundling of actin by the SipC protein of invasive *Salmonella*. *EMBO J* **18**, 4926–4934 (1999).
32. Stender, S. *et al.* Identification of SopE2 from *Salmonella typhimurium*, a conserved guanine nucleotide exchange factor for Cdc42 of the host cell. *Mol Microbiol* **36**, 1206–1221 (2000).
33. McGhie, E. J., Hayward, R. D. & Koronakis, V. Cooperation between actin-binding proteins of invasive *Salmonella*: SipA potentiates SipC nucleation and bundling of actin. *EMBO J* **20**, 2131–2139 (2001).
34. Zhou, D., Mooseker, M. S. & Galán, J. E. Role of the *S. typhimurium* Actin-Binding Protein SipA in Bacterial Internalization. *Science* **283**, 2092–2095 (1999).
35. Hernandez, L. D. *Salmonella* Modulates Vesicular Traffic by Altering Phosphoinositide Metabolism. *Science* **304**, 1805–1807 (2004).
36. Zhou, D., Chen, L.-M., Hernandez, L., Shears, S. B. & Galán, J. E. A *Salmonella* inositol polyphosphatase acts in conjunction with other bacterial effectors to promote host cell actin cytoskeleton rearrangements and bacterial internalization. *Mol Microbiol* **39**, 248–259 (2001).
37. Fu, Y. & Galan, J. E. A *Salmonella* protein antagonizes Rac-1 and Cdc42 to mediate host-cell recovery after bacterial invasion. *Nature* **401**, 293–297 (1999).
38. Steele-Mortimer, O., Meresse, S., Gorvel, J. P., Toh, B. H. & Finlay, B. B. Biogenesis of *Salmonella typhimurium*-containing vacuoles in epithelial cells involves interactions with the early endocytic pathway. *Cell Microbiol* **1**, 33–49 (1999).
39. Brawn, L. C., Hayward, R. D. & Koronakis, V. *Salmonella* SPI1 Effector SipA Persists after Entry and Cooperates with a SPI2 Effector to Regulate Phagosome Maturation and Intracellular Replication. **1**, 63–75 (2007).
40. Ye, Y. Diverse functions with a common regulator: Ubiquitin takes command of an AAA ATPase. *Journal of Structural Biology* **156**, 29–40 (2006).
41. Humphreys, D., Hume, P. J. & Koronakis, V. The *Salmonella* effector SptP

- dephosphorylates host AAA+ ATPase VCP to promote development of its intracellular replicative niche. *Cell Host and Microbe* **5**, 225–233 (2009).
42. Ye, Z., Petrof, E. O., Boone, D., Claud, E. C. & Sun, J. *Salmonella* Effector AvrA Regulation of Colonic Epithelial Cell Inflammation by Deubiquitination. *The American Journal of Pathology* **171**, 882–892 (2007).
43. Wu, H., Jones, R. M. & Neish, A. S. The *Salmonella* effector AvrA mediates bacterial intracellular survival during infection in vivo. *Cell Microbiol* **14**, 28–39 (2012).
44. Knodler, L. A., Finlay, B. B. & Steele-Mortimer, O. The *Salmonella* Effector Protein SopB Protects Epithelial Cells from Apoptosis by Sustained Activation of Akt. *Journal of Biological Chemistry* **280**, 9058–9064 (2005).
45. Woods, M. W. *et al.* The secreted effector protein of *Salmonella* dublin, SopA, is translocated into eukaryotic cells and influences the induction of enteritis. *Cell Microbiol* **2**, 293–303 (2000).
46. Layton, A. N., Brown, P. J. & Galyov, E. E. The *Salmonella* Translocated Effector SopA Is Targeted to the Mitochondria of Infected Cells. *Journal of Bacteriology* **187**, 3565–3571 (2005).
47. Zhang, Y., Higashide, W. M., McCormick, B. A., Chen, J. & Zhou, D. The inflammation-associated *Salmonella* SopA is a HECT-like E3 ubiquitin ligase. *Mol Microbiol* **62**, 786–793 (2006).
48. Zhang, S. *et al.* The *Salmonella* enterica Serotype Typhimurium Effector Proteins SipA, SopA, SopB, SopD, and SopE2 Act in Concert To Induce Diarrhea in Calves. *Infection and Immunity* **70**, 3843–3855 (2002).
49. Kamanova, J., Sun, H., Lara-Tejero, M. & Galán, J. E. The *Salmonella* Effector Protein SopA Modulates Innate Immune Responses by Targeting TRIM E3 Ligase Family Members. *PLoS Pathog* **12**, e1005552 (2016).
50. Brennan, M. A. & Cookson, B. T. *Salmonella* induces macrophage death by caspase-1-dependent necrosis. *Mol Microbiol* **38**, 31–40 (2000).
51. Hersh, D. *et al.* The *Salmonella* invasin SipB induces macrophage apoptosis by binding to caspase-1. *Proc Natl Acad Sci U S A* **96**, 2396–2401 (1999).
52. Kubori, T. & Galán, J. E. Temporal regulation of *Salmonella* virulence effector function by proteasome-dependent protein degradation. *Cell* **115**, 333–342 (2003).
53. Drecktrah, D., Knodler, L. A., Ireland, R. & Steele-Mortimer, O. The Mechanism of *Salmonella* Entry Determines the Vacuolar Environment and Intracellular Gene Expression. *Traffic* **7**, 39–51 (2005).
54. Fass, E. & Groisman, E. A. Control of *Salmonella* pathogenicity island-2 gene expression. *Current Opinion in Microbiology* **12**, 199–204 (2009).
55. Deiwick, J., Nikolaus, T., Erdogan, S. & Hensel, M. Environmental regulation of *Salmonella* pathogenicity island 2 gene expression. *Mol Microbiol* **31**, 1759–1773 (1999).
56. Rathman, M., Sjaastad, M. D. & Falkow, S. Acidification of phagosomes containing *Salmonella typhimurium* in murine macrophages. *Infection and Immunity* **64**, 2765–2773 (1996).
57. Yu, X.-J., McGourty, K., Liu, M., Unsworth, K. E. & Holden, D. W. pH sensing by intracellular *Salmonella* induces effector translocation. *Science* **328**, 1040–1043 (2010).
58. Freeman, J. A., Rappl, C., Kuhle, V., Hensel, M. & Miller, S. I. SpiC Is Required for Translocation of *Salmonella* Pathogenicity Island 2 Effectors and Secretion of Translocon Proteins SseB and SseC. *Journal of Bacteriology* **184**, 4971–4980 (2002).
59. Uchiya, K. *et al.* A *Salmonella* virulence protein that inhibits cellular trafficking.

- EMBO J* **18**, 3924–3933 (1999).
60. Shotland, Y., Krämer, H. & Groisman, E. A. The *Salmonella* SpiC protein targets the mammalian Hook3 protein function to alter cellular trafficking. *Mol Microbiol* **49**, 1565–1576 (2003).
  61. Schroeder, N., Mota, L. J. & Méresse, S. *Salmonella*-induced tubular networks. *Trends in Microbiology* **19**, 268–277 (2011).
  62. Krieger, V. *et al.* Reorganization of the Endosomal System in *Salmonella*-Infected Cells: The Ultrastructure of Salmonella-Induced Tubular Compartments. *PLoS Pathog* **10**, e1004374 (2014).
  63. Zhao, Y., Gorvel, J.-P. & Méresse, S. Effector proteins support the asymmetric apportioning of *Salmonella* during cytokinesis. *virulence* **7**, 669–678 (2016).
  64. Kuhle, V. & Hensel, M. SseF and SseG are translocated effectors of the type III secretion system of *Salmonella* pathogenicity island 2 that modulate aggregation of endosomal compartments. *Cell Microbiol* **4**, 813–824 (2002).
  65. Müller, P., Chikkaballi, D. & Hensel, M. Functional Dissection of SseF, a Membrane-Integral Effector Protein of Intracellular *Salmonella enterica*. *PLoS ONE* **7**, e35004 (2012).
  66. Kuhle, V., Abrahams, G. L. & Hensel, M. Intracellular *Salmonella enterica* Redirect Exocytic Transport Processes in a Salmonella Pathogenicity Island 2-Dependent Manner. *Traffic* **7**, 716–730 (2006).
  67. Beuzón, C. R., Meresse, S. & Unsworth, K. E. *Salmonella* maintains the integrity of its intracellular vacuole through the action of SifA. *EMBO* (2000).
  68. Dumont, A. *et al.* SKIP, the Host Target of the Salmonella Virulence Factor SifA, Promotes Kinesin-1-Dependent Vacuolar Membrane Exchanges. *Traffic* **11**, 899–911 (2010).
  69. Brumell, J. H., Tang, P., Zaharik, M. L. & Finlay, B. B. Disruption of the *Salmonella*-containing vacuole leads to increased replication of *Salmonella enterica* serovar typhimurium in the cytosol of epithelial cells. *Infection and Immunity* **70**, 3264–3270 (2002).
  70. Beuzón, C. R., Salcedo, S. P. & Holden, D. W. Growth and killing of a *Salmonella enterica* serovar Typhimurium sifA mutant strain in the cytosol of different host cell lines. *Microbiology* **148**, 2705–2715 (2002).
  71. Ohlson, M. B. *et al.* Structure and Function of *Salmonella* SifA Indicate that Its Interactions with SKIP, SseJ, and RhoA Family GTPases Induce Endosomal Tubulation. *Cell Host and Microbe* **4**, 434–446 (2008).
  72. Ruiz-Albert, J. *et al.* Complementary activities of SseJ and SifA regulate dynamics of the *Salmonella typhimurium* vacuolar membrane. *Mol Microbiol* **44**, 645–661 (2002).
  73. Lossi, N. S., Rolhion, N., Magee, A. I., Boyle, C. & Holden, D. W. The *Salmonella* SPI-2 effector SseJ exhibits eukaryotic activator-dependent phospholipase A and glycerophospholipid : cholesterol acyltransferase activity. *Microbiology* **154**, 2680–2688 (2008).
  74. Christen, M. *et al.* Activation of a Bacterial Virulence Protein by the GTPase RhoA. *Science Signaling* **2**, ra71–ra71 (2009).
  75. Catron, D. M. *et al.* The *Salmonella*-containing vacuole is a major site of intracellular cholesterol accumulation and recruits the GPI-anchored protein CD55. *Cell Microbiol* **4**, 315–328 (2002).
  76. Brumell, J. H. *et al.* SopD2 is a novel type III secreted effector of *Salmonella typhimurium* that targets late endocytic compartments upon delivery into host cells. *Traffic* **4**, 36–48 (2003).
  77. Schroeder, N. *et al.* The Virulence Protein SopD2 Regulates Membrane Dynamics

- of *Salmonella*-Containing Vacuoles. *PLoS Pathog* **6**, e1001002 (2010).
78. Birmingham, C. L., Jiang, X., Ohlson, M. B., Miller, S. I. & Brumell, J. H. *Salmonella*-Induced Filament Formation Is a Dynamic Phenotype Induced by Rapidly Replicating *Salmonella* enterica Serovar Typhimurium in Epithelial Cells. *Infection and Immunity* **73**, 1204–1208 (2005).
79. Freeman, J. A., Ohl, M. E. & Miller, S. I. The *Salmonella* enterica Serovar Typhimurium Translocated Effectors SseJ and SifB Are Targeted to the *Salmonella*-Containing Vacuole. *Infection and Immunity* **71**, 418–427 (2003).
80. Smith, A. C., Cirulis, J. T., Casanova, J. E., Scidmore, M. A. & Brumell, J. H. Interaction of the *Salmonella*-containing vacuole with the endocytic recycling system. *Journal of Biological Chemistry* **280**, 24634–24641 (2005).
81. Smith, A. C. *et al.* A network of Rab GTPases controls phagosome maturation and is modulated by *Salmonella* enterica serovar Typhimurium. *The Journal of Cell Biology* **176**, 263–268 (2007).
82. Mota, L. J., Ramsden, A. E., Liu, M., Castle, J. D. & Holden, D. W. SCAMP3 is a component of the *Salmonella*-induced tubular network and reveals an interaction between bacterial effectors and post-Golgi trafficking. *Cell Microbiol* **11**, 1236–1253 (2009).
83. Kuhle, V., Jäckel, D. & Hensel, M. Effector Proteins Encoded by *Salmonella* Pathogenicity Island 2 Interfere with the Microtubule Cytoskeleton after Translocation into Host Cells. *Traffic* **5**, 356–370 (2004).
84. Deiwick, J. *et al.* The Translocated *Salmonella* Effector Proteins SseF and SseG Interact and Are Required To Establish an Intracellular Replication Niche. *Infection and Immunity* **74**, 6965–6972 (2006).
85. Yu, X.-J., Liu, M. & Holden, D. W. *Salmonella* Effectors SseF and SseG Interact with Mammalian Protein ACBD3 (GCP60) To Anchor *Salmonella*-Containing Vacuoles at the Golgi Network. *mBio* **7**, e00474–16 (2016).
86. Henry, T., Gorvel, J.-P. & Méresse, S. Molecular motors hijacking by intracellular pathogens. *Cell Microbiol* **8**, 23–32 (2006).
87. Odendall, C. *et al.* The *Salmonella* Kinase SteC Targets the MAP Kinase MEK to Regulate the Host Actin Cytoskeleton. *Cell Host and Microbe* **12**, 657–668 (2012).
88. Poh, J. *et al.* SteC is a *Salmonella* kinase required for SPI-2-dependent F-actin remodelling. *Cell Microbiol* **10**, (2007).
89. Miao, E. A. *et al.* *Salmonella* effectors translocated across the vacuolar membrane interact with the actin cytoskeleton. *Mol Microbiol* **48**, 401–415 (2003).
90. McLaughlin, L. M. *et al.* The *Salmonella* SPI2 Effector Ssel Mediates Long-Term Systemic Infection by Modulating Host Cell Migration. *PLoS Pathog* **5**, e1000671 (2009).
91. Worley, M., Nieman, G. S., Geddes, K. & Heffron, F. *Salmonella* typhimurium disseminates within its host by manipulating the motility of infected cells. *PNAS* **103**, 17915–17920 (2006).
92. Quezada, C. M. C., Hicks, S. W. S., Galán, J. E. J. & Stebbins, C. E. C. A family of *Salmonella* virulence factors functions as a distinct class of autoregulated E3 ubiquitin ligases. *Proc Natl Acad Sci U S A* **106**, 4864–4869 (2009).
93. Bhavsar, A. P. *et al.* The *Salmonella* Type III Effector SspH2 Specifically Exploits the NLR Co-chaperone Activity of SGT1 to Subvert Immunity. *PLoS Pathog* **9**, e1003518 (2013).
94. Pilar, A. V. C., Reid-Yu, S. A., Cooper, C. A., Mulder, D. T. & Coombes, B. K. GogB Is an Anti-Inflammatory Effector that Limits Tissue Damage during *Salmonella* Infection through Interaction with Human FBXO22 and Skp1. *PLoS Pathog* **8**, e1002773 (2012).

95. Le Negrate, G. *et al.* *Salmonella* secreted factor L deubiquitinase of *Salmonella typhimurium* inhibits NF-kappa B, suppresses I kappa B alpha ubiquitination and modulates innate immune responses. *Journal of Immunology* **180**, 5045–5056 (2008).
96. Knodler, L. A. *et al.* *Salmonella* type III effectors PipB and PipB2 are targeted to detergent-resistant microdomains on internal host cell membranes. *Mol Microbiol* **49**, 685–704 (2003).
97. Ebers, K. L., Zhang, C. Y., Zhang, M. Z., Bailey, R. H. & Zhang, S. Transcriptional profiling avian beta-defensins in chicken oviduct epithelial cells before and after infection with *Salmonella enterica* serovar Enteritidis. *BMC Microbiology* **9**, 153 (2009).
98. Bakowski, M. A., Cirulis, J. T., Brown, N. F., Finlay, B. B. & Brumell, J. H. SopD acts cooperatively with SopB during *Salmonella enterica* serovar Typhimurium invasion. *Cell Microbiol* **9**, 2839–2855 (2007).
99. Spano, S., Liu, X. & Galán, J. E. Proteolytic targeting of Rab29 by an effector protein distinguishes the intracellular compartments of human-adapted and broad-host *Salmonella*. *Proc Natl Acad Sci U S A* **108**, 18418–18423 (2011).
100. Knodler, L. A. & Steele-Mortimer, O. The *Salmonella* effector PipB2 affects late endosome/lysosome distribution to mediate sif extension. *Molecular Biology of the Cell* **16**, 4108–4123 (2005).
101. Henry, T. *et al.* The *Salmonella* effector protein PipB2 is a linker for kinesin-1. *Proc Natl Acad Sci U S A* **103**, 13497–13502 (2006).
102. n-Olmo, F. B., Cardenal-Muñoz, E. & Ramos-Morales, F. PipB2 is a substrate of the *Salmonella* pathogenicity island 1-encoded type III secretion system. *Biochemical and Biophysical Research Communications* **423**, 240–246 (2012).
103. Van Engelenburg, S. B. & Palmer, A. E. Imaging type-III secretion reveals dynamics and spatial segregation of *Salmonella* effectors. *Nat Meth* **7**, 325–330 (2010).
104. Domingues, L., Holden, D. W. & Mota, L. J. The *Salmonella* Effector SteA Contributes to the Control of Membrane Dynamics of *Salmonella*-Containing Vacuoles. *Infection and Immunity* **82**, 2923–2934 (2014).
105. Domingues, L. *et al.* The *Salmonella* effector SteA binds phosphatidylinositol 4-phosphate for subcellular targeting within host cells. *Cell Microbiol* **18**, 949–969 (2016).
106. Mazurkiewicz, P. *et al.* SpvC is a *Salmonella* effector with phosphothreonine lyase activity on host mitogen-activated protein kinases. *Mol Microbiol* **67**, 1371–1383 (2008).
107. Haraga, A. & Miller, S. I. A *Salmonella enterica* Serovar Typhimurium Translocated Leucine-Rich Repeat Effector Protein Inhibits NF-kB-Dependent Gene Expression. *Infection and Immunity* **71**, 4052–4058 (2003).
108. Haraga, A. & Miller, S. I. A *Salmonella* type III secretion effector interacts with the mammalian serine/threonine protein kinase PKN1. *Cell Microbiol* **8**, 837–846 (2006).
109. Bernal-Bayard, J. & Ramos-Morales, F. *Salmonella* Type III Secretion Effector SlrP Is an E3 UbiquitinLigase for Mammalian Thioredoxin. *Journal of Biological Chemistry* **284**, 1–9 (2009).
110. Bernal-Bayard, J., Cardenal-Munoz, E. & Ramos-Morales, F. The *Salmonella* Type III Secretion Effector, *Salmonella* Leucine-rich Repeat Protein (SlrP), Targets the Human Chaperone ERdj3. *Journal of Biological Chemistry* **285**, 16360–16368 (2010).
111. Hardt, W. D. & Galan, J. E. A secreted *Salmonella* protein with homology to an avirulence determinant of plant pathogenic bacteria. *Proc Natl Acad Sci U S A* **94**,

- 9887–9892 (1997).
112. Kaniga, K., Uralil, J. & Bliska, J. B. A secreted protein tyrosine phosphatase with modular effector domains in the bacterial pathogen *Salmonella typhimurium*. *Mol Microbiol* (1996).
  113. Galán, J. E. Common Themes in the Design and Function of Bacterial Effectors. *Cell Host and Microbe* **5**, 571–579 (2009).
  114. Diao, J., Zhang, Y., Huibregtse, J. M., Zhou, D. & Chen, J. Crystal structure of SopA, a *Salmonella* effector protein mimicking a eukaryotic ubiquitin ligase. *Nat Struct Mol Biol* **15**, 65–70 (2007).
  115. Sory, M. P. & Cornelis, G. R. Translocation of a hybrid YopE-adenylate cyclase from *Yersinia enterocolitica* into HeLa cells. *Mol Microbiol* **14**, 583–594 (1994).
  116. Briones, G., Hofreuter, D. & Galan, J. E. Cre Reporter System To Monitor the Translocation of Type III Secreted Proteins into Host Cells. *Infection and Immunity* **74**, 1084–1090 (2006).
  117. Charpentier, X. & Oswald, E. Identification of the Secretion and Translocation Domain of the Enteropathogenic and Enterohemorrhagic *Escherichia coli* Effector Cif, Using TEM-1  $\beta$ -Lactamase as a New Fluorescence-Based Reporter. *Journal of Bacteriology* **186**, 5486–5495 (2004).
  118. Santiviago, C. A. *et al.* Analysis of Pools of Targeted *Salmonella* Deletion Mutants Identifies Novel Genes Affecting Fitness during Competitive Infection in Mice. *PLoS Pathog* **5**, e1000477 (2009).
  119. Sieuwerts, S., de Bok, F. A. M., Mols, E., de Vos, W. M. & van Hylckama Vlieg, J. E. T. A simple and fast method for determining colony forming units. *Letters in Applied Microbiology* **47**, 275–278 (2008).
  120. Figueiredo, J. F., Barhoumi, R., Raffatellu, M. & Lawhon, S. D. *Microbes and Infection* **11**, 850–858 (2009).
  121. Lara-Tejero, M. & Galan, J. E. *Salmonella enterica* Serovar Typhimurium Pathogenicity Island 1-Encoded Type III Secretion System Translocases Mediate Intimate Attachment to Nonphagocytic Cells. *Infection and Immunity* **77**, 2635–2642 (2009).
  122. Misselwitz, B. *et al.* Near Surface Swimming of *Salmonella* Typhimurium Explains Target-Site Selection and Cooperative Invasion. *PLoS Pathog* **8**, e1002810 (2012).
  123. Dai, S., Sarmiere, P. D., Wiggan, O., Bamburg, J. R. & Zhou, D. Efficient *Salmonella* entry requires activity cycles of host ADF and cofilin. *Cell Microbiol* **6**, 459–471 (2004).
  124. Li, D., Wang, X., Wang, L. & Zhou, D. The Actin-Polymerizing Activity of SipA Is Not Essential for *Salmonella enterica* Serovar Typhimurium-Induced Mucosal Inflammation. *Infection and Immunity* **81**, 1541–1549 (2013).
  125. Helaine, S. *et al.* Dynamics of intracellular bacterial replication at the single cell level. *Proceedings of the National Academy of Sciences* **107**, 3746–3751 (2010).
  126. McQuate, S. E. *et al.* Long-term live-cell imaging reveals new roles for *Salmonella* effector proteins SseG and SteA. *Cell Microbiol* **19**, e12641 (2016).
  127. Bujny, M. V. *et al.* Sorting nexin-1 defines an early phase of *Salmonella*-containing vacuole-remodeling during *Salmonella* infection. *Journal of Cell Science* **121**, 2027–2036 (2008).
  128. Choi, H. W. *et al.* *Salmonella* Typhimurium Impedes Innate Immunity with a Mast-Cell-Suppressing Protein Tyrosine Phosphatase, SptP. *IMMUNI* **39**, 1108–1120 (2013).
  129. Knodler, L. A. *et al.* Dissemination of invasive *Salmonella* via bacterial-induced extrusion of mucosal epithelia. *Proceedings of the National Academy of Sciences* **107**, 17733–17738 (2010).

130. Enninga, J., Mounier, J., Sansonetti, P. & Van Nhieu, G. T. Secretion of type III effectors into host cells in real time. *Nat Meth* **2**, 959–965 (2005).
131. Griffin, B. A., Adams, S. R. & Tsien, R. Y. Specific covalent labeling of recombinant protein molecules inside live cells. *Science* **281**, 269–272 (1998).
132. Rajashekar, R., Liebl, D., Chikkaballi, D., Liss, V. & Hensel, M. Live Cell Imaging Reveals Novel Functions of *Salmonella* enterica SPI2-T3SS Effector Proteins in Remodeling of the Host Cell Endosomal System. *PLoS ONE* **9**, e115423 (2014).
133. Akeda, Y. & Galán, J. E. Chaperone release and unfolding of substrates in type III secretion. *Nature* **437**, 911–915 (2005).
134. Tsai, C.-L., Burkinshaw, B. J., Strynadka, N. C. & Tainer, J. A. The *Salmonella* Type III Secretion System Virulence Effector Forms a New Hexameric Chaperone Assembly for Export of Effector/Chaperone Complexes. *Journal of Bacteriology* **197**, 672–675 (2015).
135. Radics, J., Königsmaier, L. & Marlovits, T. C. Structure of a pathogenic type 3 secretion system in action. *Nat Struct Mol Biol* **21**, 82–87 (2014).
136. Gawthorne, J. A. *et al.* Express Your LOV: An Engineered Flavoprotein as a Reporter for Protein Expression and Purification. *PLoS ONE* **7**, e52962 (2012).
137. Gawthorne, J. A. *et al.* Visualizing the Translocation and Localization of Bacterial Type III Effector Proteins by Using a Genetically Encoded Reporter System. *Applied and Environmental Microbiology* **82**, 2700–2708 (2016).
138. Buckley, A. M., Petersen, J., Roe, A. J., Douce, G. R. & Christie, J. M. ScienceDirectLOV-based reporters for fluorescence imaging. *Current Opinion in Chemical Biology* **27**, 39–45 (2015).
139. Xu, X. & Hensel, M. Systematic Analysis of the SsrAB Virulon of *Salmonella* enterica. *Infection and Immunity* **78**, 49–58 (2009).
140. Cabantous, S. & Waldo, G. S. In vivo and in vitro protein solubility assays using split GFP. *Nat Meth* **3**, 845–854 (2006).
141. Cabantous, S., Terwilliger, T. C. & Waldo, G. S. Protein tagging and detection with engineered self-assembling fragments of green fluorescent protein. *Nat Biotechnol* **23**, 102–107 (2005).
142. Brenner, F. W., Villar, R. G., Angulo, F. J., Tauxe, R. & Swaminathan, B. *Salmonella* Nomenclature. *Journal of Clinical Microbiology* **38**, 2465–2467 (2000).
143. Cornelis, G. R. The type III secretion injectisome. *Nat Rev Micro* **4**, 811–825 (2006).
144. Galán, J. E., Lara-Tejero, M., Marlovits, T. C. & Wagner, S. Bacterial Type III Secretion Systems: Specialized Nanomachines for Protein Delivery into Target Cells. *Annu. Rev. Microbiol.* **68**, 415–438 (2014).
145. Patel, J. C., Hueffer, K., Lam, T. T. & Galán, J. E. Diversification of a *Salmonella* Virulence Protein Function by Ubiquitin-Dependent Differential Localization. *Cell* **137**, 283–294 (2009).
146. Burkinshaw, B. J. & Strynadka, N. C. J. Assembly and structure of the T3SS. *BBA - Molecular Cell Research* **1843**, 1649–1663 (2014).
147. Ibarra, J. A. & Steele-Mortimer, O. *Salmonella*- the ultimate insider. Salmonellavirulence factors that modulate intracellular survival. *Cell Microbiol* **11**, 1579–1586 (2009).
148. Malik-Kale, P. *et al.* *Salmonella* – At Home in the Host Cell. *Front. Microbio.* **2**, 1–9 (2011).
149. Srikanth, C. V., Mercado-Lubo, R., Hallstrom, K. & McCormick, B. A. *Salmonella* effector proteins and host-cell responses. *Cellular and Molecular Life Sciences* **68**, 3687–3697 (2011).

150. Janssen, R., van der Straaten, T., van Diepen, A. & van Dissel, J. T. Responses to reactive oxygen intermediates and virulence of *Salmonella typhimurium*. *Microbes and Infection* **5**, 527–534 (2003).
151. Galán, J. E. SALMONELLA INTERACTIONS WITH HOST CELLS: Type III Secretion at Work. *Annu. Rev. Cell Dev. Biol.* **17**, 53–86 (2001).
152. Chakravorty, D., Hansen-Wester, I. & Hensel, M. Salmonella Pathogenicity Island 2 Mediates Protection of Intracellular Salmonella from Reactive Nitrogen Intermediates. *Journal of Experimental Medicine* **195**, 1155–1166 (2002).
153. Figueira, R. & Holden, D. W. Functions of the *Salmonella* pathogenicity island 2 (SPI-2) type III secretion system effectors. *Microbiology* **158**, 1147–1161 (2012).
154. Coombes, B. K. *et al.* Analysis of the Contribution of Salmonella Pathogenicity Islands 1 and 2 to Enteric Disease Progression Using a Novel Bovine Ileal Loop Model and a Murine Model of Infectious Enterocolitis. *Infection and Immunity* **73**, 7161–7169 (2005).
155. Bruno, V. M. *et al.* Salmonella Typhimurium Type III Secretion Effectors Stimulate Innate Immune Responses in Cultured Epithelial Cells. *PLoS Pathog* **5**, (2009).
156. Desin, T. S. *et al.* Salmonella enterica Serovar Enteritidis Pathogenicity Island 1 Is Not Essential for but Facilitates Rapid Systemic Spread in Chickens. *Infection and Immunity* **77**, 2866–2875 (2009).
157. Zhang, S. *et al.* Transcriptional response of chicken macrophages to Salmonella enterica serovar enteritidis infection. **132**, 141–151 (Developments in Biologicals, 2008).
158. Rosselin, M. *et al.* Rck of *Salmonella enterica*, subspecies enterica serovar Enteritidis, mediates Zipper-like internalization. *Nature Publishing Group* **20**, 647–664 (2010).
159. Velge, P. *et al.* Multiplicity of Salmonella entry mechanisms, a new paradigm for Salmonella pathogenesis. *MicrobiologyOpen* **1**, 243–258 (2012).
160. Boumart, Z., Velge, P. & Wiedemann, A. Multiple invasion mechanisms and different intracellular Behaviors: a new vision of *Salmonella*-host cell interaction. *FEMS Microbiol Lett* **361**, 1–7 (2014).
161. Miller, M. R. & Blystone, S. D. Reliable and inexpensive expression of large, tagged, exogenous proteins in murine bone marrow-derived macrophages using a second generation lentiviral system. *J Biol Methods* **2**, 23 (2015).
162. Monack, D. M., Navarre, W. W. & Falkow, S. Salmonella-induced macrophage death: the role of caspase-1 in death and inflammation. *Microbes and Infection* **3**, 1201–1212 (2001).
163. Brumell, J. H., Rosenberger, C. M., Gotto, G. T., Marcus, S. L. & Finlay, B. B. SifA permits survival and replication of *Salmonella typhimurium* in murine macrophages. *Cell Microbiol* **3**, 75–84 (2001).
164. Malik-Kale, P., Winfree, S. & Steele-Mortimer, O. The Bimodal Lifestyle of Intracellular *Salmonella* in Epithelial Cells: Replication in the Cytosol Obscures Defects in Vacuolar Replication. *PLoS ONE* **7**, e38732 (2012).
165. Knodler, L. A., Nair, V. & Steele-Mortimer, O. Quantitative Assessment of Cytosolic *Salmonella* in Epithelial Cells. *PLoS ONE* **9**, 1–13 (2013).
166. Guo, M. *et al.* High-resolution quantitative proteome analysis reveals substantial differences between phagosomes of RAW 264.7 and bone marrow derived macrophages. *Proteomics* **15**, 3169–3174 (2015).
167. Mullins, C. S., Wegner, T., Klar, E., Classen, C.-F. & Linnebacher, M. Optimizing the process of nucleofection for professional antigen presenting cells. *BMC Research Notes* 1–7 (2015). doi:10.1186/s13104-015-1446-8
168. Mills, E., Baruch, K., Charpentier, X., Kobi, S. & Rosenshine, I. Real-Time Analysis

- of Effector Translocation by the Type III Secretion System of Enteropathogenic *Escherichia coli*. *Cell Host and Microbe* **3**, 104–113 (2008).
169. Knodler, L. A. *et al.* Cloning Vectors and Fluorescent Proteins Can Significantly Inhibit *Salmonella enterica* Virulence in Both Epithelial Cells and Macrophages: Implications for Bacterial Pathogenesis Studies. *Infection and Immunity* **73**, 7027–7031 (2005).
170. Clark, L., Martinez-Argudo, I., Humphrey, T. J. & Jepson, M. A. GFP plasmid-induced defects in *Salmonella* invasion depend on plasmid architecture, not protein expression. *Microbiology* **155**, 461–467 (2009).
171. Kudla, G., Murray, A. W., Tollervey, D. & Plotkin, J. B. Coding-Sequence Determinants of Gene Expression in *Escherichia coli*. *Science* **324**, 255–258 (2009).
172. Salis, H. M., Mirsky, E. A. & Voigt, C. A. Automated design of synthetic ribosome binding sites to control protein expression. *Nat Biotechnol* **27**, 946–950 (2009).
173. Allert, M., Cox, J. C. & Hellinga, H. W. Multifactorial Determinants of Protein Expression in Prokaryotic Open Reading Frames. *Journal of Molecular Biology* **402**, 905–918 (2010).
174. Deutscher, M. P. Degradation of RNA in bacteria: comparison of mRNA and stable RNA. *Nucleic Acids Research* **34**, 659–666 (2006).
175. Goodman, D. B., Church, G. M. & Kosuri, S. Causes and Effects of N-Terminal Codon Bias in Bacterial Genes. *Science* **342**, 475–478 (2013).
176. Napolitano, M. G. *et al.* Emergent rules for codon choice elucidated by editing rare arginine codons in *Escherichia coli*. *Proceedings of the National Academy of Sciences* **113**, E5588–E5597 (2016).
177. Xayaphoummine, A., Bucher, T. & Isambert, H. Kinefold web server for RNA/DNA folding path and structure prediction including pseudoknots and knots. *Nucleic Acids Research* **33**, W605–W610 (2005).
178. Bajar, B. T. *et al.* Fluorescent indicators for simultaneous reporting of all four cell cycle phases. *Nat Meth* (2016). doi:10.1038/nmeth.4045
179. Salcedo, S. P. & Holden, D. W. SseG, a virulence protein that targets *Salmonella* to the Golgi network. *EMBO J* **22**, 5003–5014 (2003).
180. Ramsden, A. E., Mota, L. J., Münter, S., Shorte, S. L. & Holden, D. W. The SPI-2 type III secretion system restricts motility of *Salmonella*-containing vacuoles. *Cell Microbiol* **9**, 2517–2529 (2007).
181. Abrahams, G. L., Müller, P. & Hensel, M. Functional Dissection of SseF, a Type III Effector Protein Involved in Positioning the *Salmonella*-Containing Vacuole. *Traffic* **7**, 950–965 (2006).
182. Guy, R. L., Gonias, L. A. & Stein, M. A. Aggregation of host endosomes by *Salmonella* requires SPI2 translocation of SseFG and involves SpvR and the *fms±aroE* intragenic region. *Mol Microbiol* **37**, 1417–1435 (2000).
183. Hyun, S.-I., Maruri-Avidal, L. & Moss, B. Topology of Endoplasmic Reticulum-Associated Cellular and Viral Proteins Determined with Split-GFP. *Traffic* **16**, 787–795 (2015).
184. Garai, P., Gnanadhas, D. P. & Chakravorty, D. *Salmonella enterica* serovars Typhimurium and Typhi as model organisms. *virulence* **3**, 377–388 (2012).
185. Rosenberger, C. M. & Finlay, B. B. Phagocyte sabotage: disruption of macrophage signalling by bacterial pathogens. *Nat Rev Mol Cell Biol* **4**, 385–396 (2003).
186. Hamm, A., Krott, N., Breibach, I., Rüdiger, B. & Bosserhoff, A. K. Efficient Transfection Method for Primary Cells. *Tissue Engineering* **8**, 1–11 (2002).
187. Lenz, P., Bacot, S. M., Frazier-Jessen, M. R. & Feldman, G. M. Nucleoporation of dendritic cells: efficient gene transfer by electroporation into human monocyte-

- derived dendritic cells 1. *FEBS Letters* **538**, 149–154 (2003).
188. Maeß, M. B., Wittig, B. & Lorkowski, S. Highly Efficient Transfection of Human THP-1 Macrophages by Nucleofection. *JoVE* (2014). doi:10.3791/51960
189. Cordero-Alba, M. & Ramos-Morales, F. Patterns of Expression and Translocation of the Ubiquitin Ligase SirP in *Salmonella enterica* Serovar Typhimurium. *Journal of Bacteriology* **196**, 3912–3922 (2014).
190. Lathrop, S. K. *et al.* Replication of *Salmonella enterica* Serovar Typhimurium in Human Monocyte-Derived Macrophages. *Infection and Immunity* **83**, 2661–2671 (2015).
191. Plant, J. & Glynn, A. A. Natural resistance to *Salmonella* infection, delayed hypersensitivity and Ir genes in different strains of mice. *Nature* **345**–347 (1974).
192. Loomis, W. P. *et al.* Temporal and Anatomical Host Resistance to Chronic *Salmonella* Infection Is Quantitatively Dictated by Nramp1 and Influenced by Host Genetic Background. *PLoS ONE* **9**, e111763 (2014).
193. Uzzau, S., Figueroa-Bossi, N., Rubino, S. & Bossi, L. Epitope tagging of chromosomal genes in *Salmonella*. *PNAS* **98**, 15264–15269 (2001).
194. Datsenko, K. A. & Wanner, B. L. One-step inactivation of chromosomal genes in *Escherichia coli* K-12 using PCR products. *PNAS* **97**, 6640–6645 (2000).
195. Engelenburg, S. B. V. & Palmer, A. E. Imaging type-III secretion reveals dynamics and spatial segregation of *Salmonella* effectors. *Nature Publishing Group* **7**, 325–330 (2010).
196. Silva-Herzog, E. & Detweiler, C. S. *Salmonella enterica* Replication in Hemophagocytic Macrophages Requires Two Type Three Secretion Systems. *Infection and Immunity* **78**, 3369–3377 (2010).
197. de Chaumont, F. *et al.* Icy: an open bioimage informatics platform for extended reproducible research. *Nat Meth* **9**, 690–696 (2012).
198. Freischmidt, A., Liss, M., Wagner, R., Kalbitzer, H. R. & Horn, G. Protein Expression and Purification. *Protein Expression and Purification* **82**, 26–31 (2012).
199. Mao, Y., Liu, H., Liu, Y. & Tao, S. Deciphering the rules by which dynamics of mRNA secondary structure affect translation efficiency in *Saccharomyces cerevisiae*. *Nucleic Acids Research* **42**, 4813–4822 (2014).
200. Kamiyama, D. *et al.* Versatile protein tagging in cells with split fluorescent protein. *Nature Communications* **7**, 1–9 (2016).
201. Los, G. V. *et al.* HaloTag: A Novel Protein Labeling Technology for Cell Imaging and Protein Analysis. *ACS Chem. Biol.* **3**, 373–382 (2008).
202. Hayashi-Takanaka, Y., Stasevich, T. J., Kurumizaka, H., Nozaki, N. & Kimura, H. Evaluation of Chemical Fluorescent Dyes as a Protein Conjugation Partner for Live Cell Imaging. *PLoS ONE* **9**, e106271 (2014).
203. Kimura, H., Hayashi-Takanaka, Y., Stasevich, T. J. & Sato, Y. Visualizing posttranslational and epigenetic modifications of endogenous proteins in vivo. *Histochem Cell Biol* **144**, 101–109 (2015).
204. Effector proteins encoded by *Salmonella* pathogenicity island 2 interfere with the microtubule cytoskeleton after translocation into host cells. **5**, 356–370 (2004).
205. Berridge, M. J., Bootman, M. D. & Roderick, H. L. Calcium: Calcium signalling: dynamics, homeostasis and remodelling. *Nat Rev Mol Cell Biol* **4**, 517–529 (2003).
206. Ruschkowski, S., Rosenshine, I. & Finlay, B. B. *Salmonella typhimurium* induces an inositol phosphate flux in infected epithelial cells. *FEMS Microbiol Lett* **74**, 121–126 (1992).
207. Mallo, G. V. *et al.* SopB promotes phosphatidylinositol 3-phosphate formation on *Salmonella* vacuoles by recruiting Rab5 and Vps34. *The Journal of Cell Biology* **182**, 741–752 (2008).

208. Bakowski, M. A. *et al.* The Phosphoinositide Phosphatase SopB Manipulates Membrane Surface Charge and Trafficking of the *Salmonella*-Containing Vacuole. *Cell Host and Microbe* **7**, 453–462 (2010).
209. Pace, J., Hayman, M. J. & Galán, J. E. Signal transduction and invasion of epithelial cells by *S. typhimurium*. *Cell* **72**, 505–514 (1993).
210. Roy, D., Liston, D. R., Idone, V. J., Di, A. & Nelson, D. J. A process for controlling intracellular bacterial infections induced by membrane injury. *Science*, **304**, 1515–1518 (2004).
211. Gewirtz, A. T. *et al.* *Salmonella typhimurium* induces epithelial IL-8 expression via Ca<sup>2+</sup>-mediated activation of the NF-kappaB pathway. *J. Clin. Invest.* **105**, 79–92 (2000).
212. Figueiredo, J. F. *et al.* *Salmonella enterica* serovar Typhimurium-induced internalization and IL-8 expression in HeLa cells does not have a direct relationship with intracellular Ca<sup>2+</sup> levels. *Microbes and Infection* **11**, 850–858 (2009).
213. McCombs, J. E. & Palmer, A. E. Measuring calcium dynamics in living cells with genetically encodable calcium indicators. *Methods* **46**, 152–159 (2008).